RESEARCH PROJECT - MASTER THESIS (45 ECTS)
MASTER IN SCIENCE "SUSTAINABLE DEVELOPMENT"
TRACK: GLOBAL CHANGE AND ECOSYSTEMS"

THESIS TITLE: Influence of Road Presence in Secondary Forest Regrowth in the Amazon

STUDENT NAME: Isabel Trujillo Rocha

STUDENT NUMBER: 4046838

EMAIL: i.trujillorocha@students.uu.nl

SUPERVISORS: Dr. Karin Rebel

Dr. Maria João Ferreira Dos Santos

SECOND READER: Dr. Jerry van Dijk

INSTITUTION: Faculty of Geosciences, Utrecht University

Utrecht, 2015

Summary

The principal predictor for deforestation of primary forests in the Amazon is distance to roads. Considering the increasing ecological importance of secondary forests (which cover from 30 to 50% of the deforested area), the present research analysed the influence of road presence in secondary forest regrowth in the Amazon. Using remote sensing, I studied the land use classification of 40 plots of 400 km^2 in the States of Pará, Rondônia and Amazonas, during a 32 year period from 1984 to 2015.

My results indicate that road presence influences secondary forest regrowth. Most of the land use change (deforestation) occurs in areas closer to the road (within 30 km) and with high road density, where the percentage of area covered by secondary forest remained at around 20% during the period studied. However, an area located further than 30 km from roads has three times this probability to remain as a secondary forest, at a distance farther 50 km this probability is four times, and areas with low road density have three to four times more secondary forests cover. While the influence of type of road pattern (Fishbone or Other) was not statistically significant.

Key Words: Secondary forest, Amazon, Road ecology

Table of Contents

Table of Figures

Table of Tables

Table of Appendices

Influence of Road Presence in Secondary Forest Regrowth in the Amazon

1. INTRODUCTION

1.1. Background

The Amazon basin represents 60% of the remaining tropical rainforest in the world (Fearnside 1999). It is one of the world's most biodiverse ecoregions with thousands of unique species of plants and animals (WWF 2015), and plays vital roles in the regulation of regional hydrology and climate (Ewers and Laurance 2006; Fearnside 1999; Fearnside 2008; Laurance et al. 2002; Yoshikawa and Sanga-Ngoie 2011). At the same time, the Amazon represents one of the largest carbon storages in the world (Brienen et al. 2015; T. R. Feldpausch et al. 2012; Houghton et al. 2000), storing around 150 – 200 Pg C in living biomass and soils (T. R. Feldpausch et al. 2012).

In Brazil, it is located 69% of the Amazon biome (IBGE 2015a). The government recognizes an area of 5.1 million km^2, 59% of Brazil´s territory, as the "Legal Amazon" (Federative Republic of Brazil 1966; IBGE 2015b). However, 20% of the original area of the Brazilian Amazon tropical forests has already been deforested (Butler 2014; INPE 2015), for timber and conversion into agriculture, mainly for large - scale soybean production and cattle pastures (Colson et al. 2009; Davidson and Martinelli 2009; Ewers and Laurance 2006; Yoshikawa and Sanga-Ngoie 2011). Once the land use changes from primary forest to agriculture, tropical soils do not remain productive for a long period of time (Chazdon 2003; Luizão et al. 2009), and they are abandoned, later forming secondary forests (Davidson and Martinelli 2009; Hirsch et al. 2004).

The Brazilian government continually monitors deforestation (INPE 2015). However, once an area is deforested it is only considered either an agricultural or degraded area (IBGE 2015a; Yoshikawa and Sanga-Ngoie 2011), and the extension of secondary forests is not assessed in official statistics (Neeff et al. 2006). Nevertheless, it is estimated that 30 to 50% of cleared land is in some stage of secondary forest succession (Hirsch et al. 2004). This is more than 16 million ha which represents a fivefold increase from that area in 1978 (Neeff et al. 2006).

Secondary succession is an important process in the Amazon with implications for the sustainable regional agricultural and pasture activities, (Fearnside 2005; Wright and Muller-Landau 2006). Secondary forests buffer the net loss of forest cover, are key sources of plant propagules and facilitate movements of animal species, many of them seed dispersers and pollinators (Chazdon 2003; Groeneveld et al. 2009; Santos et al. 2014). Secondary forests play an increasingly important role as complementary conservation services, for example: reservoirs of genetic diversity, stocks of biomass, carbon and nutrients, and moderators of hydrologic cycles (Perz and Skole 2003b; Perz and Skole 2003a; Vieira et al. 2003).

However, the dynamics of secondary forest regrowth have been poorly studied. Secondary forests biomass accumulates more slowly, and even 70-year-old secondary forests are still distinguishable from primary forests (Vieira et al. 2003). Secondary forests become far more vulnerable to wildfires (Cochrane and Laurance 2002), droughts (Vasconcelos et al. 2012), predatory logging (D. C. Nepstad et al. 1999), hunting (Peres 2001) and other degrading activities (Laurance et al. 2002).

The primary determinant of land use change in the Amazon is access through roads (Laurance et al. 2002; Soares-Filho et al. 2004). Roads open the forest to exploitative activities such as logging and hunting, leading to new land colonization (Barber et al. 2014; Ewers and Laurance 2006). It is estimated that 95% of deforestation in the Brazilian Amazon occurs within 5.5 km of a road (Barber et al. 2014). As a consequence of deforestation and increase of roads in the Brazilian Amazon, the proportion of forest further than 1 km from the forest edge has decreased from 90% in 1970 to 75% (Haddad et al. 2015). Nearly 75,000 km of officially constructed roads intersect the Amazon rainforest (IBGE 2015a), with an additional 190,500 km of the unofficial road network, which are rapidly growing without any government oversight or incentives (Barber et al. 2014; Laurance and Balmford 2013). Construction of roads through rainforest is widely recognized as a primary cause of ecological degradation, affecting vegetation, animals, air and water quality, and even regional hydrology (Forman et al. 2003; Jaeger et al. 2005). Roads induce fragmentation, isolating endemic species, interfering with the genetic flow and reducing biodiversity (Epps et al. 2005; Haddad et al. 2015), enhance the spread of invasive species (Forman et al. 2003; Gelbard and Belnap 2003), increase human access to pristine ecosystems (Jaeger et al. 2005), and increase fire risk (D. Nepstad et al. 2001; D. C. Nepstad et al. 1999). Also, roads promote edge-related loss of forest carbon up to 150 million ton year^{-1} C, beyond that from deforestation alone (Laurance et al. 1997).

Considering roads are the principal determinants of deforestation, and driver of land use dynamics in the Amazon, they should also exert a major effect in secondary forest regrowth. Because, they are susceptible to be deforested again interrupting the vegetation regrowth. Furthermore, it is considered secondary forest are in a four times greater risk of deforestation than an intact forest (Asner et al. 2006), because settlers in the Amazon tend to not considered them as natural forests (Diniz et al., 2013).

The present thesis research has the objective to analyse whether there is an influence of roads in the remotely-sensed secondary forest regrowth dynamics.

1.2. Problem Description

Secondary forests have an increasing ecological importance in the Amazon considering the steady rates of deforestation. It is estimated that between 30 to 50% of the deforested area is covered by secondary forest (Hirsch et al. 2004). Distance to roads has been identified as the most important predictor of deforestation (Barber et al., 2014; Laurance et al., 2002).

However, currently there are no studies on the influence of roads to secondary forests. This is important because secondary forest regrowth dynamics should be studied, so regrowth is encouraged to develop mature forests. Consequently secondary forest could fulfil better conservation services in the Amazon and this conservation efforts should be coordinated with the development of new road construction projects.

1.3. State of the Art

Ecological succession is defined as the process of change of species structure in an ecological community over time. Succession initiated by some form of disturbance on a community such as fire or deforestation, is called secondary succession. In the case of tropical forests, like the Amazon, succession following fire and deforestation has been studied for more than 30 years (Acevedo L 1981; Fox 1976).

Deforestation in the Amazon is mainly due to the farming system known as slash and burn. Which involves the cutting and burning of forests to create fields or pastures. Livestock production has been the dominant land use because requires little labour, generates decent profits, and grass grows easily in the poor Amazon soil (Davidson and Martinelli 2009; D. C. Nepstad et al. 1999). Once productivity of pastures decline, settlers tend to leave the areas 'resting' for some years, aiming at natural soil recovery through organic matter and nutrient accumulation (Diniz et al. 2013; Ted R. Feldpausch et al. 2004).

Settlers do not consider successional areas as forest, but rather as potential areas to be cropped in the future and, therefore, they are under high risk of deforestation (Diniz et al., 2013). The probability of logging secondary forests between 5 to 25 km away from roads is two to four times greater than that of an intact forest in the same area (Asner et al. 2006), and in some areas the re-clearing of secondary forests occurs on average every 5 years (Neeff et al. 2006). These are considered the most important reasons for lack of large-statured, advanced secondary forests in the Amazon region (Davidson and Martinelli 2009).

Nevertheless, there is an ongoing transitional process of recovery in the Amazon forest (Yoshikawa and Sanga-Ngoie 2011). Remotely sensed land cover maps have been developed for the Amazon (Barber et al. 2014; Yoshikawa and Sanga-Ngoie 2011), and provide consistent spatial data on the extent and age class distribution of tropical secondary forests (Carreiras et al. 2014; Diniz et al. 2013; Neeff et al. 2006; Vieira et al. 2003).

Roads and their associated vehicular traffic have mainly adverse impacts to the natural environment (Forman and Alexander 1998; Forman et al. 2003). In the case of secondary forests, vegetation succession is affected by fragmentation and consequent edge effects (Laurance et al. 2011), which also are effects by roads (Forman et al. 2003). Forest fragmentation impairs key ecosystem functions by decreasing biomass and altering nutrient cycles (Haddad et al., 2015). The loss of area, increase in isolation, and greater exposure to human land uses along edges (edge-effect) initiate long-term changes to the structure and function of the remaining fragments (Lindenmayer and Fischer 2006). Fragmentation alters community composition, reducing biodiversity and richness of species (Haddad et al. 2015; Laurance et al. 1997). Roads also provide invasion corridors for seeds of invasive non-native species (Forman and Alexander 1998; Forman et al. 2003; Laurance, Goosem, and Laurance 2009, 200), Other edge effects include increased desiccation stress, windshear, and wind turbulence, increasing rates of tree mortality and damage (Laurance 2000; Laurance et al. 2001; D. Nepstad et al. 2001).

The principal parameters to define the influence of roads on forests, are distance to roads, and their spatial configuration in terms of density and type of pattern formed by the roads (Forman et al. 2003). However, there are no studies relating these parameters with secondary forests.

The distance to which different edge effects affect into forest fragments varies widely, ranging from 10 to 300 m in primary forests and considerably further (at least 2–3 km) in areas of the Amazon where edge-related fires are common (Cochrane and Laurance 2002; Laurance et al. 2011).

Road density is the average total road length per unit area of landscape (kilometres of road per square kilometres). Road density strongly affects spatial effects on the ecosystem because it increases human access. Many ecological phenomena affecting wildlife and biodiversity have been related to road density (Forman and Alexander 1998; Forman et al. 2003). Road density is inversely related to "effective mesh size" (Forman et al. 2003). "Effective mesh size" measures ecosystem fragmentation, in terms of the likelihood that two randomly chosen points in a region may be connected, converted into the size of an area (Jaeger 2000; Moser et al. 2007). However, this metric has not been calculated for the Amazon or other tropical forests.

Road networks may take an infinity variety of patterns, considering natural landscapes are heterogeneous and irregular that influence the construction of roads (Forman et al. 2003). However, the most common road pattern in the Amazon is the fishbone, which is defined as a straight principal road (commonly a highway) from which perpendicular smaller roads originate. The design of these roads was made by the government. Other road patterns, like radial, dendritic or irregular, normally follow the topography of the region. Studies suggest that the fishbone pattern increases rainfall in a mesoscale of 100x100 km and promotes regeneration of the forest (Garcia-Carreras and Parker 2011; Roy 2009). Therefore this pattern is considered less detrimental for primary forest, given that connectivity among the remnant forest patches is preserved (Filho and Metzger 2006). Other patterns may result in less fragmentation of the forests (Soler, Escada, and Verburg 2009).

1.4. Research Aim and Research Questions

The aim of my thesis research is to determine if an influence of roads in secondary forest regrowth dynamics in the Amazon exists.

The central research question is:

Does road presence influence secondary forest regrowth in the Amazon?

The following sub questions represent the logical steps to answer the main question of this research:

- Is secondary forest regrowth influenced by road presence in terms of:
    - **SQ1.** Distance to roads?
    - **SQ2.** Road density?
    - **SQ3.** Spatial configuration of the roads?

The present research tests the hypothesis that road presence influences the dynamics of secondary forest regrowth of the Amazon. I expect that the probability of forest regrowth is inversely correlated with the 1) distance, 2) higher density and 3) other patterns than fishbone (dendritic, radial or rectangular) of roads.

1.5. Relevance

Even though the secondary forest play an important ecological role in the Amazon, the dynamics of secondary forest regrowth are still poorly understood. Although there have been studies that analyse area and characteristics of secondary forest regrowth, using field measurements and remote sensing methods, no study has analysed the influence of roads on secondary forests.

The results of the present research will help the stakeholders in the decision making process for new road construction projects, considering their effect on secondary forests.

2. METHODS

2.1. Study Area

The study was carried out in the States of Pará, Rondônia and Amazonas, which are located in the "Brazilian Legal Amazon" (Figure 1). These states were selected because they all form part of the Amazon rainforest biome, have similar ecological characteristics, while having different levels of deforestation, population density and economic activities. According to statistical data, Rondônia is the state with higher levels of deforestation in the Legal Amazon (Butler 2014), Pará is the most populous state of the Northern Brazil, and Amazonas is the least populous state with lower deforestation levels (IBGE 2015a). The total area of these states covers more than 3 million km^2 (IBGE 2015b). This region includes several protected areas, agrarian colonization projects and urban areas. The region has a humid tropical climate, flat topography, predominantly lower than 400 m above sea level. The area is connected by highways, state and municipal roads, as well as a network of unofficial and illegal roads (IBGE 2015b; IBGE 2015b).

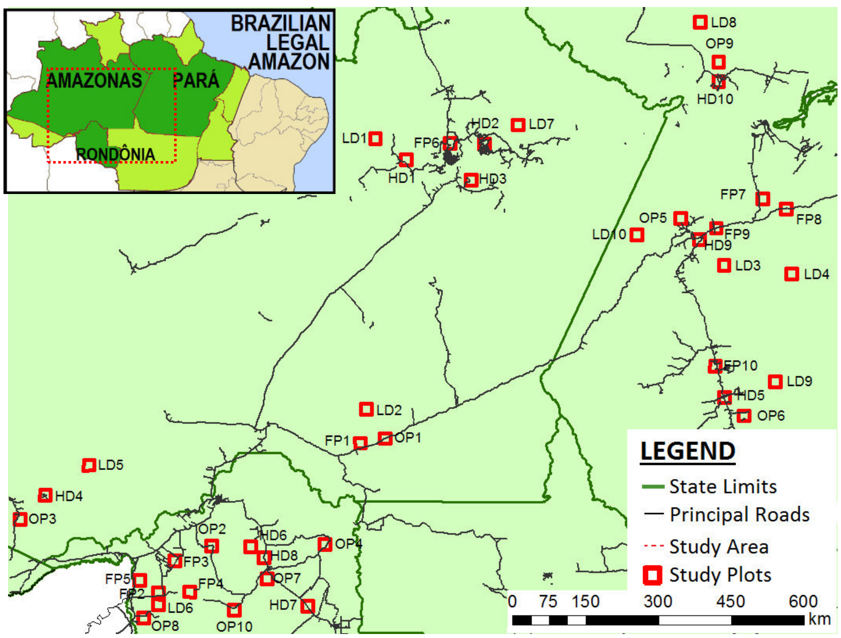

Figure 1. Distribution of the study plots (red squares) in the study area (states of Pará, Rondônia and Amazonas), with respect to the Brazilian Legal Amazon

2.2. Sampling design

To study the effect of roads on secondary forest regrowth I established a set of 40 plots, using a stratified sampling strategy. The selection of the plots was done based on the images available in Google Earth by June 2015 (Google 2015), to posteriorly check the availability of suitable historic satellite images.

I chose a plot size of 20 x 20 km because it was considered representative area of forest fragmentation in the Amazon. "Effective mesh size", which is the most common metric to measure ecosystem fragmentation, has not been measured for the Amazon. Therefore, this plot size was based on previous research where several studies (Baldi and Paruelo 2008; Jaeger 2000; Jaeger 2007; Moser et al. 2007) suggested an effective mesh size of 400 km^2.

Plots were assigned one of four categories, high and low road density and either fishbone or other road pattern (Figure 2).

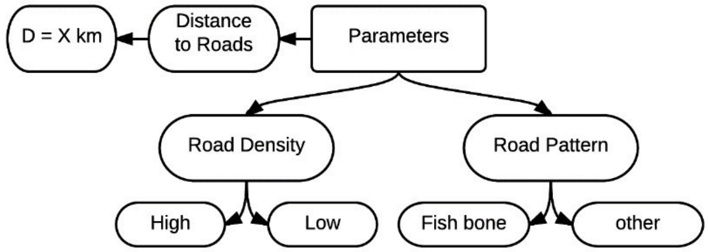

Figure 2. Characteristics of road presence that could affect secondary forest regrowth (Based on (Forman et al. 2003)

Distance to roads has been identified as the principal predictor of deforestation in the Amazon, and 95% of deforestation occurs in the first 5 km away from a road (Barber et al. 2014). Therefore to quantify the distance to roads I used the road network present in the Open Street Map crowdsourcing database (OpenStreetMap 2015). The Open Street Map database only includes the principal roads, mainly highways, as updated to their database by July 2015, and therefore does not allow testing the effects of unofficial and small roads on secondary forest. This choice was done because I could not get access to the map of unofficial network of roads, digitalized by Imazon using the methodology of (Brandão and Souza 2006), which used in the research of (Barber et al. 2014). I also chose not to use the global database of roads map (CIESIN and ITOS 2013), because the scale of this road dataset is not comparable to that of the satellite images, affecting its accuracy. The Open Street map road data set was clipped to the extent of my 40 plots and for each plot I used the "Euclidean distance" tool in ArcGIS (ESRI 2015), which gives the distance from each cell in the raster image to the closest road in the map (ESRI 2015). I also calculated the **distance to cities**, because cities include small municipal roads and also human settlements might influence land use change.

Road density is defined as the average road length per unit area of landscape (Forman et al. 2003). In the present research I only used two extremes of low and high road density based on estimates according to the road network shown in the images of Google Earth currently available. This was done because to measure density it is necessary to have the complete road map to measure length of roads per area. Also, road density of the plots would change during the temporal analysis making the classification in categories more difficult.

As detailed above, road patterns may have different effects on secondary forest regrowth. I considered two **Road Pattern** categories: fishbone and other (for example radial, rectangular, dendritic).

I selected 40 plots distributed in the study area, according to their current relation to roads. I selected plots that: were not crossed by rivers or lakes, were uniform in their characteristics, had similar Euclidian distances to roads and cities, and were distributed across the study area (Figure 3). Plots were then chosen based on their density (high (HD) and low (LD)), and spatial configuration (fishbone pattern (FP) and other pattern (OP)), 10 plots in each case. A complete list of the geographic coordinates of the plots is present in Appendix 1.

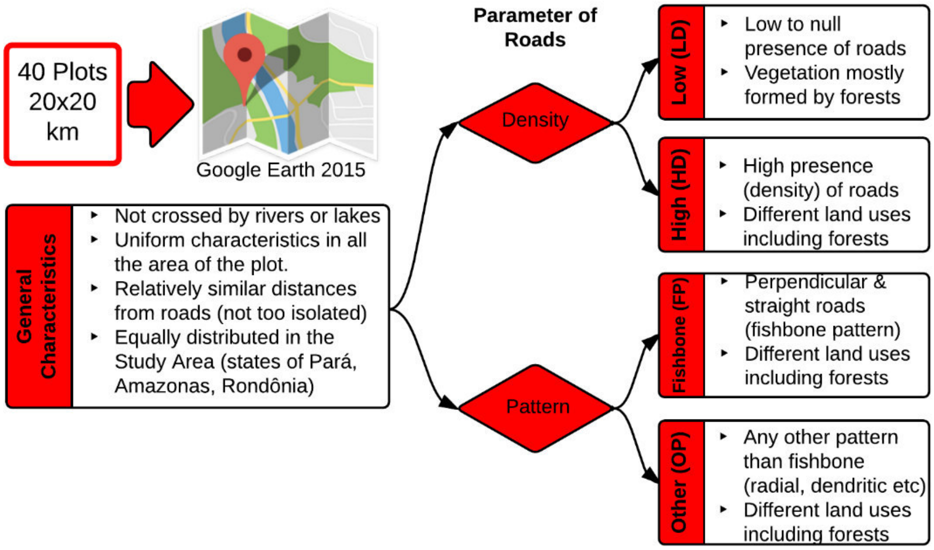

Figure 3. Decision tree for the sampling of the plots

2.3. Landsat Images

I chose the Landsat satellite images for this study because Landsat program is the largest program for acquisition of imagery of Earth from space, having images from the Amazon since 1984. These satellite images have a have a spatial resolution of 30 m, and a temporal resolution (time between imagery collection periods)of 16 days. Landsat offers already processed images, available in the user-friendly database, that are freely available to the public (NASA Official 2015; USGS 2014a).

Specifically I used Landsat Surface Reflectance images, which are generated by a specialized software of NASA to apply an atmospheric correction to the raw-data satellite images, taking into account water vapor, ozone, geopotential height, aerosol optical thickness, and digital elevation. Therefore, surface reflectance images are processed images that are better suitable for land surface change studies (USGS 2015b; USGS 2014a).

The study plots are covered by 11 Landsat scenes. For each scene I downloaded surface reflectance data from the United States Geographical Survey website (http://earthexplorer.usgs.gov/) (USGS 2015a), for the period between 1984 to 2015. Landsat scenes were clipped to the study plots and the following analysis refers to a total of 1280 individual images (40 plots over 32 years).

I used annual images of between the years 1984 to 2011 from Landsat 5 thematic mapper (TM) and Landsat 7 enhanced thematic mapper (ETM+) and from 2013 to 2015 from Landsat 8 (operational land imager (OLI). In 2003 there was a failure in the Scan Line Corrector (SLC) of the Landsat 7, which since then traced a zig-zag pattern, generating images with an increased area and data gaps(USGS 2013). I chose not to use these images and since these were the only available for 2012, this year was omitted.

As far as possible, I tried to use images that were one year apart, to analyse the annual variation of the vegetation and keep the same climatic conditions. In general, I selected only images with less than 10% cloud cover, as clouds limit visibility. I chose images from the sunnier dry season (June to November), because during that period there is minimal cloud cover and there is increased forest productivity that enhances the difference between primary forest with other types of land use

(Huete et al. 2006; Martins et al. 2015). However, 34 images (plots per year) were not available, and these were omitted from this study. This represents only 5.8% of the images were not available for the study, not affecting the analysis of this research. The complete list of images used are presented in Table 1.

Table 1. Landsat images (scenes per month), in respect to the plots.

Type of image Landsat available: TM (normal format), ETM+ (**bold**), OLI (*italics*).

Scene	Plots	84	85	86	87	88	89	90	91	92	93	94	95	96	97	98	99	00	01	02	03	04	05	06	07	08	09	10	11	12	13	14	15
001/066	HD4, OP3, LD5	jul	aug	jul	jul	jul	aug	jul	jul	jul	jul	jul	jul	jul	jul	jul	**jul**	**jul**	**jul**	**jul**	jul	jul	jul	jul	jul	jul	jul	jul	jul	**jul**	*jul*	*jul*	
227/063	FP7, FP8, LD3, LD4	aug	aug	nov	oct	jul	aug	aug	jul	jul	may	jul	jul	jul	jul	jun	aug	aug	jul	jul	jul	jul	jul	aug	jul	jul	jul	jul	jul	**jul**	*sep*	*jul*	
227/065	HD5, FP10, OP6, LD9	jun	aug	jul	jun	jul	aug	aug	jul	jul	aug	jul	jul	jul	jun	jul	**jul**		**jul**	**jul**	jul	jul	jul	jun	jun	jul	jul	jul	jul	**jul**	*aug*	*sep*	*jun*
228/061	HD10, OP9, LD8		oct	jul	jul	jul	sep	nov	aug	sep	jul	jul	jul	jun	jul	aug	jul	aug	jul	**jul**	jul	**jul**	**jul**	**aug**	**jul**	**jul**	**jul**	**aug**	jul	**jul**	**sep**	*aug*	
228/063	HD9, FP9, OP5, LD10	jul	jul	aug	jul	jul	sep	aug	jul	jun	jul	aug	jun	oct	jul	jul	jul	aug	**aug**	**aug**	jul	aug	jul	jun	jun	jul	jul	jul	aug	**jul**	*jun*	*aug*	
230/062	HD2, HD3		jul	aug	aug	sep	sep	aug	aug	jul	sep	oct	aug	oct	jun	aug	sep	aug	**aug**	**jul**	jul	aug	aug	aug		jul	aug		jul	**aug**	*jul*		*jun*
231/062	HD1, FP6, LD1	aug	jul	aug	jul	aug	aug	aug	aug	jul	jul	jul	sep	aug	jul	jul	jul	jun	aug	**aug**	jul	sep	jul	jul	jul	jul	jul	jul	aug	**jul**	*jul*	*jul*	*jul*
231/065	FP1, OP1, LD2	jul	jul	jul	jul	jul	jul	jul	jul	jul	aug	jul	aug	jul	jul	jul	jul	jul	**jul**	**jul**	jul	jul	jul	jul	jul	jul	jul	jul	jul	**jul**	*aug*	*jul*	*jun*
231/067	HD7, OP4, LD7	aug	jul	aug	jul	jul	jul	jun	jul	jun	jul	jul	aug	jul	jul	jul	jul	jul	aug	**jun**	jul	jul	jul	jul	jul	jul	aug	jun	jul	**jul**	*aug*	*jul*	*jul*
232/067	HD6, HD8, FP4, OP10, OP2,	jun	jul	jul	jul	jul	jul	apr	jul	jul	jul	jul	jul	jul	jul	jul	jul	jul	jun	aug	jul	aug	aug	jul	jun	jul	jul	aug	jul	**jul**	*jul*	*jul*	*jun*
233/067	FP2, FP3, FP5, OP8, LD6	jul	sep	jul	jul	jul	jul	jul		jul	jul	jul	jul	jul	jul	jul	jul	jul	aug	**jul**	jul	jul	jul	jul	jul	jul	jul	jul	jul	**jul**	*jun*	*jun*	*jun*

(grey) Image with < 10% of cloud coverage not available in the USGS database

(yellow) Only images with gaps (ETM+SLC-off data) available

2.4. Image Classification

Secondary forest is defined as vegetation succession in the tropical forest of the Brazilian Amazon, in which forest has regenerated on land that has been previously used for agriculture or as cattle pasture (Neeff et al., 2006).

It is widely recognized that remote sensing is among the best methods for consistently quantifying areas under different forest cover (Steininger, 2000). Land cover change can be analysed through time-series comparison of image classifications (Neeff et al. 2006).

Landsat 5, 7 and 8 satellites collect spatial information over 7 spectral bands, with different wavelength (USGS 2014a).

Table 2. Wavelengths according to bands of Landsat 5, 7 y 8 (USGS 2014b)

Colour	Landsat 5 & 7 # Band	Wavelength (µm)	Landsat 8 # Band	Wavelength (µm)
			1	0.43 – 0.45
Blue (B)	1	0.45 – 0.52	2	0.45 – 0.51
Green (G)	2	0.52 – 0.60	3	0.53 – 0.59
Red (R)	3	0.63 – 0.69	4	0.64 – 0.67
Near Infrared	4	0.77 – 0.90	5	0.85 – 0.88
Short wave Infrared 1	5	1.55 – 1.75	6	1.57 – 1.65
Short wave Infrared 2	7	2.09 – 2.35	7	2.11 – 2.29

I used the true colour and the colour infrared composites to identify and differentiate forests. The natural colour composite (RGB) serves for recognizing, and classifying most of the natural features. The colour infrared composite (CIR) is that where green wavelength is displayed in blue, red is displayed in green, and near infrared is displayed in red. Colour infrared composite serves to differentiate Secondary forest from Primary (mature) forest because secondary forest regrowth is recognizable in a brighter red colour, as suggested by (Carreiras et al. 2014; Neeff et al. 2006; Soler, Escada, and Verburg 2009) (Figure 4).

a) b)

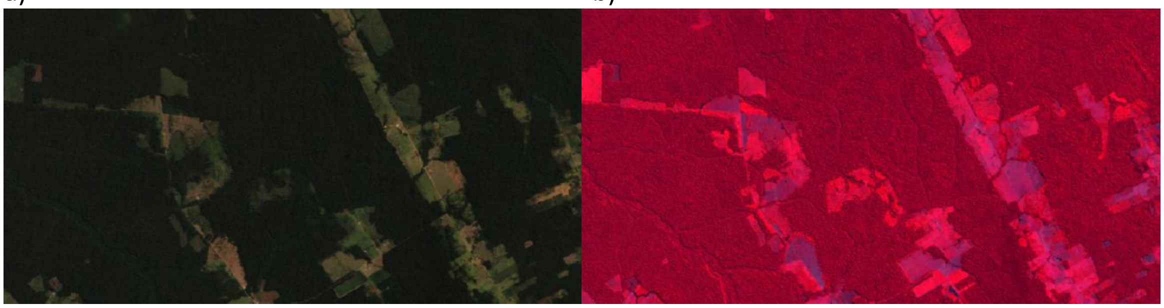

Figure 4. Difference between Landsat satellite images a) true colour composite, and b) colour infrared composite

There are several challenges in discriminating It must be noted that several studies carried out in the Amazon have acknowledged some issues in discriminating secondary and primary forest in the Amazon, especially when forest is older than 15 years. This is largely because of spectral similarities between different successional stages, considering that secondary forest is a transitional class between other vegetation (agriculture or pasture) and primary or mature forest (Carreiras et al. 2014; Neeff et al. 2006).

Other reason is because the specific characteristics of secondary forests like vegetation structure and species composition and its consequent accumulation of biomass, may vary across regions and are influenced by several factors like differences in edaphic and climatic conditions, history of land use, proximity to seed sources, and management practices such as the frequency of burning and grazing intensity (Davidson and Martinelli 2009; Rebel et al. 2001; Vieira et al. 2003).

I classified Landsat satellite images using the Spatial Analysis tools in ArcGIS v.10.3 (ESRI 2014). I ran **Supervised Image Classification,** based on the maximum likelihood algorithms (ESRI 2015). Supervised image classification is a multistep process that follows the workflow presented in Figure 5.

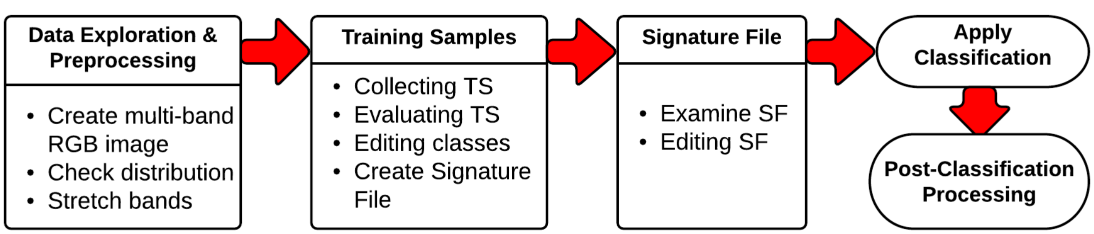

Figure 5. Supervised image classification workflow (ESRI 2015)

First I created a true colour composite, checked that all the bands have a normal distribution. This because the supervised image classification analysis is based on the assumption that the band data and the training sample data follow normal distribution in order that the range of values in each band is considered equally. Thus if the value range of one band was too small (or too large) relative to the other bands I stretched the bands using the Spatial Analyst toolbox (ESRI 2015).

Second, for every scene I collected representative training samples, which are specific areas that represent the different types of land use or forest cover to be analysed. In this case, I chose four classes: Primary Forest, Clear Cut (recently deforested), Other (pastures, agriculture, and all other land covers), and Secondary Forest. The change between these classes represents dynamics of land use in the Amazon (Figure 6).

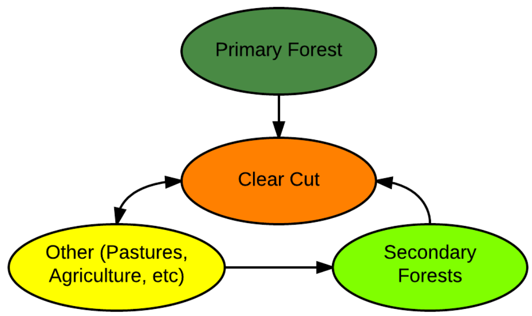

Figure 6. Dynamics of Land Use in the Amazon

The selected training samples were evaluated to assess whether they would be representative (not intersect or overlap with other classes). For this, I used the histogram and dendogram tools.

During the evaluation of the training samples, I noticed the presence of other land use classes that were intersecting and overlapping with the initial four classes. For example I considered urban areas (more reflective), clouds, shadows of clouds, and clouded areas which could still be recognized as belonging to a certain class (i.e. clouded primary forest). I also grouped areas that do not support forest (water bodies) with areas of cloud and cloud shadow as ''no data''. Therefore it was necessary to add them for the image classification.

The final classification had the land cover classes, which are summarized in Figure 7:

1) Primary Forest (**P.F.**) comprises primary forest and clouded forest areas,

2) Clear Cut (**C.C.**), recently deforested areas without vegetation or burned,

3) Other (**Oth.**), comprises pasture, agricultural crops, urban areas, or other clouded areas,

4) Secondary Forest (**S.F.**) secondary forest and clouded secondary forest,

5) No Data (**N.D**.) areas covered by clouds, shadows or water and therefore not relevant for the land use and cover change dynamics.

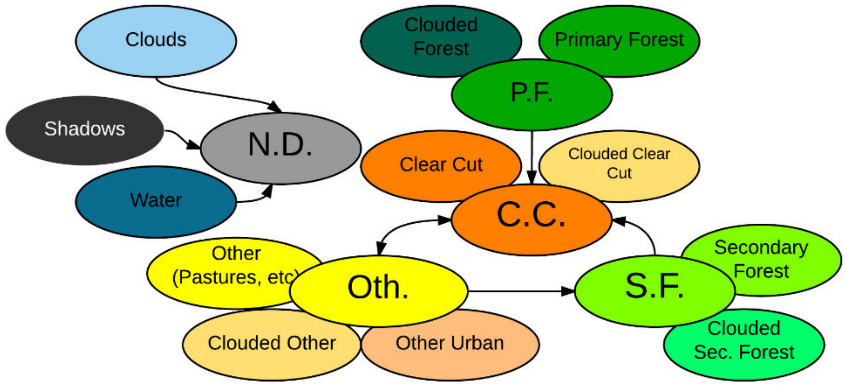

Figure 7. Classes of land use for image classification of Landsat images

I created a signature file for the selected training points (Figure 5), which was examined prior to being used. I then performed a classification using the **Maximum Likelihood Classification** tool, which assigns each pixel of the image to one of the different classes based on the means and variances of each signature (Ahmad 2012; Lu et al. 2012; Strahler 1980). The maximum likelihood classification is still an important method for providing reasonably good accuracy, because even though there are other classification algorithms available, they often require more time to achieve parametric optimization and require high spatial resolution images (Lu et al. 2012).

The classification was improved by the **post-classification processing**, which filters isolated pixels and cleans boundaries. The final image classification presents areas with cleaner borders. I then calculated the area (in square kilometres) of the different classes of land use in the final classification.

2.5. Data Quality Assessment

I based the accuracy assessment of the time-series classification in the methodology of (Carreiras et al. 2014), Foody (2009), and (Vieira et al. 2003). For each individual scene of the Landsat images, test points were generated for each class, using the original true colour composite image. It is not possible to use the same points used as training points for the classification, because it will result in a sampling error for the assessment.

An error matrix was derived by overlaying the test points on the classified image, and comparing the field observations with the classification for each test point. I calculated the omission and commission errors, which represent the percentage of false negative and false positive points, respectively (Gallego 2004). False negatives represent points that were not correctly classified with the right class and false positives represent points that were wrongly attributed a certain class.

To further evaluate the quality of the classification, I used two indexes. First, I used the Overall Accuracy that quantifies the number of points correctly classified divided with the total of points used in the classification. Second, I used the Kappa coefficient, which quantifies the overall accuracy of the classification relative to that expected by chance (Czaplewski, 2000 in (Vieira et al. 2003); (Stehman 1996). According to the following equation:

$$K = \frac{observed\ accuracy - chance\ agreement}{1 - chance\ agreement} = \frac{(N \sum_k X_{kk} - \sum_k (x_{k+} * x_{+k}))}{(N^2 - \sum_k (x_{k+} * x_{+k}))}$$

Where k = kappa, N = total number of pixels in all ground classes, $\sum_k X_{kk}$= the sum of the matrix diagonal classes, + = summation over the index, x_{k+} = the sum of the ground truth pixels in that class, and x_{+k} = the sum of the classified pixels in that class (Congalton 1991; Congalton and Mead 1983; Stehman 1996). This indicates the percentage of error avoided in comparison to what a completely random classification would generate (Vieira et al. 2003).

Therefore, for further statistical analysis I decided not to take into account individual plots with more than 10% of cloud coverage. In total, these are 173 individual images (plot per year) from the different time series, besides the scenes omitted for lack of availability in the USGS database. The complete list of plots and years that were eliminated of the image classification because of presence of cloud coverage or shadows (no data) is presented in Appendix 2.

2.6. Statistical Analysis

I analysed the relation between the Euclidean distance map to the roads and cities in respect to plots, using the spatial analysis in ArcGIS to separate the different classes according to the image classification. The measures obtained are the total statistics (one measure): mean, minimum, and maximum distance. Later, I analysed the relation between type of plot (Low and High Density, and Fishbone and Other pattern) and the distance to roads and cities, I used the "One-Way Analysis of Variance" (ANOVA). This test compares the difference in mean scores between multiple groups (Rencher 2012).

To further analyse the image classification in respect to distance, I classified all the time-series according to the distance to roads and cities in eight categories (< 5, 5 – 10, 10-20, 20-30, 30-40, 40-50, 50-100 and > 100 km). I tested the hypothesis, that there is a statistically significant difference in S.F. between the different distances to roads and cities. The most adequate statistical analysis to analyse and compare this change in areas over the time-series is "Multivariate Analysis of Variance" (MANOVA) because the dependent variables (classes of land use) are correlated, therefore the change of one land use affects the distribution or others. MANOVA compares the difference in mean scores between multiple groups, using multiple variables (Rencher 2012).

I analysed the change of percentage of land cover in the different plots the areas of the classes of land use (in km^2). The response of dependent variable are the areas of different classes of land use (P.F., C.C., Oth., S.F. and N.D.). I tested the hypothesis, that there is a statistically significant difference in S.F. between the plots with different road densities (Low and High) and road pattern (Fishbone and Other), using MANOVA.

I also used "Multivariate Analysis of Covariance" (MANCOVA) to consider if the influence of distance to roads and cities (in terms of mean, minimum and maximum distance) affects the independent variables (density and pattern). The purpose of this analysis is to 'factor out' the possible error introduced by these covariables in the analysis (Rencher 2012).

ANOVA, MANOVA and MANCOVA analyses were ran in SPSS version 17 (SPSS Inc. 2008), considering a 95% of confidence for testing the hypothesis. The result statistics for both analysis are expressed in four different multivariate tests analysis: Pillai's Trace, Wilks' Lambda, Hotelling's Trace, and Roy's Largest Root, because each test has its own associated F ratio. In cases where their P values differ, Pillai's trace is used because it is considered the most powerful and robust of the four (Carey 1998).

A P value less than 0.05 indicates that the mean of the variables are different and therefore corroborate my original hypothesis (Carey 1998).

3. RESULTS

3.1. Image Classification

The results of the image classification show a difference between the plots with high/low density and the fishbone/other road pattern. Some examples of this classification are presented in Figure 8. As can be seen in Figure 8, the types of plots have visually different characteristics, and their image classification follows the land use. In general, the results of the image classification are similar to the ones presented as example, but the final 1280 images (40 plots over 32 years) are not presented in this report because of space.

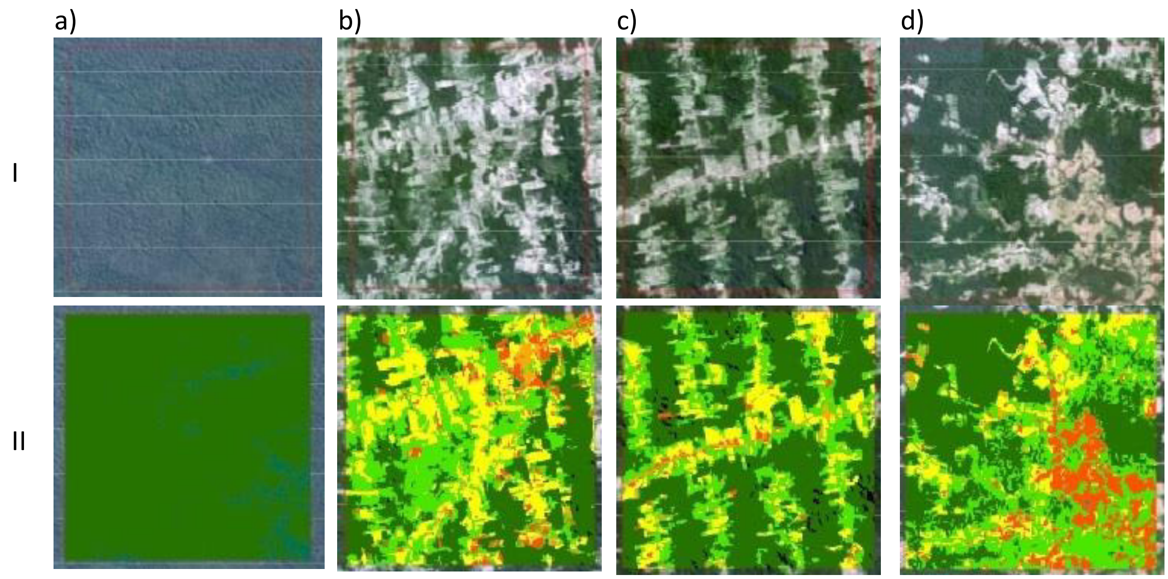

Figure 8. Different types of plots used in the image classification. I. Original satellite image, II. Images with image classification. Types of plots: a) Low Density (LD10 2014), b) High Density (HD9 2014), c) Fishbone Pattern (FP9 2014), d) Other Pattern (OP5 2015)

In the Appendices, I present a complete report of the image classification resulted by the Supervised classification done in ArcGIS. The percentage distribution of the plots are in Appendix 3.

On the bases of these image classifications, I obtained the areas (in square kilometres) of each land cover type in the plots: 1) Primary Forest (P.F.), 2) Clear Cut (C.C.), 3) Other (Oth.), 4) Secondary Forest (S.F.), and 5) No Data (N.D). The mean composition (in area percentage) of each land cover is presented in Figure 9.

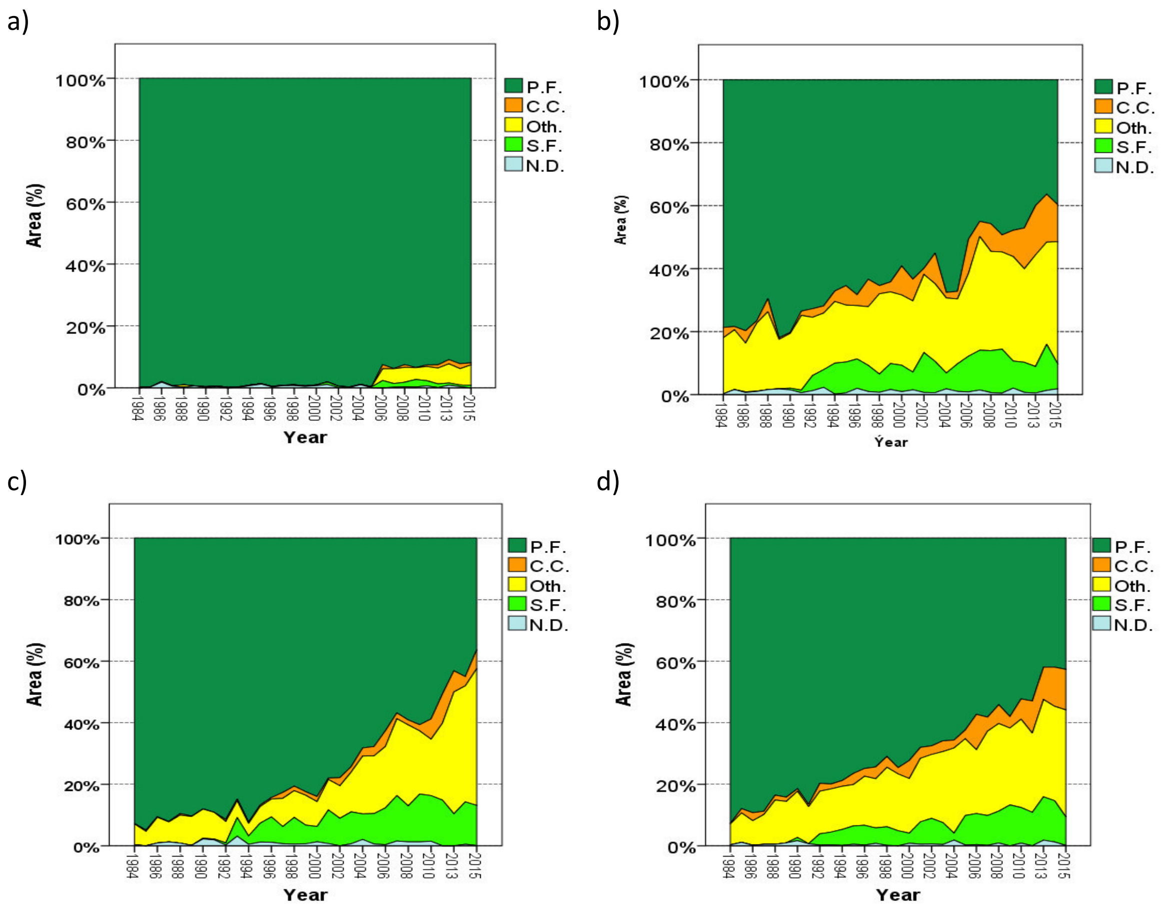

Figure 9. Mean composition (in area percentage) of image classification of the time-series, Primary Forest (P.F.), Clear Cut (C.C.), Other (Oth.), Secondary Forest (S.F.), No Data (N.D.), according type of plot: a) Low Density, b) High Density, c) Fishbone Pattern, and d) Other Pattern

Figure 9 shows that the percentage of P.F. are decreasing from 1984 to 2015. The mean percentage of P.F. all types, with exception to Low Density, at the end of the study is around 40%. The mean percentage of S.F. also increases reaching less than 20% for all types, being also lower for Low Density plots.

In the appendices I present a complete report of the image classification reports, using the supervised classification in ArcGIS. The figures with the percentage distribution of each plot's time-series are presented in Appendix 3. The figures are similar to the ones presented in Figure 9, which are representative of their mean values.

3.2. Accuracy Assessment

In general, the accuracy indexes show lower results for the scenes with cloud coverage, and the accuracy varies for some years and scenes. Nevertheless, the mean value of overall accuracy is 0.92 with a standard error of 0.05, while the Kappa coefficient is 0.85 with a standard error of 0.08. This result indicates that the image classifications are reliable for further analysis.

The most common misclassifications in the research were secondary forests being misclassified as primary forests and pastures being misclassified as secondary forests. However, in general terms, the accuracy values were lower in clouded plots, because cloudy areas with different consistency were classified as other classes and their shadows also affected the classification.

The accuracy assessment of the image classification was done for all the scenes of the time-series, generating an error matrix for each of them. However, considering reasons of space (they are 1033 tables), only the tables with the summary of the results, overall accuracy and Kappa coefficients of all the time series, are presented in Appendix 4.

3.3. Distance to Roads and Cities

First the Euclidian distance was measured between the plots in respect to roads and cities. These thematic maps are presented in Appendix 5. The measures of distances to roads and cities, in terms of mean, minimum, and maximum is presented in Appendix 6.

The distance between plots in relation with roads and cities was analysed using an ANOVA, the complete results of this analysis are presented in Appendix 7. The ANOVA results show that the type of plot are significantly different in respect to the distance to roads (Sig < 0.05). The Low Density (LD) plots are located significantly further from the roads (mean 54.8 km), while Fishbone (FP), Other Pattern (OP) and High Density (HD) are statistically located at similar mean distance to roads (3.4 to 6.2 km from roads). For cities, the difference in mean distance is significant between types of plot (Sig < 0.05). The Low Density plots are located significantly further from the roads (mean 90.9 km), Other and Fishbone Pattern are in a similar mean distance of 43.6 and 47.8 km, and High Density Plots are in a mean of 31.8 km (Figure 10).

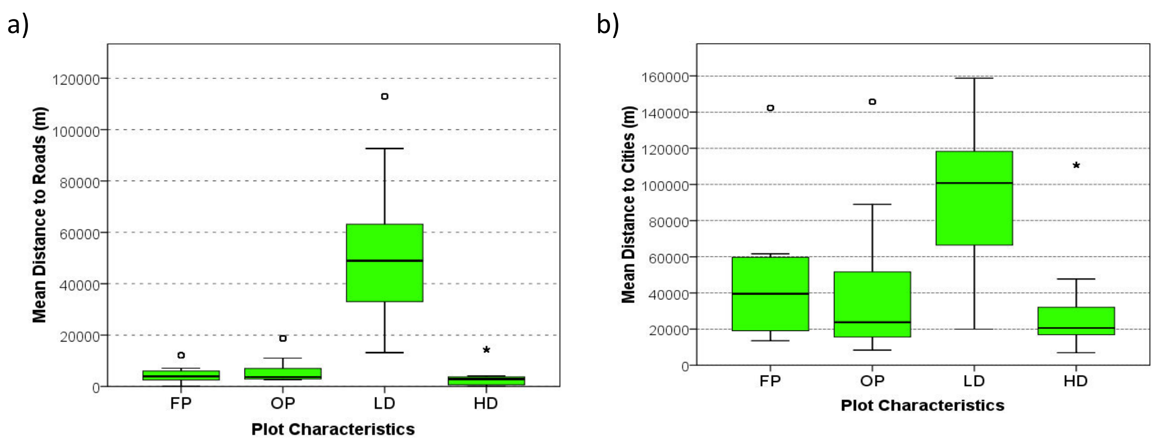

Figure 10. Boxplots of the mean distance from the plots of Fishbone Pattern (FP), Other Pattern (OP), Low Density (LD), and High Density (HD) in respect to a) Roads, and b) Cities

In Figure 11, we can see that Primary Forest (P.F.) is located farther from the roads (between 10 000 and 40 000 m) than the other land cover types, including Secondary Forest (S.F.). While distance to cities is more variable between land cover types.

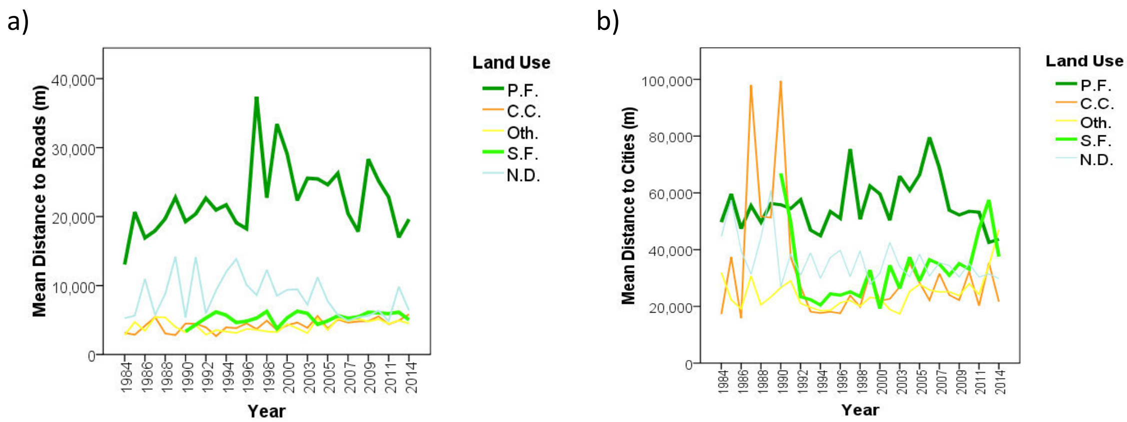

Figure 11. Mean distance in meters from the land cover types, Primary Forest (P.F.), Clear Cut (C.C.), Other (Oth.), Secondary Forest (S.F.), No Data (N.D.), in relation to a) Roads, and b) Cities

The MANOVA analysis shows that distance to roads and cities is statistically different for all the land cover types ($F < 0.05$). The results of the MANOVA are presented in the Appendix 8. The distribution of the land cover types according to the distance to roads and cities classification, in values and in percentages, is presented in Figure 12.

Figure 12.I. shows that roads are a stronger indicator for land use change dynamics than cities, because land use change is concentrated in the first 30 km from roads (Ia), while land use change is distributed in all the categories from the distance to cities (Ib).

Figure 12.II shows the different land use cover in percentage of the area correlated with the distance to roads and cities. For distances from roads greater than 30 km, more than 90% is primary forest. While, for cities, those categories farther than 30 km show more than 80% as primary forest.

Figure 12.III shows the percentage omitting the primary forest category, in order to only analyse land use change once the land is deforested. The results show that the percentage distribution of secondary forest remains constant at a 20 % of the total land use within a distance < 30 km of roads, while the next category (30-40 km) shows a 60% of the land use as secondary forest, increasing until 80% in those areas with a distance > 50 km. In the case of distance to roads, there is a similar effect of secondary forest remaining around 20% within 30 km from cities. However, the increase in secondary forest is not continuous, only increasing to 40% within 30 to 50 km, descending again for higher distances.

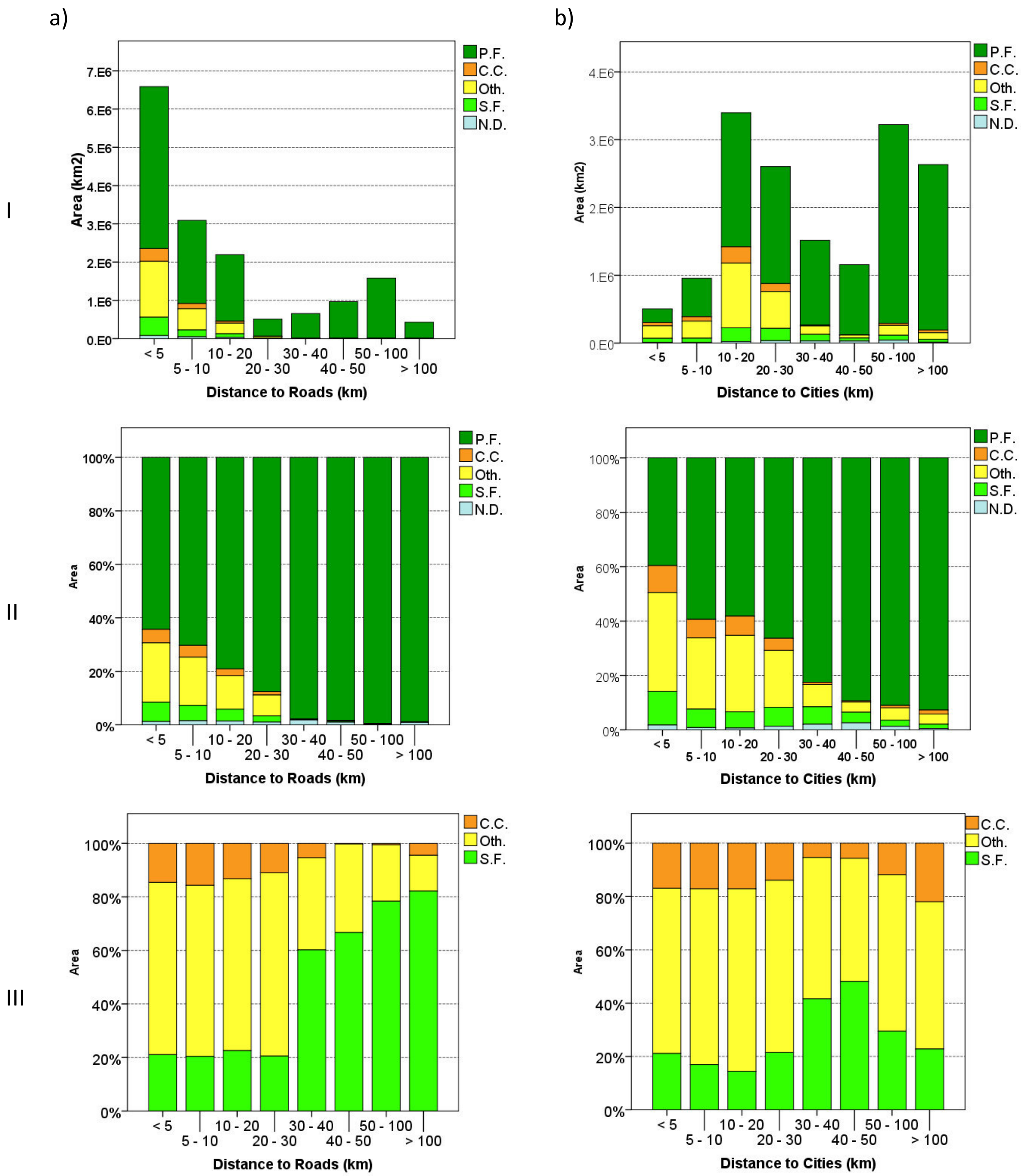

Figure 12. Different land use types, Primary Forest (P.F.), Clear Cut (C.C.), Other (Oth.), Secondary Forest (S.F.), No Data (N.D.), in relation to the distance classification to a) Roads, b) Cities. I. Total values in area (km^2), II. Total classification in percentage, III. Percentage excluding Primary Forest

I also considered important to analyse the weight of each of these categories, according to distance to roads and cities. In consequence, the total area of the different classes of land cover, in terms of percentage, is presented in Figure 13. Which shows that the classification according to roads is clearer for the categories of distance to roads (Figure 13a) than to cities (Figure 13b), as was previously pointed in Figure 12.I. A high percentage of the land use changes are in the first 5 km, and almost all of them are within the first 30 km to roads. In detailed values: Clear Cut (62.4% - <5km, 98.8% <30km), Other (62.6% - <5km, 98.2% <30 km) and Secondary Forest (61.8% < 5 km, 97.2% < 30km). In the case of distance to cities, more than 80% of Clear Cut and Other are situated within the first 30 km. However, these percentage is lower (65%) for Secondary Forest.

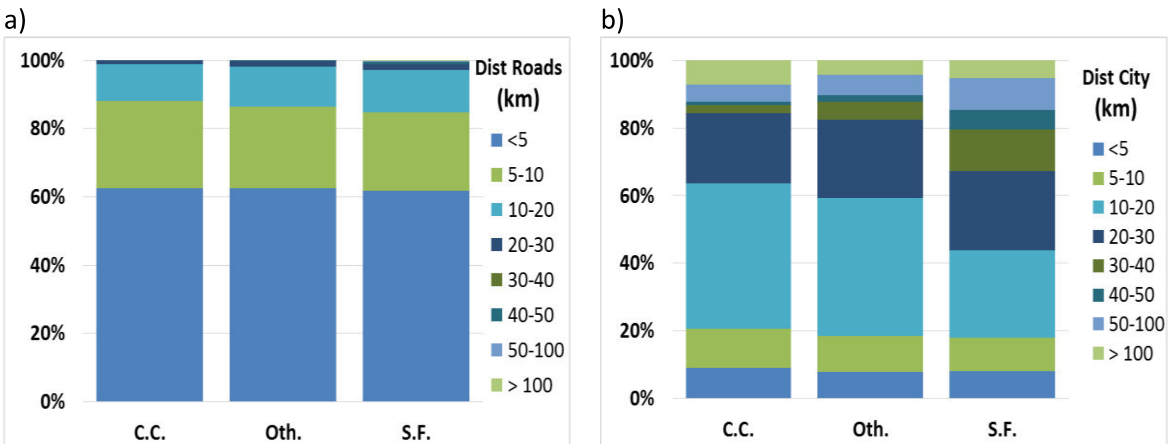

Figure 13. Percentage of different land cover classification of Clear Cut (C.C.), Other (Oth.), and Secondary Forest (S.F.), according to distance to a) Roads, and b) Cities

3.4. Road Density

The results of MANOVA and MANCOVA show a statistically difference between the Low and High Density plots for the time-series analysed. The complete statistical results and tables are present in the Appendix 9. Considering all the multivariate tests (Pillai's Trace, Wilks' Lambda, Hotelling's Trace, and Roy's Largest Root) show a significant statistically different ($p<0.05$) land use composition according to the density, I only present the Pillai's Trace value in Table 3, which is considered the most powerful and robust of the four tests (Carey 1998).

Table 3. Results of the Pillai's Trace multivariate test of the analysis MANOVA and MANCOVA according to road density

Effect (Year * Density)		Value	F	Hypothesis df	Error df	Sig. (p)
Pillai's Trace	MANOVA	0.399	1.274	150.000	2205.000	0.016
	MANCOVA (roads & cities as covariables)	0.577	1.896	150.000	2180.000	0.000

According to Table 3, in MANOVA there was a statistically significant difference in the land use classification between High and Low road density, $F(150 \pm 2.2) = 1.274$, $p < 0.05$ (0.016); Pillai's Trace = 0.399. Considering the covariables (MANCOVA), the land use classification between High and Low Density is also statistically different, $p < 0.05$.

Table 4 presents only the results of MANOVA. This shows that the different land cover types are statistically ($p<0.05$) different for High and Low Density, with the only exception of Other ($p=0.840$) and No Data ($p=0.783$). Primary Forest is the only land cover type that has higher mean in the Low Density Plot.

Table 4. MANOVA statistics for land cover type according to High and Low Density

Source	Dependent Variable	F	Sig. (p)	Road Density	Mean	Std. Error
Year * Density	Primary Forest	2.150	0.001	Low	399.440	4.642
				High	251.555	4.764
	Clear Cut	1.911	0.003	Low	0.050	1.692
				High	22.650	1.737
	Other	0.741	0.840	Low	0.462	3.282
				High	94.150	3.368
	Secondary Forest	2.750	0.000	Low	1.180	1.549
				High	28.558	1.590
	No Data	0.846	0.703	Low	1.856	0.417
				High	4.687	0.428

In Figure 14 I present the estimated mean area result from the MANOVA and MANCOVA analysis for Primary and Secondary Forest, considering these are the principal land-use changes analysed in this research. It can be seen that using the distances to roads and cities as covariables for the analysis improves the results of the graphs, especially the temporal decrease of Primary Forest in High Density plots. It must be noted that both primary and secondary forest remain almost constant during the analysed period for the Low Density plots.

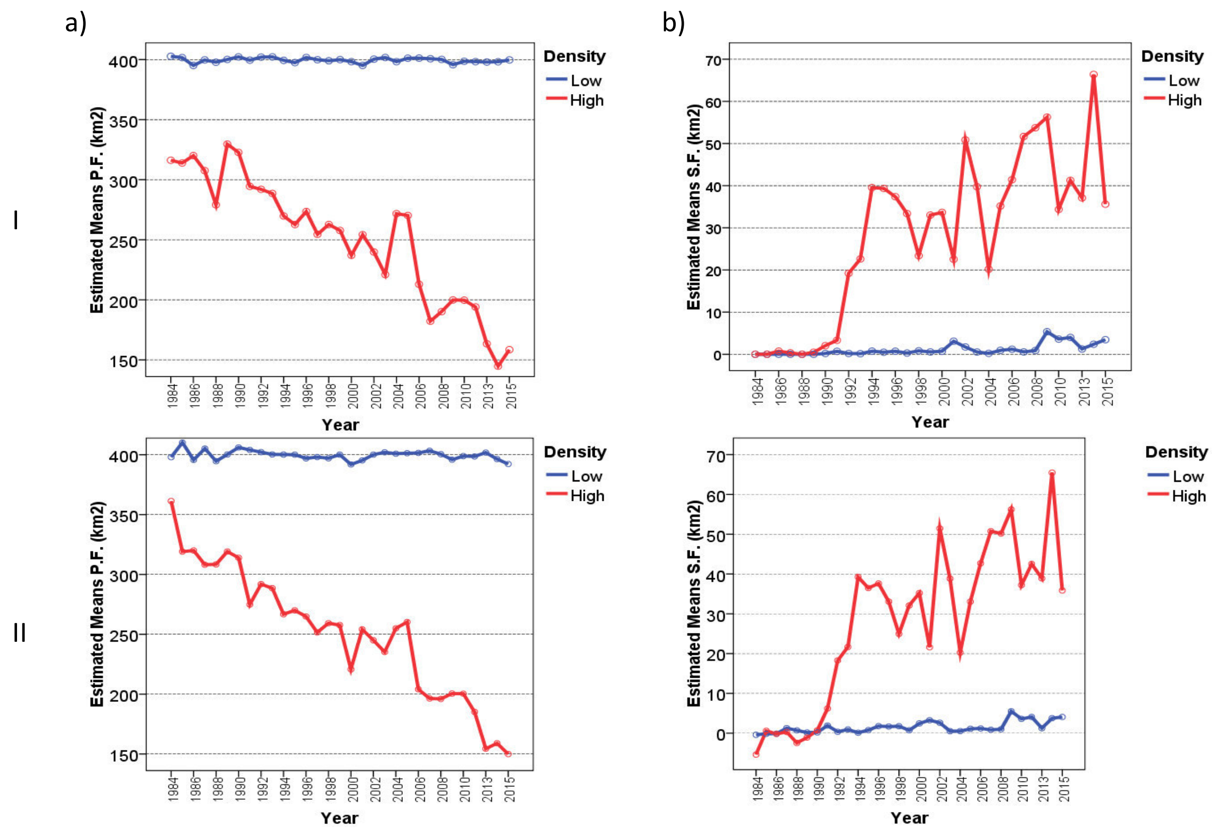

Figure 14. Estimated means according to Road Density of a) Primary Forest, and b) Secondary Forest. For I. MANOVA of the density analysis alone, II. MANCOVA including distance to roads and cities as covariables

The distribution of the land cover types according to the road density, in percentages, is presented in Figure 15.

Figure 15.I. shows that Low Density plots are principally composed by Primary Forests for all the time-series (Ia). For High Density the composition of Primary Forest reduces from 80 % in 1984 to 40% in 2015 (Ib).

Figure 15.II shows the percentage composition of the different land use types omitting the primary forest. For Low Density (IIa), even though the total percentage of land use affected (deforested) is lower in total terms, the percentage that becomes Secondary Forest is constantly higher than 20% reaching 80%. Secondary Forest area shows higher rates of regrowth even after being re-logged during all the time-series. Secondary Forest for High Density (IIb), shows a level of around 20%, and a slower rate of regrowth.

Figure 15.III shows the total percentage of land cover, again omitting Primary Forest, to better compare the dynamics of land use change. For Low Density a 69.4% of the total land cover is Secondary Forest, while for High Density it is only 19.6%.

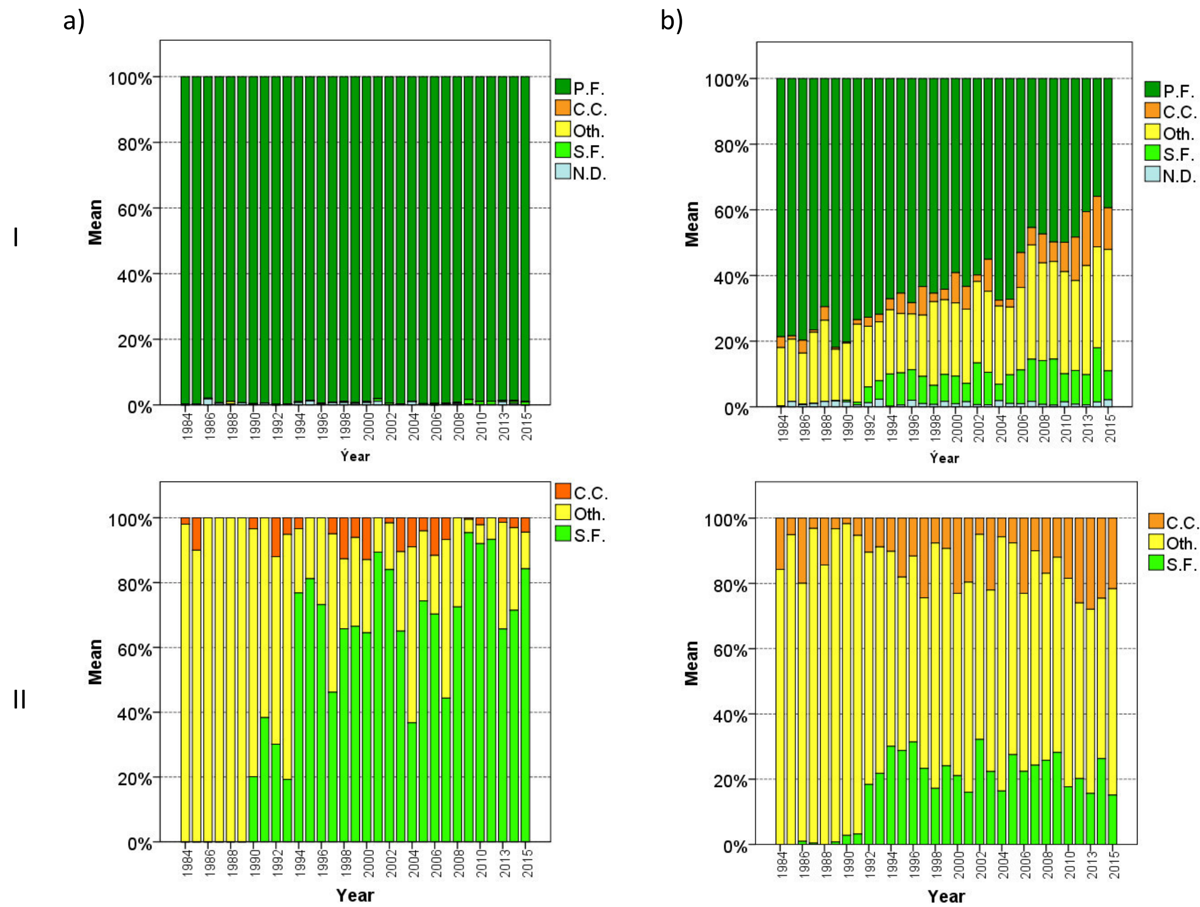

III

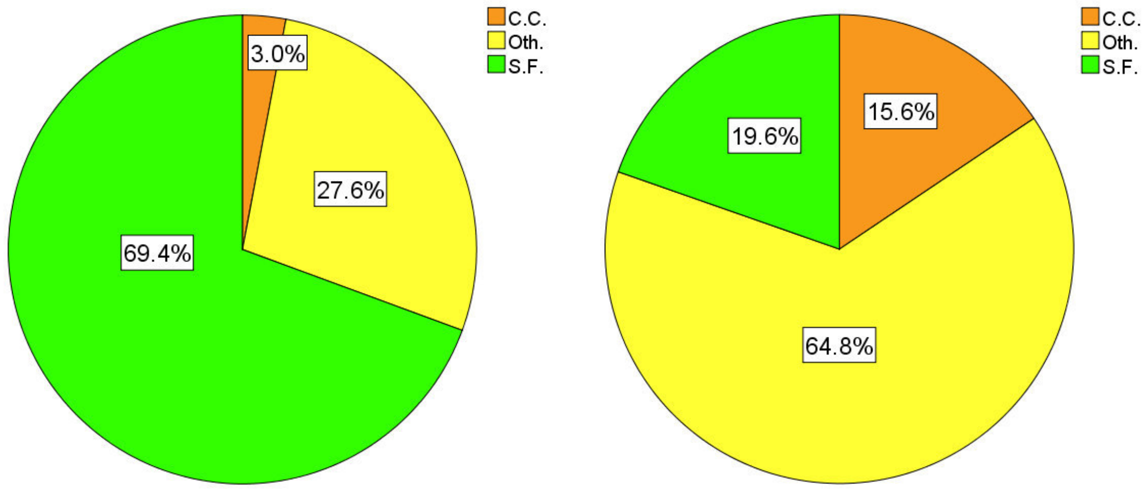

Figure 15. Different land use types, Primary Forest (P.F.), Clear Cut (C.C.), Other (Oth.), Secondary Forest (S.F.), No Data (N.D.), in relation to Road Density a) Low, b) High. I. Total values in area (in percentage), II. Classification of the time-series in percentage excluding P.F., III. Total percentage composition excluding P.F.

3.5. Road Pattern

The results of the MANOVA for the Road Pattern do not show a statistically difference between the Fishbone and Other plots for the time-series analysed. All the statistical results of P are higher than 0.05 (Appendix 10). Meaning that for the time-series none of the land use classes are significantly different based in their road pattern, even using roads and cities as covariables.

4. DISCUSSION

4.1. Distance to Roads and Cities

I found that secondary forest regrowth is influenced by distance to roads. My results show that primary forest is located further from roads (20 km) than secondary forest (<10 km), with an increasing trend getting further from the roads in recent years (Figure 11). More than 60% of secondary forest occurs within the first 5 km from a road, and more than 97% within 30 km from roads (Figure 12.I and Figure 14). Within this 30 km, the percentage of secondary forest keeps at a constant of 20% of the total affected (deforested) area. However, for areas located further than 30 km are three times more likely (60%) to develop secondary forest regrowth than one located within 30 km. In distances higher than 50 km this probability increases to even four times (80%) (Figure 12.III).

The percentage of secondary forest found in this research is coherent to Hirsch et al. (2004), which reported that 30 to 50% of the deforested area was covered by secondary forests, and Carreiras et al. (2014) that found values between 40 to 55% in separated studies of small regions of the Legal Amazon.

This influence of secondary forest regrowth to the proximity to the principal roads is coherent to the relation found between distance to roads and deforestation by earlier studies. (Alves 2002) reported 90% of deforestation within 100 km, (D. Nepstad et al. 2001) indicated that two thirds of deforestation occurred within 50 km to major paved highways. However, the threshold distance found in this research (30 km) is closer than that presented in these studies that used only principal roads and highway. This higher influence might be because the increase of deforestation levels in the last 15 years since these studies were elaborated. This is similar to what was found by (Asner et al. 2006), which was focused on selective logging, that found that nearly 80% of deforestation was within 5 km from roads, and the probability of clearing a secondary forest was two to four times higher than primary forest in the area within 5 to 25 km.

In the other hand, the more recent study of (Barber et al. 2014), which linked 95% of deforestation to the first 5.5 km from roads. However, this study digitalized a map roads present in the Amazon up to 2007, including small and unofficial roads. Therefore, I would expect that the relation between secondary forests to roads would be lower (closer) in case of using a more complete road network of the Amazon.

Also, it would be interesting to analyse a temporal model of the development of roads. This considering the construction of new roads since the seventies and the improvements realized to them, from unpaved small roads to highways. This considering that temporally, (Barber et al. 2014) used only the 2006 land cover and 2007 road maps to assess the relation of past deforestation with roads. Also that (D. Nepstad et al. 2001) found that deforestation of forests within 50 km of paved roads is of 29±58%, compared to 0±9% along the same distance of unpaved roads. Therefore, using a temporal map including the construction and changes to the roads related to the complete time-series of the Amazon land cover, would give a clearer vision of the land use and land cover change dynamics of the Amazon, being able to predict future behaviour.

Finding this clear correlation between secondary forest regrowth and distance to roads is a first step towards new studies. The distance of 30 km to principal roads as a threshold that could predict a three times higher probability of regrowth of secondary forests (Figure 12.III) could help stakeholders to put more resources to protect abandoned pastures and areas with initial successional vegetation situated further than this distance. It must be noted that previous studies that focused in secondary forests in the Amazon region (Carreiras et al. 2014; Soler, Escada, and Verburg 2009) do not take into account road presence.

Finally, indicate that distance to roads is a stronger indicator than distance to cities for the land use change dynamics. This because, mean distance from cities to primary forest is 50 km, and secondary forest is around 20 km. However, the land use changes are more distributed along the distance to cities, although secondary forest regrowth is double between 30 and 50 km than that within the first 30 km. Therefore, in case of counting with a more complete map of the road network analysing the relationship to distance with roads might not be as relevant. This might be because the primary determinant of the spatial distribution and land use change in the Amazon is access through roads and not urban settlement (Laurance et al. 2002; Soares-Filho et al. 2004).

4.2. Road Density

I found that secondary forest regrowth is influenced by road density. My results show that high density plots have lower percentage of primary forest, with a steady decrease during the time-series, and secondary forest show an increase in the time-series, peaking since 1992. Low density plots have higher percentage of primary forest, with a composition that remains stable during the time-series, while secondary forest remains low. (Figure 14). This is because low density plots also have lower deforestation rates, therefore secondary forest is higher (in general terms) in high density plots only because these are the ones more affected for land use changes.

Nevertheless, the area affected by deforestation in low density plots was three to four times more likely to develop secondary forest regrowth than one located in high road density plots. Even though it shows some increases in the time series (regrowth), the percentage of secondary forest in high road density remains relatively constant about 20%, while it is around 70% for low density (Figure 15.II and Figure 15.III). This ratio (3.5:1) between secondary forest in Low Density compared with High Density is similar to the one found for distance to roads in this same research. This is a ratio of 3:1 of secondary forests for distances further than 30 km from roads, and 4:1 for distances further than 50 km (Figure 12.III). This might be related to the fact that mean distance to roads from Low Density Plots is 54.8 km (Figure 10). However, the ratio of secondary forest is slightly higher for density than distance, suggesting that road density is a factor more important.

These results are similar to those of (Forman et al. 2003), who indicates that higher road density increases fragmentation and edge-effects of forests. Therefore, a higher road density would negatively affect secondary forest regrowth. Also, the higher percentage of secondary forest regrowth in Low Road Density might be a consequence to their proximity to Primary Forests. Proximity to primary forests is mentioned as a source of seeds and nutrients for vegetation succession (Davidson and Martinelli 2009; Myster 2008; Vasconcelos et al. 2012). However, it must be noted that there are no specific studies that analyse the direct influence of road density to secondary forests in the Amazon.

However, it has to be mentioned that, by the sampling design of my research, I only selected plots with low (near to zero) road densities according to the 2015 data of Google Earth (Figure 3). Therefore, the levels of anthropogenic disturbance in the area since 1984 are minimal and therefore the land use change analysed in these plots is limited.

It would be interesting to use different categories of road density for future studies. This analysis can be done with a complete road network to properly calculate road density in length per square kilometre. This measure will allow to further knowledge of the dynamics of land cover change in the Amazon.

4.3. Road Pattern

I found that secondary forest regrowth is not influenced by spatial configuration of roads (road pattern). My results show that Fishbone and Other Pattern have not a statistically different land use classification for the Amazon.

This result might be a consequence of the selection of the plots, existing the probability that the plots were not significantly different in their spatial configuration along the time-series. This considering the plots were chosen based only in their final road configuration (in 2015), and during the time-series analysis I saw different development stages in the spatial configuration of the roads. This factor (development along time) should be taken into consideration for future studies. Also, the category “other pattern” aggregates several types of configuration: dendritic, rectangular, and radial, thus it is harder to make a clear categorization to analyse the difference between them.

Another reason that might have influenced these results are the processes behind the land cover dynamics. It is indicated that fishbone pattern increases rainfall thus promoting the regeneration of the forest (Garcia-Carreras and Parker 2011; Roy 2009), while dendritic or radial patterns result in less fragmentation of the forests (Soler, Escada, and Verburg 2009), which can also help with the dispersion of seeds. Therefore, both processes might help the secondary forest regrowth via positive feedback processes.

4.4. Accuracy Assessment

Previous studies carried out in the Amazon have already acknowledged some issues in discriminating Secondary from Primary Forest (Carreiras et al. 2014; Caviglia-Harris et al. 2014; Neeff et al. 2006). This issue in differentiating primary and secondary forest was noticeable in the later years of the time-series, where the secondary forest were older. In these cases I had to try several training points before having a successful classification. However, the general accuracy of the time-series classification was of 85±8%. This level of quality is good, considering it is very difficult to exceed 85% of accuracy using only Landsat images (Gallego 2004).

Even though Gallego (2004) indicates that methods that do not use ground field measurements are deemed insufficient for the needs of national administrations. (Lu et al. 2012) consider maximum likelihood classification using training locations a good method of classification for remote sensing data. For future analysis it should be considered complement the results of this research using ground field measurements or Very High Resolution images for the accuracy assessment.

5. CONCLUSIONS

Land cover change should be understood as a dynamic process not a simple change from primary forest to secondary forest, because by definition secondary forest regrowth grows in an area that was previously affected by anthropogenic activities. Thus any analysis should also include the process of deforestation (clear cut areas) and agricultural or rural areas (other land uses). In this sense, it is undeniable that the presence of roads affect the land use and land cover change dynamics of the Amazon. During this research I analysed the influence that roads have, in terms of distance, road density (High and Low), and road pattern (Fishbone and Other), to land use classification, that included both primary and secondary forest. This using 40 study plots distributed in the Legal Amazon during a 32 year period.

The results of this research show that if a primary forest is closer to roads and has a higher road density, that area is more susceptible to be deforested and consequently suffer a land use change, while road pattern does not show a significant effect. Considering the land use dynamics of the Amazon, a percentage of this area will be abandoned after its period of productivity has ended and consequently will develop a secondary forest regrowth, which is highly susceptible to be re-deforested in the future.

However, the key findings of my research are that if the area affected by deforestation and land use change is further than 30 km from the principal roads it has at three times more probability to remain as a secondary forest, in terms of percentage of area. If this distance to further than 50 km the probability increases to a 4:1 ratio. The same is applicable to road density, where I found that in Low Density plots, areas affected by land use change have three to four times more percentage of secondary forest than those of High Density plots. Meanwhile, areas within 30 km from a road and with high density plots remained with a relatively constant 20% of secondary forests coverage.

Considering the scope of this research and that the level of accuracy reached with the method of image classification (85±8%), these results can provide a guideline for the government and stakeholders. These results indicate that, for conservation efforts to promote the regrowth of secondary forest to reach a mature state, areas with low road density located further than 30 km from roads should be prioritized. Also, development of new road construction projects should not be considered in these areas.

The results of this research also provide the opportunity for further research in the topic, which can be validated at a bigger scale (for example the whole Brazilian Amazon), it would be interesting to very high resolution (VHR) imagery, and in situ assessment of secondary forest to have a higher level of accuracy.

Acknowledgements

I would like to thank my supervisors Dr. Maria João Ferreira Dos Santos and Dr. Karin Rebel for all the collaboration, continuous support and feedback they gave me during this research. Thanks for making me see the bigger picture and not get lost in the details.

To Dr. William Laurance, Dr. Barber without whose previous research this project would have never been possible. Thanks for always answering my emails and give me valuable information.

To the United States Geographical Services and Open Street Maps, my total support for these organizations that offer free and accessible availability of data for the scientific community. This research would not be possible without these satellite images and maps of road network and cities.

To my family and friends who supported me no matter the distance and to Geert who always was there for me. Thanks for everything.

REFERENCES

Acevedo L, Miguel F. 1981. “On Horn’s Markovian Model of Forest Dynamics with Particular Reference to Tropical Forests.” *Theoretical Population Biology* 19 (2): 230–50. doi:10.1016/0040-5809(81)90019-8.

Ahmad, Asmala. 2012. “Analysis of Maximum Likelihood Classification on Multispectral Data.” *Applied Mathematical Sciences* 6 (129): 6425–36.

Alves, D. S. 2002. “Space-Time Dynamics of Deforestation in Brazilian Amazônia.” *International Journal of Remote Sensing* 23 (14): 2903–8. doi:10.1080/01431160110096791.

Asner, Gregory P., Eben N. Broadbent, Paulo J. C. Oliveira, Michael Keller, David E. Knapp, and José N. M. Silva. 2006. “Condition and Fate of Logged Forests in the Brazilian Amazon.” *Proceedings of the National Academy of Sciences* 103 (34): 12947–50. doi:10.1073/pnas.0604093103.

Baldi, Germán, and José M. Paruelo. 2008. “Land-Use and Land Cover Dynamics in South American Temperate Grasslands.” *Ecology and Society* 13 (2): 6.

Barber, Christopher P., Mark A. Cochrane, Carlos M. Souza, and William F. Laurance. 2014. “Roads, Deforestation, and the Mitigating Effect of Protected Areas in the Amazon.” *Biological Conservation* 177 (September): 203–9. doi:10.1016/j.biocon.2014.07.004.

Brandão, A. O., and C. M. Souza. 2006. “Mapping Unofficial Roads with Landsat Images: A New Tool to Improve the Monitoring of the Brazilian Amazon Rainforest.” *International Journal of Remote Sensing* 27 (1): 177–89. doi:10.1080/01431160500353841.

Brienen, R. J. W., O. L. Phillips, T. R. Feldpausch, E. Gloor, T. R. Baker, J. Lloyd, G. Lopez-Gonzalez, et al. 2015. “Long-Term Decline of the Amazon Carbon Sink.” *Nature* 519 (7543): 344–48. doi:10.1038/nature14283.

Butler, Rhett A. 2014. “Calculating Deforestation in the Amazon. Sourced from INPE and FAO Figures.” *Mongabay.com*. http://rainforests.mongabay.com/amazon/deforestation_calculations.html.

Carey, Gregory. 1998. “Multivariate Statistics: MANOVA Handouts.” *University of Colorado*. http://psych.colorado.edu/~carey/Courses/PSYC7291/index.html.

Carreiras, João M. B., Joshua Jones, Richard M. Lucas, and Cristina Gabriel. 2014. “Land Use and Land Cover Change Dynamics across the Brazilian Amazon: Insights from Extensive Time-Series Analysis of Remote Sensing Data.” *PLoS ONE* 9 (8): e104144. doi:10.1371/journal.pone.0104144.

Caviglia-Harris, Jill L., Michael Toomey, Daniel W. Harris, Katrina Mullan, Andrew Reid Bell, Erin O. Sills, and Dar A. Roberts. 2014. “Detecting and Interpreting Secondary Forest on an Old Amazonian Frontier.” *Journal of Land Use Science* 0 (0): 1–24. doi:10.1080/1747423X.2014.940614.

Chazdon, Robin L. 2003. “Tropical Forest Recovery: Legacies of Human Impact and Natural Disturbances.” *Perspectives in Plant Ecology, Evolution and Systematics* 6 (1–2): 51–71. doi:10.1078/1433-8319-00042.

CIESIN, and ITOS. 2013. “Global Roads Open Access Data Set (gROADS), v1: Global Roads | SEDAC. Center for International Earth Science Information Network (CIESIN) - Columbia University and Information Technology Outreach Services (ITOS) - University of Georgia.” http://sedac.ciesin.columbia.edu/data/set/groads-global-roads-open-access-v1/metadata.

Cochrane, Mark A., and William F. Laurance. 2002. “Fire as a Large-Scale Edge Effect in Amazonian Forests.” *Journal of Tropical Ecology* 18 (3): 311–25.

Colson, Filip, Jan Bogaert, Arnaldo Carneiro Filho, Bruce Nelson, Ekena Rangel Pinagé, and Reinhart Ceulemans. 2009. “The Influence of Forest Definition on Landscape Fragmentation Assessment in Rondônia, Brazil.” *Ecological Indicators* 9 (6): 1163–68. doi:10.1016/j.ecolind.2009.02.001.

Congalton, Russell G. 1991. “A Review of Assessing the Accuracy of Classifications of Remotely Sensed Data.” *Remote Sensing of Environment* 37 (1): 35–46. doi:10.1016/0034-4257(91)90048-B.

Congalton, Russell G., and R. A. Mead. 1983. “A Quantitative Method to Test for Consistency and Correctness in Photointerpretation.” *Photogrammetric Engineering & Remote Sensing* 49 (1): 69–74.

Davidson, Eric A., and Luiz A. Martinelli. 2009. “Nutrient Limitations to Secondary Forest Regrowth.” In *Amazonia and Global Change*, edited by Michael Keller, Michael Bustamante, John Gash, and Pedro Silva Dias, 299–309. American Geophysical Union. http://onlinelibrary.wiley.com.proxy.library.uu.nl/doi/10.1029/2009GM000905/summary.

Diniz, F.H., K. Kok, M.C. Hott, M.A. Hoogstra-Klein, and B. Arts. 2013. “From Space and from the Ground: Determining Forest Dynamics in Settlement Projects in the Brazilian Amazon.” *International Forestry Review* 15 (4): 442–55. doi:10.1505/146554813809025658.

Epps, Clinton W., Per J. Palsbøll, John D. Wehausen, George K. Roderick, Rob R. Ramey, and Dale R. McCullough. 2005. “Highways Block Gene Flow and Cause a Rapid Decline in Genetic Diversity of Desert Bighorn Sheep.” *Ecology Letters* 8 (10): 1029–38. doi:10.1111/j.1461-0248.2005.00804.x.

ESRI. 2014. *ArcGIS v10* (version 10.x). Environmental Systems Research Institute Inc. http://desktop.arcgis.com/en/.

———. 2015. “Help ArcGIS Desktop.” http://help.arcgis.com/en/arcgisdesktop/10.0/help/index.html#//00nv00000002000000.htm.

Ewers, Robert M., and William F. Laurance. 2006. “Scale-Dependent Patterns of Deforestation in the Brazilian Amazon.” *Environmental Conservation* null (03): 203–11. doi:10.1017/S0376892906003250.

Fearnside, Philip M. 1999. “Biodiversity as an Environmental Service in Brazil’s Amazonian Forests: Risks, Value and Conservation.” *Environmental Conservation* null (04): 305–21. doi:null.

———. 2005. “Deforestation in Brazilian Amazonia: History, Rates, and Consequences.” *Conservation Biology* 19 (3): 680–88.

———. 2008. “Will Urbanization Cause Deforested Areas to Be Abandoned in Brazilian Amazonia?” *Environmental Conservation* 35 (03): 197–99. doi:10.1017/S0376892908004906.

Federative Republic of Brazil. 1966. *Law N 5.173*.

Feldpausch, Ted R., Marco A. Rondon, Erick CM Fernandes, Susan J. Riha, and Elisa Wandelli. 2004. “Carbon and Nutrient Accumulation in Secondary Forests Regenerating on Pastures in Central Amazonia.” *Ecological Applications* 14 (sp4): 164–76.

Feldpausch, T. R., J. Lloyd, S. L. Lewis, R. J. W. Brienen, M. Gloor, A. Monteagudo Mendoza, G. Lopez-Gonzalez, et al. 2012. “Tree Height Integrated into Pantropical Forest Biomass Estimates.” *Biogeosciences* 9 (8): 3381–3403. doi:10.5194/bg-9-3381-2012.

Filho, Francisco José Barbosa Oliveira de, and Jean Paul Metzger. 2006. “Thresholds in Landscape Structure for Three Common Deforestation Patterns in the Brazilian Amazon.” *Landscape Ecology* 21 (7): 1061–73. doi:10.1007/s10980-006-6913-0.

Forman, Richard T. T., and Lauren E. Alexander. 1998. “Roads and Their Major Ecological Effects.” *Annual Review of Ecology and Systematics* 29 (1): 207–31. doi:10.1146/annurev.ecolsys.29.1.207.

Forman, Richard T. T., Daniel Sperling, John A. Bissonette, Anthony P. Clevenger, Carol D. Cutshall, Virginia H. Dale, Lenore Fahrig, et al. 2003. *Road Ecology: Science and Solutions*. 2nd edition. Washington, DC: Island Press.

Fox, J. E. D. 1976. “Constraints on the Natural Regeneration of Tropical Moist Forest.” *Forest Ecology and Management* 1: 37–65. doi:10.1016/0378-1127(76)90006-2.

Gallego, F. J. 2004. “Remote Sensing and Land Cover Area Estimation.” *International Journal of Remote Sensing* 25 (15): 3019–47. doi:10.1080/01431160310001619607.

Garcia-Carreras, L., and D. J. Parker. 2011. “How Does Local Tropical Deforestation Affect Rainfall?” *Geophysical Research Letters* 38 (19): L19802. doi:10.1029/2011GL049099.

Gelbard, Jonathan L., and Jayne Belnap. 2003. “Roads as Conduits for Exotic Plant Invasions in a Semiarid Landscape.” *Conservation Biology* 17 (2): 420–32. doi:10.1046/j.1523-1739.2003.01408.x.

Google. 2015. “Google Earth.” https://www.google.com/earth/explore/products/.

Groeneveld, J., L. F. Alves, L. C. Bernacci, E. L. M. Catharino, C. Knogge, J. P. Metzger, S. Pütz, and A. Huth. 2009. “The Impact of Fragmentation and Density Regulation on Forest Succession in the Atlantic Rain Forest.” *Ecological Modelling* 220 (19): 2450–59. doi:10.1016/j.ecolmodel.2009.06.015.

Haddad, N. M., L. A. Brudvig, J. Clobert, K. F. Davies, A. Gonzalez, R. D. Holt, T. E. Lovejoy, et al. 2015. “Habitat Fragmentation and Its Lasting Impact on Earth’s Ecosystems.” *Science Advances* 1 (2): e1500052–e1500052. doi:10.1126/sciadv.1500052.

Hirsch, Adam I., William S. Little, Richard A. Houghton, Neal A. Scott, and Joseph D. White. 2004. “The Net Carbon Flux due to Deforestation and Forest Re-Growth in the Brazilian Amazon: Analysis Using a Process-Based Model.” *Global Change Biology* 10 (5): 908–24. doi:10.1111/j.1529-8817.2003.00765.x.

Houghton, R. A., D. L. Skole, Carlos A. Nobre, J. L. Hackler, K. T. Lawrence, and W. H. Chomentowski. 2000. “Annual Fluxes of Carbon from Deforestation and Regrowth in the Brazilian Amazon.” *Nature* 403 (6767): 301–4. doi:10.1038/35002062.

Huete, Alfredo R., Kamel Didan, Yosio E. Shimabukuro, Piyachat Ratana, Scott R. Saleska, Lucy R. Hutyra, Wenze Yang, Ramakrishna R. Nemani, and Ranga Myneni. 2006. “Amazon Rainforests Green-up with Sunlight in Dry Season.” *Geophysical Research Letters* 33 (6): L06405. doi:10.1029/2005GL025583.

IBGE. 2015a. “IBGE :: Instituto Brasileiro de Geografia E Estatística.” http://www.ibge.gov.br/home/.

———. 2015b. “IBGE :: Instituto Brasileiro de Geografia E Estatística. Legal Amazon.” http://www.ibge.gov.br/english/geociencias/geografia/amazonialegal.shtm?c=2.

INPE. 2015. “INPE - National Institute For Space Research.” http://www.inpe.br/ingles/.

Jaeger, Jochen A. G. 2000. “Landscape Division, Splitting Index, and Effective Mesh Size: New Measures of Landscape Fragmentation.” *Landscape Ecology* 15 (2): 115–30. doi:10.1023/A:1008129329289.

———. 2007. “Effects of the Configuration of Road Networks on Landscape Connectivity.” *Road Ecology Center*, May. http://escholarship.org/uc/item/10d5q9nj.

Jaeger, Jochen A. G., Jeff Bowman, Julie Brennan, Lenore Fahrig, Dan Bert, Julie Bouchard, Neil Charbonneau, Karin Frank, Bernd Gruber, and Katharina Tluk von Toschanowitz. 2005. “Predicting When Animal Populations Are at Risk from Roads: An Interactive Model of Road Avoidance Behavior.” *Ecological Modelling* 185 (2–4): 329–48. doi:10.1016/j.ecolmodel.2004.12.015.

Laurance, William F. 2000. “Mega-Development Trends in the Amazon: Implications for Global Change.” *Environmental Monitoring and Assessment* 61 (1): 113–22. doi:10.1023/A:1006374320085.

Laurance, William F., Ana K. M. Albernaz, Götz Schroth, Philip M. Fearnside, Scott Bergen, Eduardo M. Venticinque, and Carlos Da Costa. 2002. “Predictors of Deforestation in the Brazilian Amazon.” *Journal of Biogeography* 29 (5-6): 737–48. doi:10.1046/j.1365-2699.2002.00721.x.

Laurance, William F., and Andrew Balmford. 2013. “Land Use: A Global Map for Road Building.” *Nature* 495 (7441): 308–9.

Laurance, William F., José L. C. Camargo, Regina C. C. Luizão, Susan G. Laurance, Stuart L. Pimm, Emilio M. Bruna, Philip C. Stouffer, et al. 2011. “The Fate of Amazonian Forest Fragments: A 32-Year Investigation.” *Biological Conservation* 144 (1): 56–67. doi:10.1016/j.biocon.2010.09.021.

Laurance, William F., Mark A. Cochrane, Scott Bergen, Philip M. Fearnside, Patricia Delamônica, Christopher Barber, Sammya D’Angelo, and Tito Fernandes. 2001. “The Future of the Brazilian Amazon.” *Science* 291 (5503): 438–39. doi:10.1126/science.291.5503.438.

Laurance, William F., Miriam Goosem, and Susan G.W. Laurance. 2009. “Impacts of Roads and Linear Clearings on Tropical Forests.” *Trends in Ecology & Evolution* 24 (12): 659–69. doi:10.1016/j.tree.2009.06.009.

Laurance, William F., Susan G. Laurance, Leandro V. Ferreira, Judy M. Rankin-de Merona, Claude Gascon, and Thomas E. Lovejoy. 1997. “Biomass Collapse in Amazonian Forest Fragments.” *Science* 278 (5340): 1117–18. doi:10.1126/science.278.5340.1117.

Lindenmayer, David B., and Joern Fischer. 2006. *Habitat Fragmentation and Landscape Change: An Ecological and Conservation Synthesis*. Island Press.

Lu, Dengsheng, Mateus Batistella, Guiying Li, Emilio Moran, Scott Hetrick, Corina da Costa Freitas, Luciano Vieira Dutra, and Sidnei João Siqueira Sant’Anna. 2012. “Land Use/cover Classification in the Brazilian Amazon Using Satellite Images.” *Pesquisa Agropecuária Brasileira* 47 (9): 1185–1208. doi:10.1590/S0100-204X2012000900004.

Luizão, Flávio J., Philip M. Fearnside, Carlos E. P. Cerri, and Johannes Lehmann. 2009. “The Maintenance of Soil Fertility in Amazonian Managed Systems.” In *Amazonia and Global Change*, edited by Michael Keller, Michael Bustamante, John Gash, and Pedro Silva Dias, 311–36. American Geophysical Union. http://onlinelibrary.wiley.com.proxy.library.uu.nl/doi/10.1029/2008GM000732/summary.

Martins, G., C. von Randow, G. Sampaio, and A. J. Dolman. 2015. “Precipitation in the Amazon and Its Relationship with Moisture Transport and Tropical Pacific and Atlantic SST from the CMIP5 Simulation.” *Hydrol. Earth Syst. Sci. Discuss.* 12 (1): 671–704. doi:10.5194/hessd-12-671-2015.

Moser, Brigitte, Jochen A. G. Jaeger, Ulrike Tappeiner, Erich Tasser, and Beatrice Eiselt. 2007. “Modification of the Effective Mesh Size for Measuring Landscape Fragmentation to Solve the Boundary Problem.” *Landscape Ecology* 22 (3): 447–59. doi:10.1007/s10980-006-9023-0.

Myster, Randall W. 2008. “Neotropic Post-Dispersal Seed Predation.” In *Post-Agricultural Succession in the Neotropics*, 216–20. Springer New York. http://link.springer.com.proxy.library.uu.nl/chapter/10.1007/978-0-387-33642-8_9.

NASA Official. 2015. “Technical Details « Landsat Science.” http://landsat.gsfc.nasa.gov/?page_id=2290.

Neeff, Till, Richard M. Lucas, João Roberto dos Santos, Eduardo S. Brondizio, and Corina C. Freitas. 2006. “Area and Age of Secondary Forests in Brazilian Amazonia 1978–2002: An Empirical Estimate.” *Ecosystems* 9 (4): 609–23. doi:10.1007/s10021-006-0001-9.

Nepstad, Daniel, Georgia Carvalho, Ana Cristina Barros, Ane Alencar, João Paulo Capobianco, Josh Bishop, Paulo Moutinho, Paul Lefebvre, Urbano Lopes Silva Jr., and Elaine Prins. 2001. “Road Paving, Fire Regime Feedbacks, and the Future of Amazon Forests.” *Forest Ecology and Management*, New Directions in Tropical Forest Research, 154 (3): 395–407. doi:10.1016/S0378-1127(01)00511-4.

Nepstad, Daniel C., Adalberto Verssimo, Ane Alencar, Carlos Nobre, Eirivelthon Lima, Paul Lefebvre, Peter Schlesinger, et al. 1999. “Large-Scale Impoverishment of Amazonian Forests by Logging and Fire.” *Nature* 398 (6727): 505–8. doi:10.1038/19066.

OpenStreetMap. 2015. “OpenStreetMap.” https://www.openstreetmap.org/#map=11/-23.1782/-53.7156.

Peres, Carlos A. 2001. “Synergistic Effects of Subsistence Hunting and Habitat Fragmentation on Amazonian Forest Vertebrates.” *Conservation Biology* 15 (6): 1490–1505. doi:10.1046/j.1523-1739.2001.01089.x.

Perz, Stephen G, and David L Skole. 2003a. “Social Determinants of Secondary Forests in the Brazilian Amazon.” *Social Science Research* 32 (1): 25–60. doi:10.1016/S0049-089X(02)00012-1.

Perz, Stephen G., and David L Skole. 2003b. “Secondary Forest Expansion in the Brazilian Amazon and the Refinement of Forest Transition Theory.” *Society & Natural Resources* 16 (4): 277–94. doi:10.1080/08941920390178856.

Rebel, K. T., S. J. Riha, M. A. Rondon, T. R. Feldpausch, and E. C. Fernandes. 2001. “Spatial Simulation of the Dynamics of Establishment of Secondary Forest in Abandoned Pasture in the Central Amazon.” *AGU Spring Meeting Abstracts*. http://adsabs.harvard.edu/abs/2001AGUSM...B32A22R.

Rencher, Alvin C. 2012. *Methods of Multivariate Analysis*. 3 edition. Hoboken, New Jersey: Wiley.

Roy, Somnath Baidya. 2009. “Mesoscale Vegetation-Atmosphere Feedbacks in Amazonia.” *Journal of Geophysical Research: Atmospheres* 114 (D20): D20111. doi:10.1029/2009JD012001.

Santos, João R., Camila V. d. J. Silva, Lênio S. Galvão, Robert Treuhaft, José C. Mura, Soren Madsen, Fábio G. Gonçalves, and Michael M. Keller. 2014. “Determining Aboveground Biomass of the Forest Successional Chronosequence in a Test-Site of Brazilian Amazon through X- and L-Band Data Analysis.” In *Proc. SPIE 9229, Second International Conference on Remote Sensing and*

Geoinformation of the Environment (RSCy2014), 9229:92291E – 92291E – 10. doi:10.1117/12.2066031.

Soares-Filho, Britaldo, Ane Alencar, Daniel Nepstad, Gustavo Cerqueira, Maria del Carmen Vera Diaz, Sérgio Rivero, Luis Solórzano, and Eliane Voll. 2004. “Simulating the Response of Land-Cover Changes to Road Paving and Governance along a Major Amazon Highway: The Santarém–Cuiabá Corridor.” *Global Change Biology* 10 (5): 745–64. doi:10.1111/j.1529-8817.2003.00769.x.

Soler, Luciana de Souza, Maria Isabel S. Escada, and Peter H. Verburg. 2009. “Quantifying Deforestation and Secondary Forest Determinants for Different Spatial Extents in an Amazonian Colonization Frontier (Rondonia).” *Applied Geography* 29 (2): 182–93. doi:10.1016/j.apgeog.2008.09.005.

SPSS Inc. 2008. *SPSS v.17* (version 17). Windows. http://www-01.ibm.com/software/analytics/spss.

Stehman, Stephen V. 1996. “Estimating the Kappa Coefficient and Its Variance under Stratified Random Sampling.” *Photogrammetric Engineering & Remote Sensing* 62 (4): 401–2.

Strahler, Alan H. 1980. “The Use of Prior Probabilities in Maximum Likelihood Classification of Remotely Sensed Data.” *Remote Sensing of Environment* 10 (2): 135–63. doi:10.1016/0034-4257(80)90011-5.

USGS. 2013. “SLC-off Products: Background.” http://landsat.usgs.gov/products_slcoffbackground.php.

———. 2014a. “Landsat FAQ.” http://landsat.usgs.gov/band_designations_landsat_satellites.php.

———. 2014b. “What Are the Band Designations for the Landsat Satellites?. Http://landsat.usgs.gov/band_designations_landsat_satellites.php.” http://landsat.usgs.gov/band_designations_landsat_satellites.php.

———. 2015a. “EarthExplorer.” *Earth Explorer USGS*. http://earthexplorer.usgs.gov/.

———. 2015b. “Product Guide. Landsat Climate Data Record (CDR) Surface Reflectance.” http://landsat.usgs.gov/documents/cdr_sr_product_guide.pdf.

Vasconcelos, Steel Silva, Daniel Jacob Zarin, Maristela Machado Araújo, and Izildinha de Souza Miranda. 2012. “Aboveground Net Primary Productivity in Tropical Forest Regrowth Increases Following Wetter Dry-Seasons.” *Forest Ecology and Management* 276 (July): 82–87. doi:10.1016/j.foreco.2012.03.034.

Vieira, Ima Célia G, Arlete Silva de Almeida, Eric A Davidson, Thomas A Stone, Cláudio J Reis de Carvalho, and José Benito Guerrero. 2003. “Classifying Successional Forests Using Landsat Spectral Properties and Ecological Characteristics in Eastern Amazônia.” *Remote Sensing of Environment*, Large Scale Biosphere Atmosphere Experiment in Amazonia, 87 (4): 470–81. doi:10.1016/j.rse.2002.09.002.

Wright, S. Joseph, and Helene C. Muller-Landau. 2006. “The Future of Tropical Forest Species1.” *Biotropica* 38 (3): 287–301. doi:10.1111/j.1744-7429.2006.00154.x.

WWF. 2015. “Amazon | Places | World Wildlife Fund.” http://www.worldwildlife.org/places/amazon.

Yoshikawa, S., and K. Sanga-Ngoie. 2011. “Deforestation Dynamics in Mato Grosso in the Southern Brazilian Amazon Using GIS and NOAA/AVHRR Data.” *International Journal of Remote Sensing* 32 (2): 523–44. doi:10.1080/01431160903475225.

APPENDICES

Table of Appendices

Appendix 1. Coordinates of the Study Plots

N	Parameter	Category	Province	Code	Latitude	Longitud
1	Density	Low	Amazon	LD1	1°51'15.23"S	58°58'6.00"W
					2° 2'10.00"S	58°47'19.00"W
2	Density	Low	Amazon	LD2	7°19'48.22"S	61°29'28.59"W
					7° 9'0.84"S	61°18'40.60"W
3	Density	Low	Pará	LD3	4°55'53.70"S	55°30'15.33"W
					4°45'2.80"S	55°19'23.36"W
4	Density	Low	Pará	LD4	5° 4'24.35"S	54°22'33.80"W
					4°53'39.47"S	54°11'49.52"W
5	Density	Low	Amazon	LD5	8°16'14.39"S	66° 8'5.13"W
					8° 5'24.44"S	65°57'9.94"W
6	Density	Low	Rondônia	LD6	10°36'44.60"S	64°58'11.49"W
					10°25'48.21"S	64°47'14.28"W
7	Density	Low	Amazon	LD7	2°34'36.47"S	58°57'10.51"W
					2°23'50.10"S	58°46'24.79"W
8	Density	Low	Pará	LD8	0°51'2.75"S	55°54'12.64"W
					0°40'12.04"S	55°43'23.40"W
9	Density	Low	Pará	LD9	6°52'27.31"S	54°38'38.78"W
					6°41'32.33"S	54°27'48.54"W
10	Density	Low	Pará	LD10	0°16'44.00"S	57°53'5.00"W
					0°27'38.00"S	57°42'20.00"W
11	Density	High	Amazon	HD1	1°57'58.00"S	59°55'32"W
					2° 8'50.00"S	60° 6'17.00"W
12	Density	High	Amazon	HD2	2°43'0.00"S	59°30'58.00"W
					2°43'0.00"S	59°20'12.00"W
13	Density	High	Amazon	HD3	3°27'4.00"S	59°52'12.00"W
					3°37'54.00"S	59°41'23.00"W
14	Density	High	Amazon	HD4	8°46'19.83"S	66°51'57.85"W
					8°35'24.55"S	66°41'4.45"W
15	Density	High	Amazon	HD5	7°12'46.73"S	59°58'4.36"W
					7° 1'59.47"S	59°47'13.33"W
16	Density	High	Rondônia	HD6	9°37'55.08"S	63°25'24.22"W
					9°27'10.50"S	63°14'33.51"W
17	Density	High	Pará	HD7	4°29'49.95"S	55°54'53.99"W
					4°18'55.97"S	55°44'12.82"W
18	Density	High	Rondônia	HD8	9°49'8.39"S	63°12'21.17"W
					9°38'14.57"S	63° 1'23.40"W
19	Density	High	Pará	HD9	5° 1'2.84"S	50°38'27.96"W
					4°50'8.81"S	50°27'37.50"W
20	Density	High	Pará	HD10	1°50'54.98"S	55°35'45.02"W
					1°40'2.85"S	55°25'0.04"W
21	Spatial Pattern	Fishbone	Amazon	FP1	7°54'7.00"S	61°24'41.00"W
					7°43'15.00"S	61°35'33.00"W
22	Spatial Pattern	Fishbone	Rondônia	FP2	10°24'26.75"S	64°58'14.58"W
					10°13'32.98"S	64°47'17.94"W
23	Spatial Pattern	Fishbone	Rondônia	FP3	9°52'11.82"S	64°41'46.56"W
					9°41'22.14"S	64°30'50.85"W
24	Spatial Pattern	Fishbone	Rondônia	FP4	10°23'19.55"S	64°27'19.09"W
					10°12'28.25"S	64°16'20.66"W

N	Parameter	Category	Province	Code	Latitude	Longitud
25	Spatial Pattern	Fishbone	Rondônia	FP5	10°11'56.00"S	65°17'21.73"W
					10° 1'6.40"S	65° 6'29.02"W
26	Spatial Pattern	Fishbone	Amazon	FP6	2°52'57.72"S	60° 5'14.10"W
					2°42'5.91"S	59°54'27.44"W
27	Spatial Pattern	Fishbone	Pará	FP7	3°48'42.34"S	54°51'6.22"W
					3°37'51.85"S	54°40'20.42"W
28	Spatial Pattern	Fishbone	Pará	FP8	3°59'5.79"S	54°27'49.83"W
					3°48'16.97"S	54°17'4.14"W
29	Spatial Pattern	Fishbone	Pará	FP9	4°18'16.08"S	55°38'7.92"W
					4° 7'19.25"S	55°27'23.27"W
30	Spatial Pattern	Fishbone	Pará	FP10	6°36'45.28"S	55°39'0.90"W
					6°25'51.41"S	55°28'10.38"W
31	Spatial Pattern	Other	Amazon	OP1	7°55'1.53"S	61°24'41.00"W
					8° 5'57.00"S	61°35'33.00"W
32	Spatial Pattern	Other	Rondonia	OP2	9°37'21.00"S	64° 5'11.00"W
					9°26'28.00"S	63°54'18.00"W
33	Spatial Pattern	Other	Amazon	OP3	8°41'12.14"S	64°13'58.87"W
					8°30'21.64"S	64° 3'6.94"W
34	Spatial Pattern	Other	Rondônia	OP4	9°35'48.86"S	62°11'25.55"W
					9°24'55.57"S	62° 0'32.76"W
35	Spatial Pattern	Other	Pará	OP5	4° 8'40.15"S	56°13'49.64"W
					3°57'48.39"S	56° 3'2.47"W
36	Spatial Pattern	Other	Pará	OP6	7°26'47.75"S	55°10'27.67"W
					7°15'53.47"S	54°59'35.97"W
37	Spatial Pattern	Other	Rondônia	OP7	10°10'13.01"S	63° 9'40.13"W
					9°59'18.60"S	62°58'43.34"W
38	Spatial Pattern	Other	Rondônia	OP8	10°49'45.15"S	65°13'4.35"W
					10°38'48.59"S	65° 2'10.29"W
39	Spatial Pattern	Other	Pará	OP9	1°31'17.80"S	55°35'48.31"W
					1°20'25.95"S	55°25'2.12"W
40	Spatial Pattern	Other	Rondônia	OP10	10°42'2.35"S	63°42'34.78"W
					10°31'19.87"S	63°31'47.52"W

Appendix 2. Time – series used in the research. Including clouded and not available plots

TOTAL:	1033	finished classification	173	Cloudy	40	Only ETM+slc off available	34	no image available
	1280	Total planned samples	13.5	%	3.1	%	2.7	%

Scene	Plots	84	85	86	87	88	89	90	91	92	93	94	95	96	97	98	99	00	01	02	03	04	05	06	07	08	09	10	11	12	13	14	15
001/066	HD4		aug	jul	jul		aug	jul	jul	jul	jul	jul	jul	jul	jul	jul	**jul**	**jul**	**jul**	**jul**	jul	jul	jul	jul	jul	jul	jul	jul	jul		*jul*	*jul*	*jul*
	OP3	jul	aug		jul	jul		jul	jul	jul		jul	jul	jul			**jul**	**jul**	**jul**	**jul**	jul	jul	jul	jul	jul	jul	jul	jul	jul		*jul*		*jul*
	LD5		aug		jul		aug	jul		jul	jul	jul	jul	jul	jul	jul	**jul**		**jul**	**jul**	jul	jul	jul	jul	jul	jul	jul	jul	jul		*jul*	*jul*	*jul*
227/063	PF7	aug				jul	aug		jul	jul	may		jul	jul	jul	jun	aug	aug	jul		jul	jul	jul	aug		jul	jul	jul	jul		*sep*	*jul*	
	PF8	aug		nov		jul	aug		jul	jul	may		jul	jul	jul	jun	aug		jul		jul	jul	jul	aug	jul	jul	jul	jul					*jul*
	LD3			nov		jul	aug			jul	may	jul		jul		jun	aug	aug	jul	jul	jul		jul	aug		jul	jul	jul	jul				*jul*
	LD4					jul	aug		jul	jul	may	jul	jul		jul	jun	aug	aug	jul	jul	jul	jul	jul	aug	jul		jul	jul				*jul*	*jul*
227/065	HD5	jun		jul	jun	jul	aug			jul	aug	jul	jul		jun	jul	**jul**		**jul**		jul	jul	jul	jun	jun	jul	jul		jul		*aug*	*sep*	*jun*
	PF10	jun		jul	jun	jul	aug	aug	jul	jul	aug	jul	jul	jul	jun	jul	**jul**		**jul**		jul	jul	jul	jun	jun		jul	jul	jul		*aug*	*sep*	*jun*
	OP6	jun		jul	jun	jul	aug	aug	jul	jul	aug	jul	jul	jul	jun	jul	**jul**	jul	**jul**		jul	jul	jul	jun	jun	jul	jul	jul	jul		*aug*	*sep*	*jun*
	LD9	jun		jul	jun	jul	aug	aug	jul	jul	aug	jul	jul	jul	jun	jul	**jul**	jul	**jul**		jul	jul	jul	jun	jun	jul	jul	jul	jul		*aug*	*sep*	*jun*
228/061	HD10		oct	jul	jul	jul	sep	nov	aug	sep	jul	jul	jul	jun	jul		jul	aug	jul	**jul**	jul		**jul**	**aug**	**jul**	**jul**	**jul**		jul			*aug*	
	OP9		oct	jul	jul	jul	sep	nov	aug	sep	jul	jul	jul	jun	jul	aug	jul	aug	jul	**jul**	jul	**jul**	**jul**	**aug**	**jul**	**jul**	**jul**		jul			*aug*	
	LD8		oct		jul	jul	sep		aug	sep		jul	jul		jul	aug	jul	aug	jul	**jul**		**jul**	**jul**		**jul**	**jul**	**jul**		jul			*aug*	
228/063	HD9	jul	jul	aug	jul		sep	aug		jun	jul	aug	jun	oct		jul	jul		**aug**	**aug**	jul	aug	jul		jun	jul	jul	jul				*aug*	
	PF9	jul		aug	jul	jul	sep	aug	jul		jul		jun	oct	jul	jul	jul		**aug**		jul	aug	jul		jun	jul	jul	jul	aug			*aug*	
	OP5	jul	jul	aug	jul	jul	sep	aug	jul	jun	jul		jun	oct	jul	jul	jul	aug	**aug**	**aug**	jul	aug	jul	jun	jun	jul	jul	jul	aug		*jun*	*aug*	
	LD10	jul	jul	aug	jul		sep	aug	jul	jun	jul		jun	oct	jul	jul	jul	aug	**aug**	**aug**	jul	aug	jul	jun	jun	jul	jul	jul	aug		*jun*	*aug*	
230/062	HD2			aug	aug			aug	aug	jul	sep	oct	aug	oct	jun	aug	sep	aug	**aug**			aug	aug	aug		jul	aug		jul		*jul*		*jun*
	HD3			aug			sep	aug	aug	jul	sep			oct			sep		**aug**			aug	aug	aug		jul			jul				*jun*
	LD7		jul	aug	aug		sep	aug	aug	jul	sep	oct	aug	oct	jun	aug	sep	aug	**aug**	**jul**	jul	aug	aug	aug		jul	aug		jul		*jul*		*jun*
231/062	HD1		jul	aug	jul	aug	aug	aug	aug	jul	jul			aug		jul	jul		aug	**aug**	jul	sep	jul	jul	jul		jul	jul	aug			*jul*	
	PF6	aug	jul	aug	jul	aug	aug	aug	aug	jul	jul		sep		jul	jul	jul	jun	aug		jul	sep	jul	jul	jul		jul	jul	aug		*jul*	*jul*	
	LD1		jul	aug	jul	aug	aug	aug	aug	jul		jul	sep				jul		aug		jul	sep	jul	jul	jul	jul	jul	jul	aug		*jul*		
231/065	PF1	jul	jul	jul	jul	jul	jul	jul	jul	jul			aug	jul			jul	jul	**jul**		jul	jul	jul	jul	jul	jul	jul	jul	**jul**		*aug*	*jul*	*jun*
	OP1	jul	jul		jul	jul	jul	jul	jul	jul			aug	jul	jul		jul	jul	**jul**	**jul**	jul	jul	jul	jul	jul	jul	jul	jul	**jul**		*aug*		*jun*
	LD2	jul	jul	jul	jul	jul	jul	jul	jul	jul			aug	jul	jul		jul		**jul**	**jul**	jul	jul	jul	jul	jul	jul	jul	jul	**jul**		*aug*	*jul*	*jun*
231/067	HD7	aug	jul	aug	jul	jul			jul	jun	jul	jul	aug	jul	jul	jul	jul	jul	aug	**jun**	jul			jul	jul	jul	aug	jun	jul		*aug*	*jul*	*jul*
	OP4	aug	jul	aug	jul	jul	jul	jun	jul	jun	jul	jul	aug	jul	jul	jul	jul	jul	aug	**jun**	jul	jul	jul	jul	jul	jul	aug	jun	jul		*aug*	*jul*	*jul*
232/067	HD6	jun	jul	jul	jul	jul	jul	apr	jul	jul	jul	jul	jul	jul	jul	jul	jul	jul	jun	aug	jul	aug		jul	jun	jul	jul	aug	jul		*jul*	*jul*	*jun*
	HD8	jun	jul	jul	jul	jul			jul	jul	jul	jul	jul	jul	jul	jul	jul	jul	jun	aug	jul			jul	jun	jul	jul	aug	jul		*jul*	*jul*	*jun*
	PF4	jun		jul	jul	jul			jul	jul	jul	jul	jul	jul	jul	jul	jul	jul	jun	aug	jul	aug		jul	jun	jul	jul		jul		*jul*	*jul*	*jun*
	OP10	jun		jul		jul			jul	jul	jul	jul	jul	jul	jul	jul			jun		jul	aug	aug	jul	jun	jul	jul	aug	jul		*jul*	*jul*	*jun*
	OP2	jun	jul	jul	jul	jul	jul		jul	jul	jul	jul	jul	jul	jul	jul	jul	jul	jun	aug	jul	aug		jul	jun	jul	jul	aug	jul		*jul*	*jul*	*jun*
	OP7	jun	jul	jul	jul	jul	jul	apr	jul	jul	jul	jul	jul	jul	jul	jul	jul	jul	jun	aug	jul	aug		jul	jun	jul	jul	aug	jul		*jul*	*jul*	*jun*
233/067	PF2	jul	sep	jul		jul	jul	jul		jul	jul	jul	jul	jul	jul	jul	jul	jul	aug	**jul**	jul	jul	jul	jul	jul	jul	jul	jul	jul		*jun*	*jun*	*jun*
	PF3	jul	sep	jul	jul	jul	jul			jul	jul	jul	jul	jul	jul	jul	jul	jul	aug	**jul**	jul	jul	jul	jul	jul	jul		jul	jul		*jun*	*jun*	*jun*
	PF5	jul	sep	jul	jul	jul	jul	jul		jul	jul	jul	jul	jul	jul	jul	jul	jul	aug	**jul**	jul	jul	jul	jul	jul	jul	jul	jul	jul		*jun*	*jun*	*jun*
	OP8	jul	sep	jul		jul	jul	jul		jul	jul	jul	jul	jul	jul	jul	jul	jul	aug	**jul**	jul	jul	jul	jul	jul	jul		jul	jul		*jun*	*jun*	*jun*
	LD6	jul	sep	jul		jul	jul	jul		jul	jul	jul	jul	jul	jul	jul	jul	jul	aug	**jul**	jul	jul	jul	jul	jul	jul	jul	jul	jul		*jun*	*jun*	*jun*

Appendix 2. Image classification of the complete plots in percentage in respect to total area (400 km^2)

Primary Forest (P.F.), Clear Cut (C.C.), Other (Oth.), Secondary Forest (S.F.), No Data (N.D.). Low Density Plots

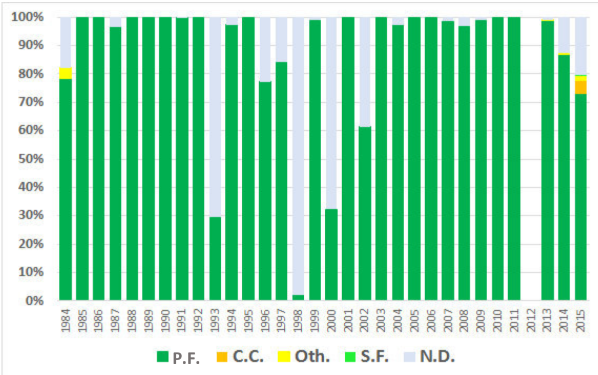

1. Image classification (%) of plot LD1

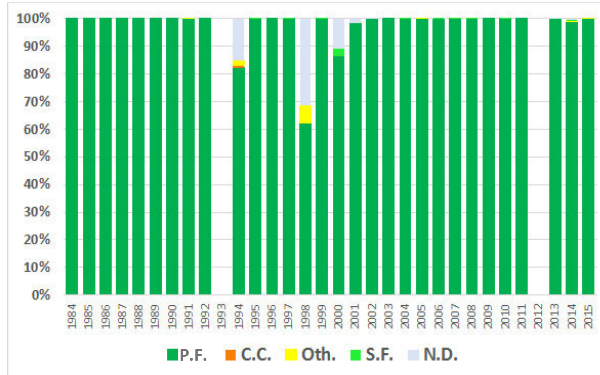

2. Image classification (%) of plot LD2

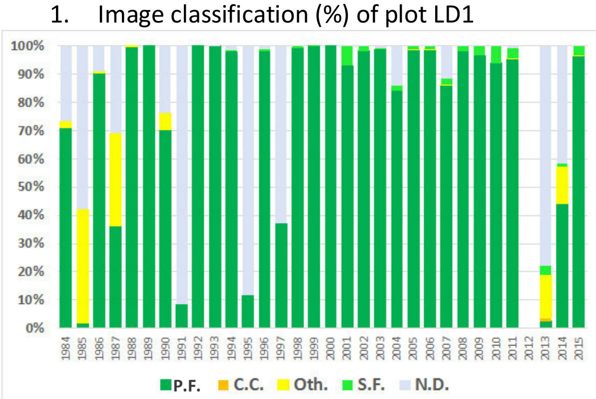

3. Image classification (%) of plot LD3

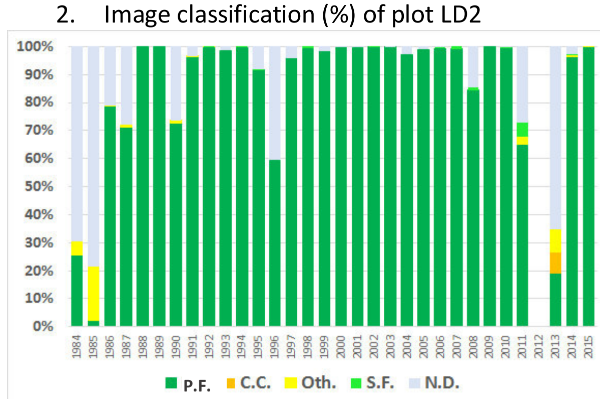

4. Image classification (%) of plot LD4

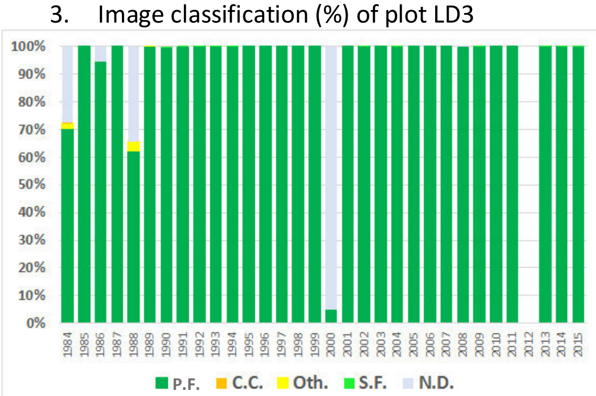

5. Image classification (%) of plot LD5

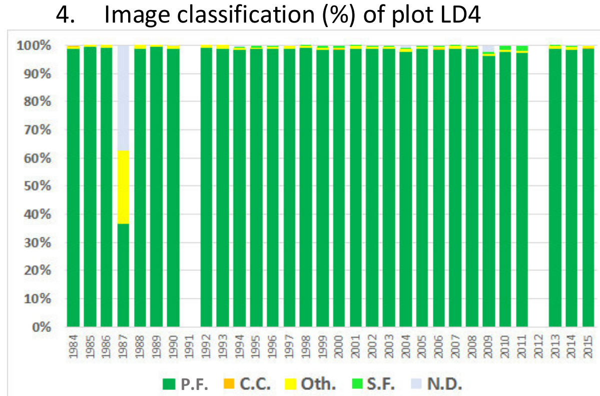

6. Image classification (%) of plot LD6

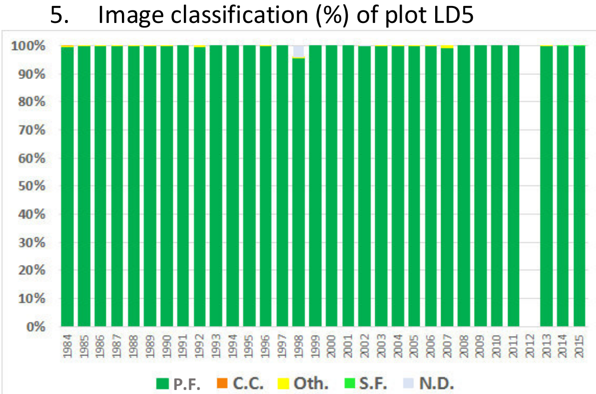

7. Image classification (%) of plot LD7

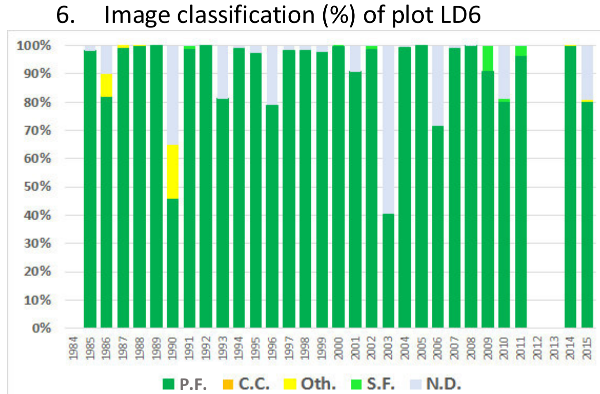

8. Image classification (%) of plot LD8

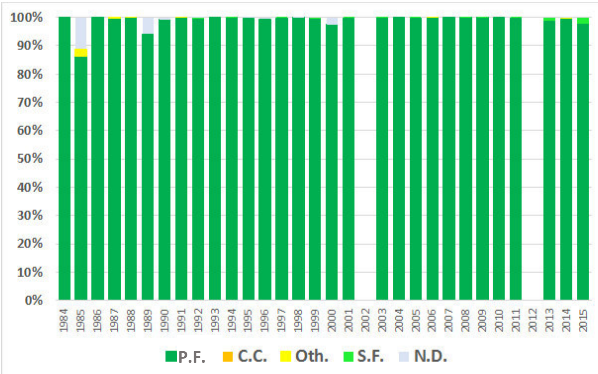

9. Image classification (%) of plot LD9

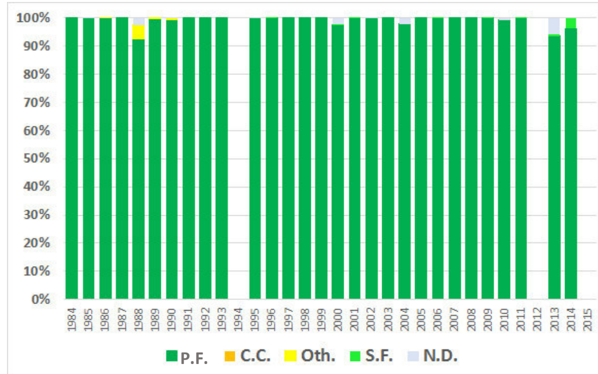

10. Image classification (%) of plot LD10

High Density Plots

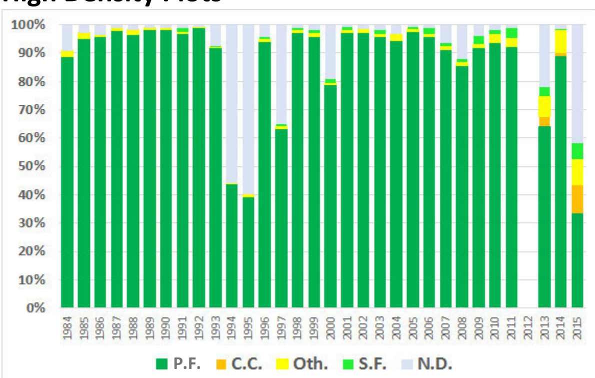

11. Image classification (%) of plot HD1

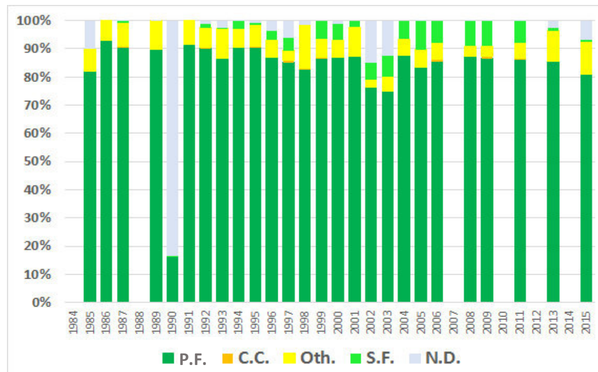

12. Image classification (%) of plot HD2

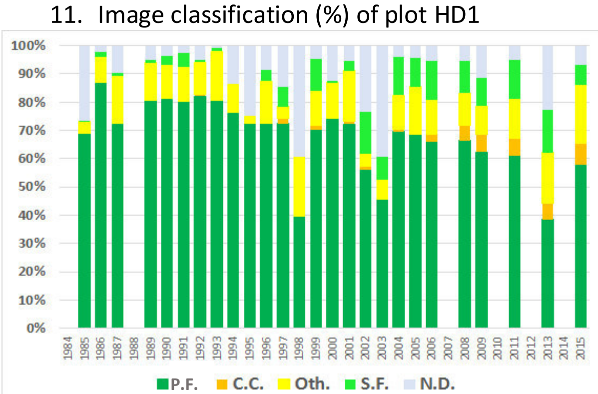

13. Image classification (%) of plot HD3

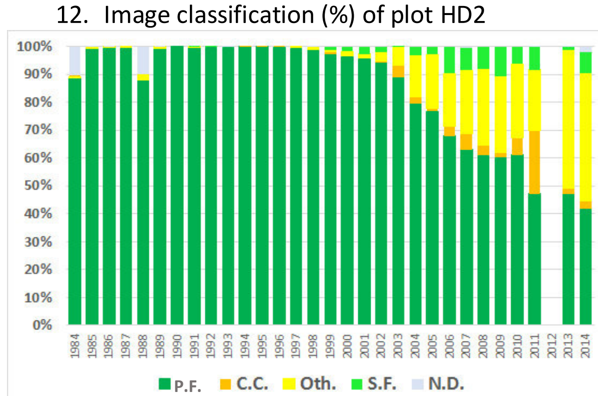

14. Image classification (%) of plot HD4

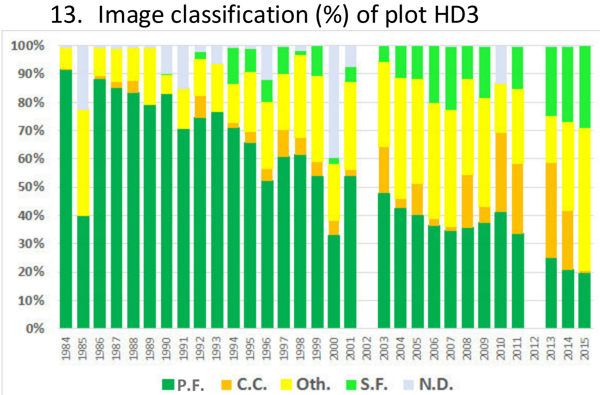

15. Image classification (%) of plot HD5

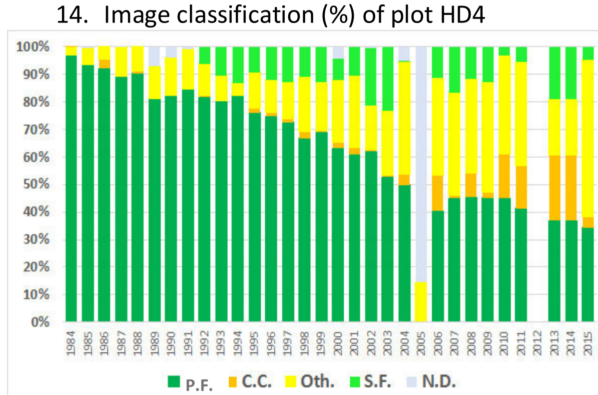

16. Image classification (%) of plot HD6

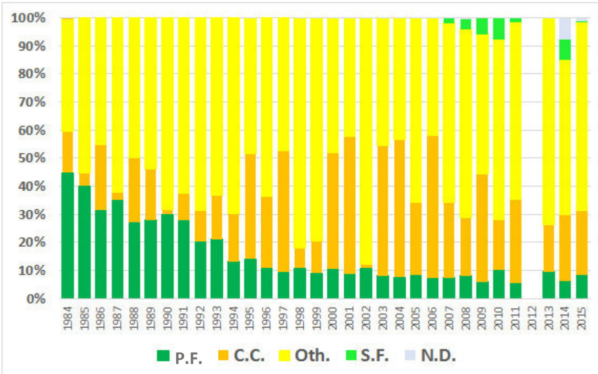

17. Image classification (%) of plot HD7

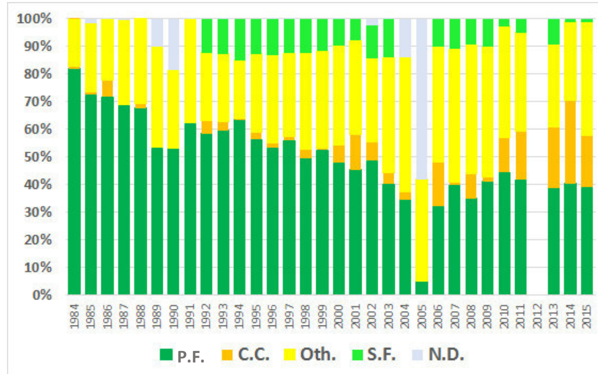

18. Image classification (%) of plot HD8

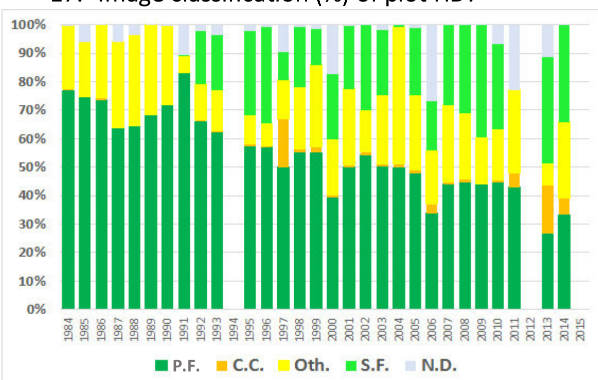

19. Image classification (%) of plot HD9

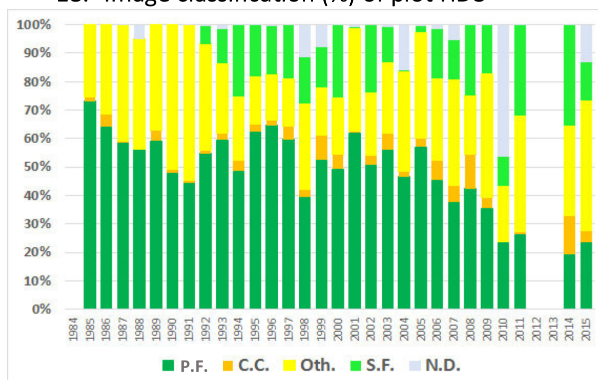

20. Image classification (%) of plot HD10

Fishbone Pattern Plots

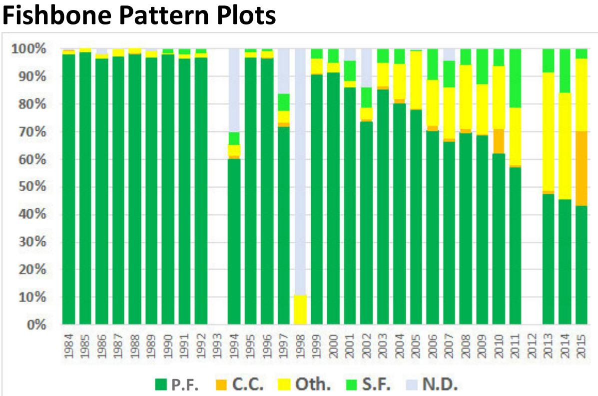

21. Image classification (%) of plot FP1

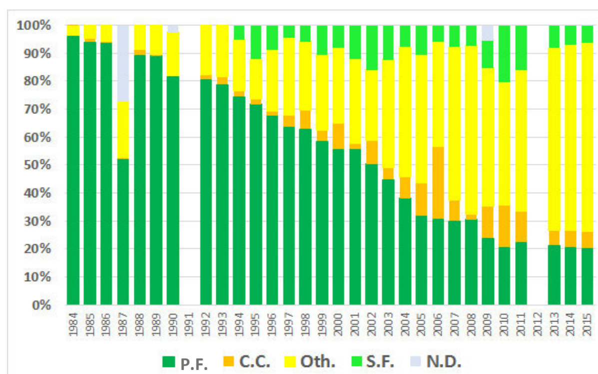

22. Image classification (%) of plot FP2

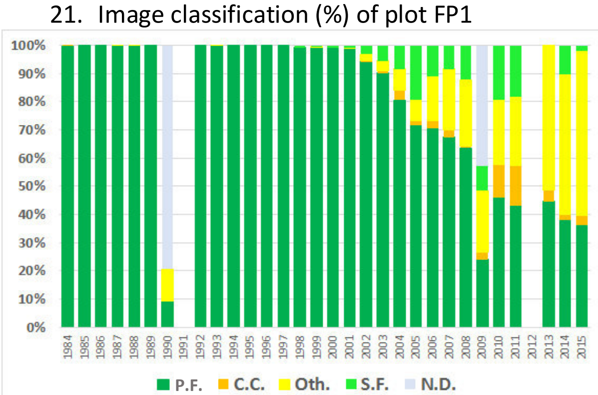

23. Image classification (%) of plot FP3

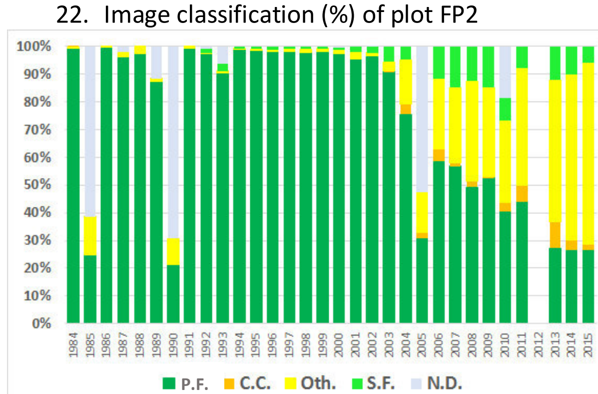

24. Image classification (%) of plot FP4

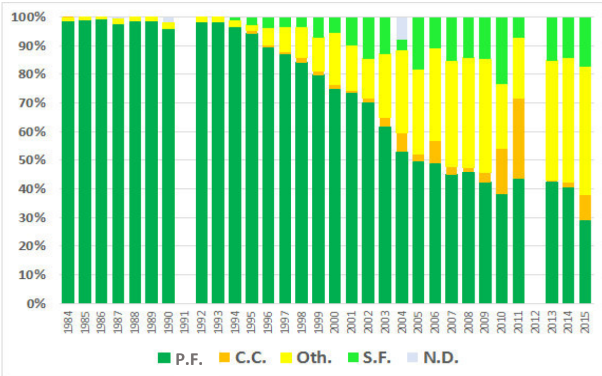

25. Image classification (%) of plot FP5

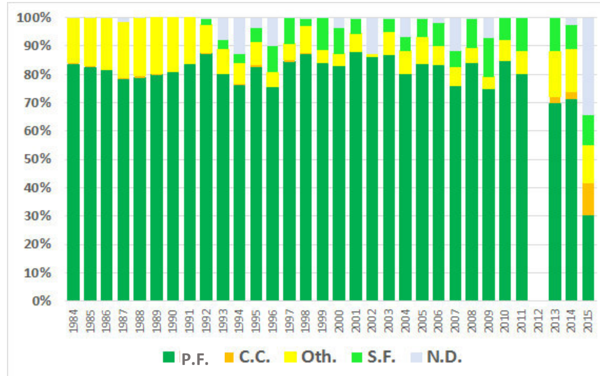

26. Image classification (%) of plot FP6

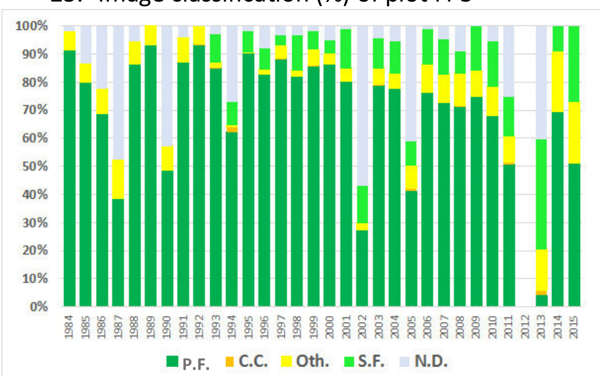

27. Image classification (%) of plot FP7

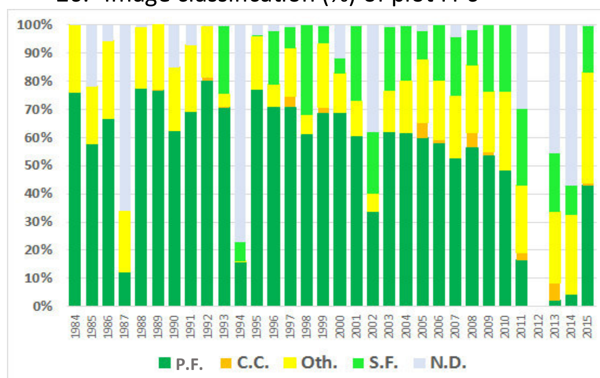

28. Image classification (%) of plot FP8

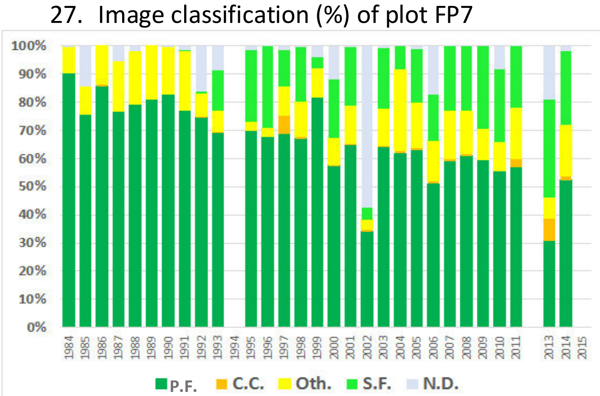

29. Image classification (%) of plot FP9

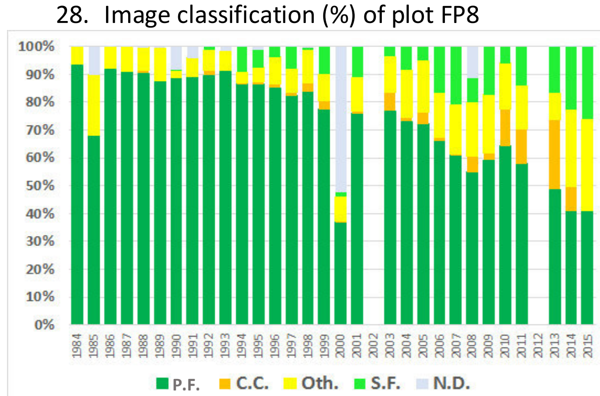

30. Image classification (%) of plot FP10

Other Pattern Plots

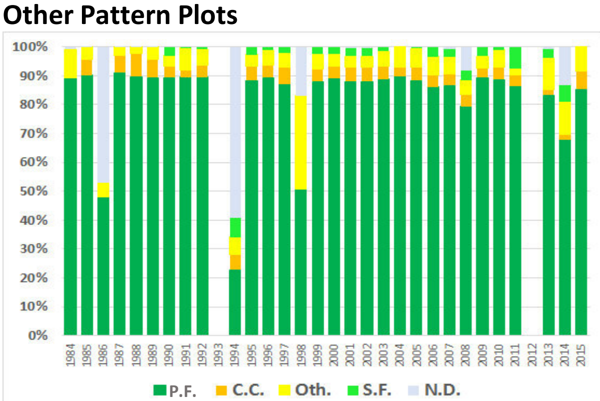

31. Image classification (%) of plot OP1

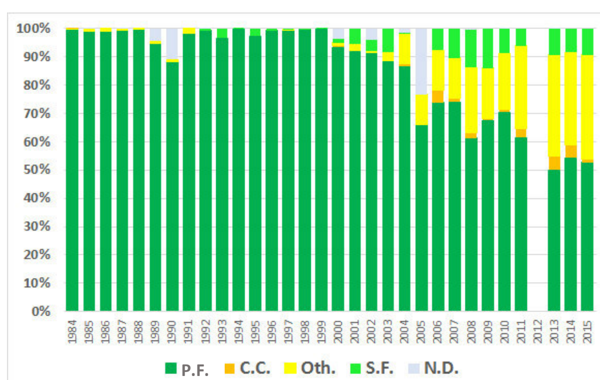

32. Image classification (%) of plot OP2

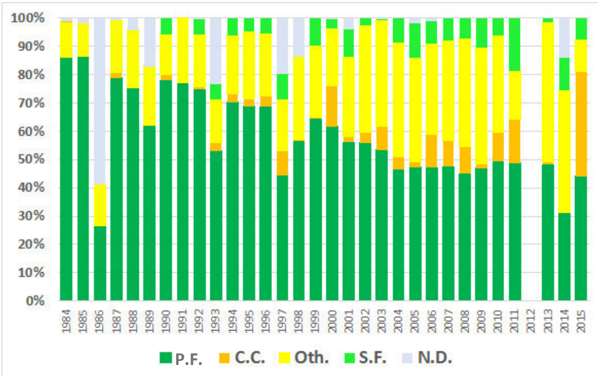

33. Image classification (%) of plot OP3

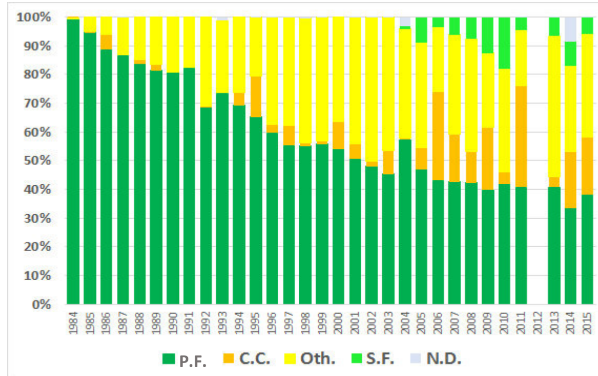

34. Image classification (%) of plot OP4

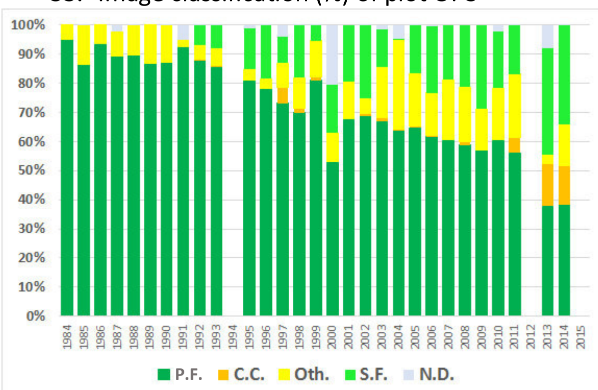

35. Image classification (%) of plot OP5

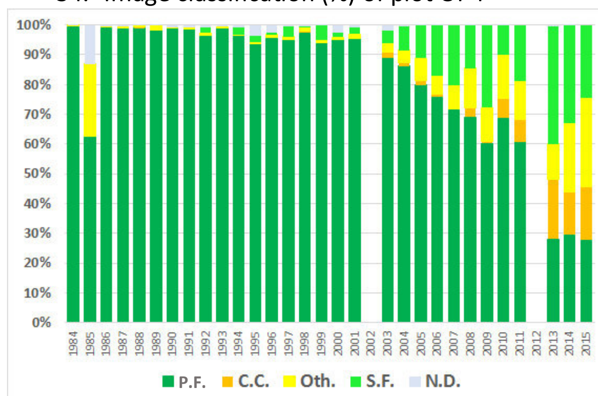

36. Image classification (%) of plot OP6

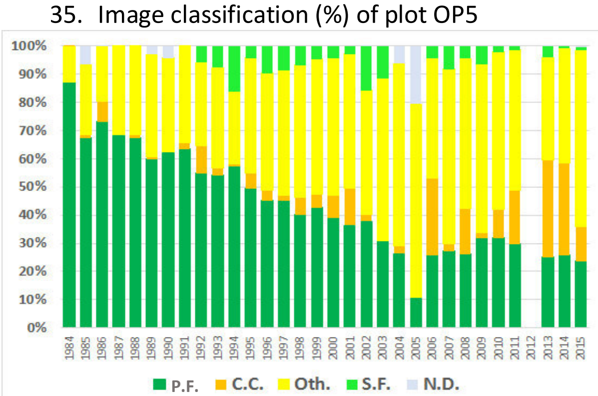

37. Image classification (%) of plot OP7

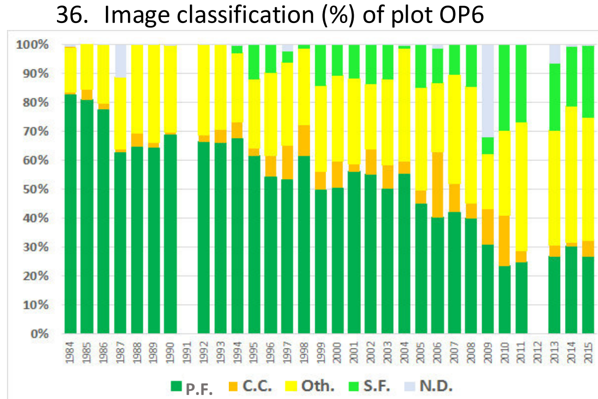

38. Image classification (%) of plot OP8

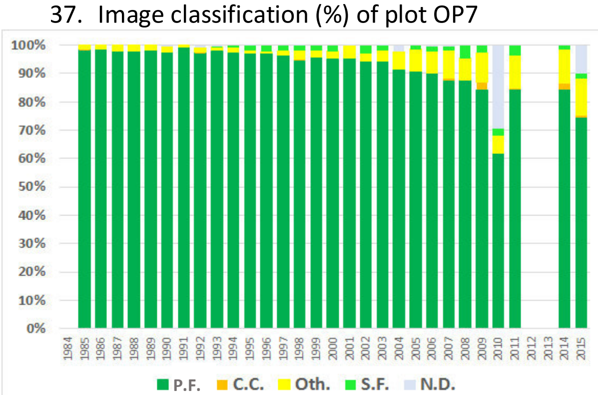

39. Image classification (%) of plot OP9

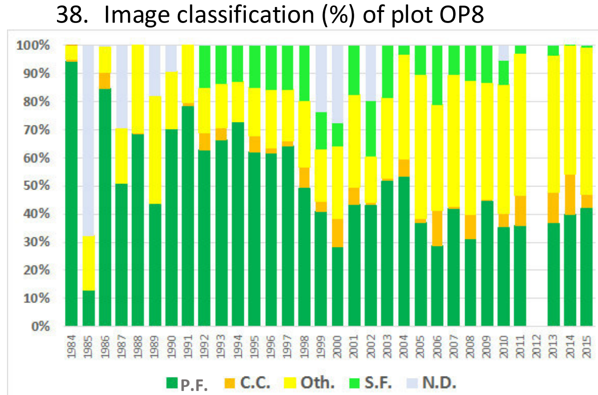

40. Image classification (%) of plot OP10

Appendix 4. Matrix of the accuracy assessment of the different scenes, according to year

1. **Overall Accuracy**

a) With clouded plots

Legend: (red) No Landsat image available; (blue) Clouded images, with lower accuracy

Scene	84	85	86	87	88	89	90	91	92	93	94	95	96	97	98	99	00	01	02	03	04	05	06	07	08	09	10	11	12	13	14	15	Mean	STD
1/066	0.75	0.99	0.26	0.94	0.67	0.81	0.99	0.74	0.95	0.84	0.96	0.98	0.99	0.80	0.86	0.97	0.89	0.99	0.96	0.67	0.98	0.99	0.98	0.92	0.98	0.94	0.91	0.89		0.93	0.81	0.87	0.88	0.15
227/063	0.74	0.65	0.61	0.67	0.96	0.82	0.59	0.62	0.96	0.94	0.61	0.51	0.60	0.90	0.84	0.94	0.79	0.91	0.71	0.86	0.71	0.97	0.95	0.59	0.88	0.96	0.79	0.46		0.44	0.72	0.80	0.76	0.16
227/065	0.82	0.61	0.83	0.97	0.94	0.86	0.70	0.61	0.95	0.84	0.93	0.88	0.79	0.97	0.90	0.98	0.60	0.93		0.79	0.91	0.97	0.92	0.92	0.60	0.87	0.82	0.83		0.91	0.90	0.88	0.85	0.12
228/061		0.98	0.34	0.90	0.97	0.87	0.87	0.98	0.97	0.81	0.93	0.93	0.78	0.94	0.81	0.94	0.89	0.95	0.93	0.68	0.82	0.94	0.87	0.96	0.93	0.89	0.71	0.89			0.95	0.67	0.87	0.13
228/063	0.94	0.37	0.96	0.96		0.92	0.99	0.52	0.62	0.84	0.72	0.98	0.97	0.72	0.85	0.97	0.80	0.97	0.53	0.92	0.94	0.98	0.89	0.89	0.88	0.91	0.89	0.72		0.72	0.91		0.84	0.16
230/062		0.78	0.91	0.40		0.66	0.96	0.88	0.96	0.96	0.79	0.79	0.94	0.64	0.81	0.97	0.79	0.96	0.81	0.63	0.94	0.93	0.94		0.96	0.80		0.87		0.64		0.95	0.83	0.14
231/062	0.76	0.97	0.79	0.96	0.94	0.87	0.93	0.91	0.96	0.78	0.73	0.82	0.75	0.73	0.83	0.97	0.83	0.91	0.75	0.95	0.95	0.97	0.97	0.79	0.64	0.91	0.92	0.81		0.83	0.79	0.83	0.86	0.09
231/065	0.89	0.99	0.31	0.94	0.95	0.87	0.99	0.87	0.95	0.76	0.86	0.92	0.97	0.80	0.85	0.95	0.78	0.94	0.78	0.83	0.98	0.97	0.98	0.82	0.95	0.94	0.91	0.86		0.91	0.82	0.93	0.88	0.13
231/067	0.89	0.96	0.79	0.96	0.93	0.81	0.80	0.89	0.97	0.84	0.97	0.96	0.95	0.87	0.90	0.98	0.92	0.99	0.91	0.89	0.80	0.79	0.91	0.94	0.91	0.93	0.86	0.84		0.94	0.95	0.81	0.90	0.06
232/067	0.91	0.81	0.79	0.89	0.84	0.79	0.86	0.89	0.95	0.88	0.86	0.90	0.98	0.85	0.91	0.83	0.81	0.99	0.72	0.83	0.79	0.73	0.99	0.87	0.96	0.96	0.79	0.87		0.89	0.91	0.95	0.87	0.07
233/067	0.94	0.94	0.86	0.64	0.95	0.87	0.79		0.95	0.95	0.96	0.88	0.99	0.80	0.92	0.97	0.88	0.97	0.96	0.83	0.90	0.93	0.98	0.88	0.98	0.69	0.91	0.89		0.93	0.93	0.93	0.90	0.08
Mean	0.85	0.82	0.68	0.84	0.91	0.83	0.86	0.79	0.93	0.86	0.85	0.87	0.88	0.82	0.86	0.95	0.82	0.96	0.81	0.81	0.88	0.92	0.94	0.86	0.88	0.89	0.85	0.81		0.81	0.87	0.86	**0.86**	**0.13**
STD	0.08	0.19	0.25	0.18	0.09	0.07	0.12	0.15	0.10	0.06	0.11	0.13	0.13	0.09	0.04	0.04	0.08	0.03	0.13	0.10	0.08	0.08	0.04	0.10	0.13	0.08	0.07	0.12		0.16	0.07	0.08		

b) Ommiting clouded plots

Scene	84	85	86	87	88	89	90	91	92	93	94	95	96	97	98	99	00	01	02	03	04	05	06	07	08	09	10	11	12	13	14	15	Mean	STD
1/066		0.99		0.94			0.99		0.95		0.96	0.98	0.99			0.97		0.99	0.96	0.67	0.98	0.99	0.98	0.92	0.98	0.94	0.91	0.89		0.93		0.87	0.94	0.07
227/063					0.96	0.82			0.96	0.94				0.90	0.84	0.94		0.91		0.86		0.97	0.95		0.88	0.96	0.79						0.91	0.06
227/065	0.82		0.83	0.97	0.94	0.86			0.95	0.84	0.93	0.88		0.97	0.90	0.98		0.93		0.79	0.91	0.97	0.92	0.92		0.87		0.83		0.91	0.90	0.88	0.90	0.05
228/061		0.98		0.90	0.97	0.87		0.98	0.97		0.93	0.93		0.94		0.94	0.89	0.95	0.93			0.94		0.96	0.93	0.89		0.89			0.95		0.93	0.03
228/063	0.94		0.96	0.96		0.92	0.99			0.84		0.98	0.97		0.85	0.97		0.97		0.92	0.94	0.98		0.89	0.88	0.91	0.89				0.91		0.93	0.05
230/062			0.91				0.96	0.88	0.96	0.96			0.94			0.97		0.96			0.94	0.93	0.94		0.96			0.87				0.95	0.94	0.03
231/062		0.97	0.79	0.96	0.94	0.87	0.93	0.91	0.96							0.97		0.91		0.95	0.95	0.97	0.97	0.79		0.91	0.92	0.81					0.92	0.06
231/065	0.89	0.99		0.94	0.95	0.87	0.99	0.87	0.95			0.92	0.97			0.95		0.94		0.83	0.98	0.97	0.98	0.82	0.95	0.94	0.91	0.86		0.91		0.93	0.93	0.05
231/067	0.89	0.96	0.79	0.96	0.93			0.89	0.97	0.84	0.97	0.96	0.95	0.87	0.90	0.98	0.92	0.99	0.91	0.89			0.91	0.94	0.91	0.93	0.86	0.84		0.94	0.95	0.81	0.91	0.05
232/067	0.91		0.79		0.84			0.89	0.95	0.88	0.86	0.90	0.98	0.85	0.91			0.99		0.83			0.99	0.87	0.96	0.96		0.87		0.89	0.91	0.95	0.90	0.06
233/067	0.94	0.94	0.86		0.95	0.87			0.95	0.95	0.96	0.88	0.99	0.80	0.92	0.97	0.88	0.97	0.96	0.83	0.90	0.93	0.98	0.88	0.98		0.91	0.89		0.93	0.93	0.93	0.92	0.05
Mean	0.90	0.97	0.85	0.95	0.93	0.87	0.97	0.90	0.96	0.89	0.93	0.93	0.97	0.89	0.89	0.96	0.90	0.96	0.94	0.84	0.94	0.96	0.96	0.89	0.94	0.92	0.88	0.86		0.92	0.93	0.90	**0.92**	**0.05**
STD	0.04	0.02	0.06	0.02	0.04	0.03	0.03	0.04	0.01	0.05	0.04	0.04	0.02	0.06	0.03	0.01	0.02	0.03	0.02	0.08	0.03	0.02	0.03	0.05	0.04	0.03	0.04	0.03		0.02	0.02	0.05		

2. Kappa Index of Accuracy

a) With clouded plots — **Legend:** No Landsat image available; Clouded images, with lower accuracy

Scene	84	85	86	87	88	89	90	91	92	93	94	95	96	97	98	99	00	01	02	03	04	05	06	07	08	09	10	11	12	13	14	15	Mean	STD
1/066	0.58	0.98	0.18	0.74	0.49	0.64	0.94	0.37	0.81	0.74	0.94	0.97	0.97	0.62	0.61	0.89	0.77	0.97	0.93	0.49	0.97	0.92	0.77	0.84	0.97	0.89	0.84	0.86		0.88	0.75	0.83	0.78	0.20
227/063	0.60	0.55	0.45	0.40	0.79	0.70	0.48	0.51	0.93	0.87	0.41	0.38	0.41	0.84	0.71	0.86	0.56	0.83	0.60	0.81	0.63	0.91	0.79	0.52	0.81	0.93	0.72	0.36		0.32	0.65	0.76	0.65	0.19
227/065	0.71	0.48	0.76	0.91	0.89	0.74	0.47	0.45	0.92	0.79	0.90	0.81	0.64	0.94	0.82	0.95	0.46	0.88		0.72	0.87	0.90	0.75	0.90	0.48	0.80	0.61	0.78		0.85	0.85	0.86	0.76	0.16
228/061		0.97	0.25	0.78	0.95	0.75	0.77	0.93	0.91	0.70	0.90	0.90	0.62	0.87	0.68	0.89	0.82	0.91	0.88	0.56	0.69	0.85	0.74	0.94	0.90	0.84	0.65	0.86			0.91	0.63	0.79	0.15
228/063	0.83	0.25	0.92	0.85		0.85	0.94	0.42	0.47	0.73	0.57	0.97	0.92	0.54	0.68	0.91	0.65	0.92	0.40	0.86	0.91	0.90	0.72	0.81	0.85	0.84	0.80	0.67		0.61	0.85		0.75	0.19
230/062		0.64	0.82	0.27		0.49	0.89	0.81	0.94	0.94	0.70	0.72	0.89	0.46	0.72	0.94	0.67	0.92	0.71	0.48	0.92	0.86	0.91		0.95	0.68		0.82		0.56		0.71	0.75	0.18
231/062	0.61	0.94	0.71	0.86	0.90	0.78	0.81	0.77	0.91	0.67	0.67	0.73	0.49	0.49	0.68	0.88	0.70	0.79	0.65	0.93	0.93	0.92	0.84	0.68	0.51	0.83	0.84	0.75		0.62	0.73	0.62	0.75	0.13
231/065	0.74	0.98	0.21	0.74	0.90	0.75	0.96	0.82	0.86	0.66	0.79	0.88	0.91	0.62	0.61	0.87	0.60	0.86	0.68	0.70	0.97	0.88	0.75	0.66	0.93	0.91	0.84	0.81		0.84	0.75	0.75	0.78	0.15
231/067	0.81	0.93	0.67	0.87	0.89	0.67	0.59	0.78	0.92	0.75	0.95	0.93	0.87	0.75	0.84	0.94	0.84	0.98	0.86	0.84	0.73	0.65	0.70	0.90	0.87	0.87	0.74	0.79		0.88	0.91	0.78	0.82	0.10
232/067	0.82	0.70	0.66	0.54	0.75	0.61	0.74	0.77	0.90	0.81	0.76	0.83	0.95	0.72	0.81	0.59	0.62	0.98	0.60	0.70	0.66	0.60	0.81	0.74	0.94	0.90	0.66	0.81		0.80	0.83	0.73	0.75	0.11
233/067	0.86	0.87	0.80	0.39	0.93	0.74	0.53		0.86	0.91	0.94	0.82	0.98	0.62	0.79	0.89	0.72	0.94	0.93	0.71	0.85	0.81	0.79	0.78	0.97	0.56	0.79	0.86		0.78	0.86	0.74	0.80	0.14
Mean	0.73	0.75	0.58	0.67	0.83	0.70	0.74	0.66	0.86	0.78	0.78	0.81	0.79	0.68	0.72	0.87	0.67	0.91	0.72	0.71	0.83	0.84	0.78	0.78	0.83	0.82	0.75	0.76		0.72	0.81	0.74	**0.76**	**0.16**
STD	0.10	0.24	0.25	0.22	0.13	0.09	0.18	0.19	0.13	0.09	0.17	0.16	0.20	0.15	0.08	0.10	0.11	0.06	0.17	0.14	0.12	0.10	0.06	0.12	0.17	0.11	0.08	0.14		0.18	0.08	0.07		

b) Ommiting Clouded Plots

Scene	84	85	86	87	88	89	90	91	92	93	94	95	96	97	98	99	00	01	02	03	04	05	06	07	08	09	10	11	12	13	14	15	Mean	STD
1/066		0.98		0.74			0.94		0.81		0.94	0.97	0.97			0.89		0.97	0.93	0.49	0.97	0.92	0.77	0.84	0.97	0.89	0.84	0.86		0.88		0.83	0.88	0.11
227/063					0.79	0.70			0.93	0.87				0.84	0.71	0.86		0.83		0.81		0.91	0.79		0.81	0.93	0.72						0.82	0.08
227/065	0.71		0.76	0.91	0.89	0.74			0.92	0.79	0.90	0.81		0.94	0.82	0.95		0.88		0.72	0.87	0.90	0.75	0.90		0.80		0.78		0.85	0.85	0.86	0.84	0.07
228/061		0.97		0.78	0.95	0.75		0.93	0.91		0.90	0.90		0.87		0.89	0.82	0.91	0.88			0.85		0.94	0.90	0.84		0.86			0.91		0.88	0.06
228/063	0.83		0.92	0.85		0.85	0.94			0.73		0.97	0.92		0.68	0.91		0.92		0.86	0.91	0.90		0.81	0.85	0.84	0.80				0.85		0.86	0.07
230/062			0.82				0.89	0.81	0.94	0.94			0.89			0.94		0.92			0.92	0.86	0.91		0.95			0.82				0.71	0.88	0.07
231/062		0.94	0.71	0.86	0.90	0.78	0.81	0.77	0.91							0.88		0.79		0.93	0.93	0.92	0.84	0.68		0.83	0.84	0.75					0.84	0.08
231/065	0.74	0.98		0.74	0.90	0.75	0.96	0.82	0.86			0.88	0.91			0.87		0.86		0.70	0.97	0.88	0.75	0.66	0.93	0.91	0.84	0.81		0.84		0.75	0.84	0.09
231/067	0.81	0.93	0.67	0.87	0.89			0.78	0.92	0.75	0.95	0.93	0.87	0.75	0.84	0.94	0.84	0.98	0.86	0.84			0.70	0.90	0.87	0.87	0.74	0.79		0.88	0.91	0.78	0.85	0.08
232/067	0.82		0.66		0.75			0.77	0.90	0.81	0.76	0.83	0.95	0.72	0.81			0.98		0.70			0.81	0.74	0.94	0.90		0.81		0.80	0.83	0.73	0.81	0.09
233/067	0.86	0.87	0.80		0.93	0.74			0.86	0.91	0.94	0.82	0.98	0.62	0.79	0.89	0.72	0.94	0.93	0.71	0.85	0.81	0.79	0.78	0.97		0.79	0.86		0.78	0.86	0.74	0.83	0.09
Mean	0.79	0.94	0.76	0.82	0.87	0.76	0.91	0.81	0.89	0.83	0.90	0.89	0.93	0.79	0.77	0.90	0.79	0.91	0.90	0.75	0.92	0.88	0.79	0.80	0.91	0.87	0.80	0.82		0.84	0.87	0.77	**0.85**	**0.08**
STD	0.05	0.04	0.08	0.06	0.06	0.04	0.05	0.06	0.04	0.07	0.07	0.06	0.04	0.11	0.06	0.03	0.05	0.06	0.03	0.12	0.04	0.03	0.06	0.09	0.05	0.04	0.05	0.04		0.04	0.03	0.05		

Appendix 5. Distribution of the plots in relation to their Euclidean distance to a) Roads, and b) Cities

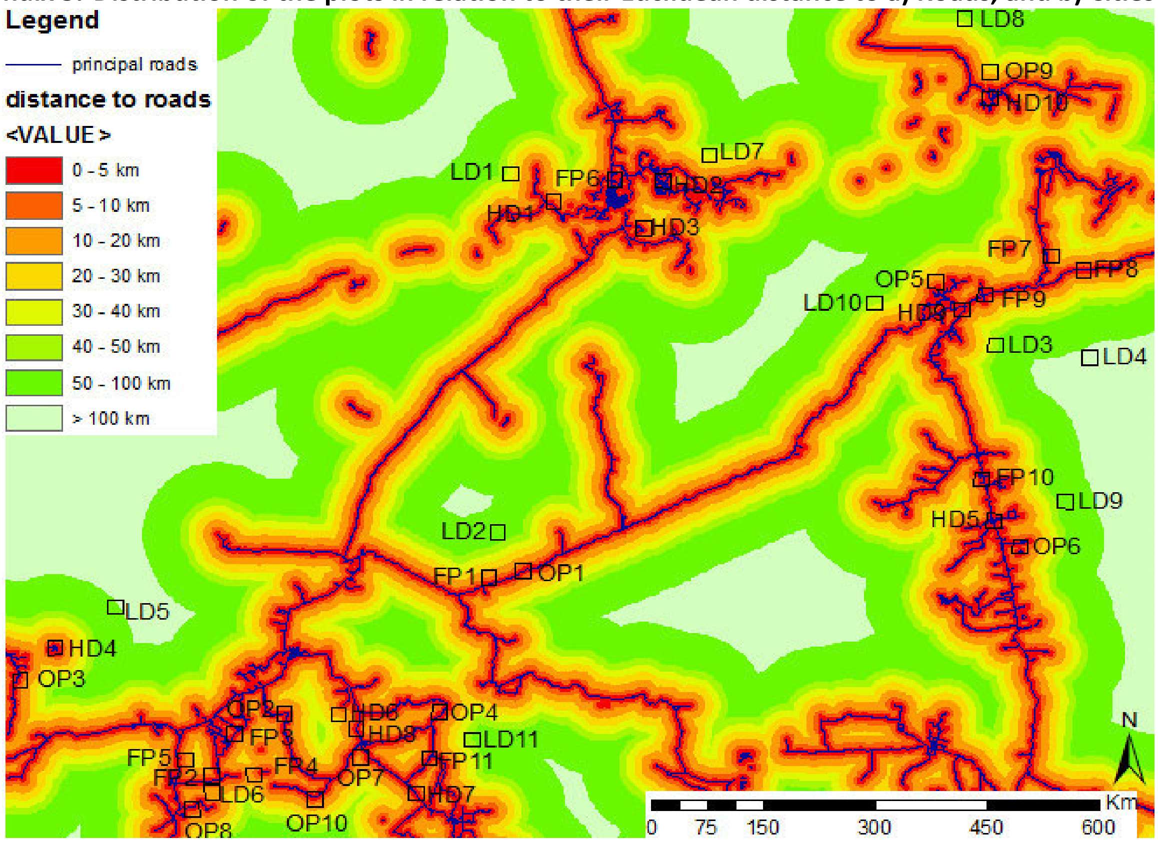

a)

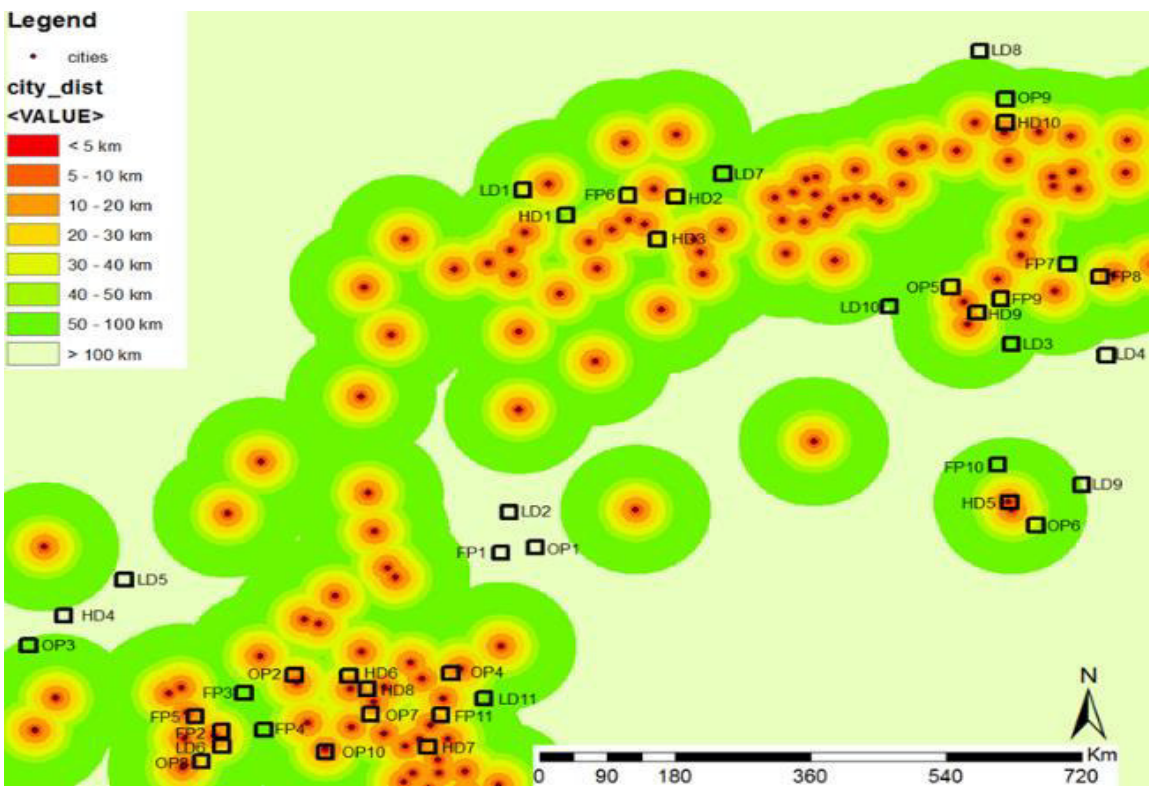

b)

Appendix 6. Values of distance to roads and cities in relation to plots

Plots	Distance to roads (m)				Distance to cities (m)			
Code	Mean	Min	Max	Std	Mean	Min	Max	Std
HD1	3612.1	0	8491.4	3314.7	47693.92	37780.95	53129.65	3315.41
HD2	0.0	0	0.0	0.0	32050.08	19284.19	44582.06	5805.829
HD3	3709.8	0	8491.4	3205.0	29699.22	15565.35	42055.68	5785.727
HD4	2501.8	0	6004.3	2960.2	110682.9	99132.64	120694	5602.639
HD5	600.4	0	6004.3	1801.3	6925.099	0	15000	2851.492
HD6	14332.1	6004.339	21649.0	4787.6	20788.53	10200	31754.69	5526.545
HD7	4063.6	0	12008.7	3877.2	15752.6	3231.099	22593.8	4120.847
HD8	3209.4	0	8491.4	3275.7	16938.41	9600	23736.05	2915.923
HD9	667.1	0	6004.3	1887.0	20388.16	9138.928	30857.74	4810.208
HD10	1501.1	0	6004.3	2600.0	16908.23	6000	27911.29	5465.904
LD1	33023.9	24017.36	42030.4	6713.1	35933	24600	47823.43	5677.951
LD2	60557.8	51301.1	70022.0	5299.9	158731.3	148819.4	169902.8	5471.725
LD3	48937.8	42030.38	55357.3	4884.6	66425.3	53261.62	79338.52	5746.44
LD4	112917.8	104861.3	120835.0	4901.0	120751	107003.7	134196.3	5746.471
LD5	92653.1	81667.84	103302.6	6152.7	118282.1	105097.7	131230	5837.356
LD6	13152.7	8491.418	18013.0	2695.8	19961.06	6029.925	32890.73	5823.765
LD7	32863.0	24017.36	42457.1	6134.8	76356.65	64702.7	83505.69	4195.063
LD8	46882.2	36522.97	56962.2	6579.8	112267.3	102000	122953.2	5880.021
LD9	63169.3	55357.27	70279.0	4610.3	100760.6	87665.73	113465.1	5900.147
LD10	42357.2	30616.24	53704.4	6672.8	95881.09	87831.88	105246.6	3978.074
OP1	2668.6	0	6004.3	2983.6	145706.5	133032.3	155446.3	5227.911
OP2	3335.7	0	6004.3	2983.6	13057.57	1200	24490	5385.159
OP3	2944.9	0	8491.4	3369.9	88968.75	76124.38	101699.6	5772.402
OP4	3688.3	0	8491.4	3344.0	15652.15	3000	27840.26	5557.882
OP5	11037.3	0	21649.0	5786.2	29157.15	15035.96	42260.62	5803.441
OP6	2668.6	0	6004.3	2983.6	41213.25	27475.81	54629.66	5844.57
OP7	6990.9	0	13426.1	3348.8	19703.67	9600	27736.62	4601.711
OP8	3709.8	0	12008.7	4035.0	23744.82	12600	33988.82	5651.377
OP9	18730.6	12008.68	25474.3	4324.2	51620.25	41260.64	62954.27	5596.185
OP10	6004.3	0	12008.7	4902.5	8353.027	0	16810.71	3625.869
FP1	7105.3	0	13426.1	4649.6	142311.8	133805.4	154498.5	4993.625
FP2	4503.3	0	12008.7	3573.3	13522.18	600	25582.81	5480.027
FP3	2501.8	0	6004.3	2960.2	61650.18	49335.18	70320.41	5262.609
FP4	12133.4	6004.339	16982.8	3001.1	57777.63	48614.81	64135.48	3935.621
FP5	6004.3	0	12008.7	4902.5	13860.36	1200	25462.91	5550.425
FP6	0.0	0	0.0	0.0	33322.44	24600	44545.71	4560.627
FP7	6004.3	0	12008.7	4902.5	45712.91	33065.39	57961.37	5797.829
FP8	3335.7	0	6004.3	2983.6	19077.87	7800	30340.07	5621.632
FP9	3202.3	0	12008.7	3712.1	31663.71	21000	42907.34	5627.454
FP10	1656.5	0	8491.4	2919.3	59678.4	47642.42	71922.46	5809.704

Appendix 7. ANOVA of the distance to roads and cities in respect to plot type

1. **Distance to roads**

ANOVA Table

			Sum of Squares	df	Mean Square	F	Sig.
Mean Distance to Roads * Plot Characteristics	Between Groups	(Combined)	5.834E11	3	1.945E11	944.407	.000
	Within Groups		2.582E11	1254	2.059E8		
	Total		8.416E11	1257			

Multiple Comparisons

Dependent Variable:Mean Distance to Roads

	(I) Plot Characteristics	(J) Plot Characteristics	Mean Difference (I-J)	Std. Error	Sig.	95% Confidence Interval	
						Lower Bound	Upper Bound
Bonferroni	Fishbone Pattern	Other Pattern	-1533.2100	1134.43678	1.000	-4530.9030	1464.4830
		Low Density	-50147.2288*	1145.43320	.000	-53173.9793	-47120.4784
		High Density	1224.9500	1143.54887	1.000	-1796.8212	4246.7212
	Other Pattern	Fishbone Pattern	1533.2100	1134.43678	1.000	-1464.4830	4530.9030
		Low Density	-48614.0188*	1145.43320	.000	-51640.7693	-45587.2684
		High Density	2758.1600	1143.54887	.096	-263.6112	5779.9312
	Low Density	Fishbone Pattern	50147.2288*	1145.43320	.000	47120.4784	53173.9793
		Other Pattern	48614.0188*	1145.43320	.000	45587.2684	51640.7693
		High Density	51372.1788*	1154.45849	.000	48321.5795	54422.7782
	High Density	Fishbone Pattern	-1224.9500	1143.54887	1.000	-4246.7212	1796.8212
		Other Pattern	-2758.1600	1143.54887	.096	-5779.9312	263.6112
		Low Density	-51372.1788*	1154.45849	.000	-54422.7782	-48321.5795

Based on observed means.
The error term is Mean Square(Error) = 205911490.395.

*. The mean difference is significant at the .05 level.

Mean Distance to Roads

	Plot Characteristics	N	Subset	
			1	2
Tukey B[a,,b,,c]	High Density	310	3419.7400	
	Fishbone Pattern	320	4644.6900	
	Other Pattern	320	6177.9000	
	Low Density	308		54791.9188

Means for groups in homogeneous subsets are displayed. Based on observed means. The error term is Mean Square(Error) = 205911490.395.

a. Uses Harmonic Mean Sample Size = 314.402.

b. The group sizes are unequal. The harmonic mean of the group sizes is used. Type I error levels are not guaranteed. c. Alpha = .05.

2. Distance to cities

ANOVA Table[a]

			Sum of Squares	df	Mean Square	F	Sig.
Mean Distance to Cities * Plot Characteristics	Between Groups	(Combined)	6.182E11	3	2.061E11	153.816	.000
	Within Groups		1.680E12	1254	1.340E9		
	Total		2.298E12	1257			

a. The grouping variable Plot Characteristics is a string, so the test for linearity cannot be computed.

Multiple Comparisons

Dependent Variable:Mean Distance to Cities

	(I) Plot Characteristics	(J) Plot Characteristics	Mean Difference (I-J)	Std. Error	Sig.	95% Confidence Interval	
						Lower Bound	Upper Bound
Bonferroni	Fishbone Pattern	Other Pattern	4182.2374	2893.63873	.892	-3464.0595	11828.5343
		Low Density	-43047.5926*	2921.68758	.000	-50768.0072	-35327.1780
		High Density	16075.0331*	2916.88118	.000	8367.3192	23782.7470
	Other Pattern	Fishbone Pattern	-4182.2374	2893.63873	.892	-11828.5343	3464.0595
		Low Density	-47229.8300*	2921.68758	.000	-54950.2446	-39509.4154
		High Density	11892.7957*	2916.88118	.000	4185.0817	19600.5096
	Low Density	Fishbone Pattern	43047.5926*	2921.68758	.000	35327.1780	50768.0072
		Other Pattern	47229.8300*	2921.68758	.000	39509.4154	54950.2446
		High Density	59122.6257*	2944.70865	.000	51341.3791	66903.8724
	High Density	Fishbone Pattern	-16075.0331*	2916.88118	.000	-23782.7470	-8367.3192
		Other Pattern	-11892.7957*	2916.88118	.000	-19600.5096	-4185.0817
		Low Density	-59122.6257*	2944.70865	.000	-66903.8724	-51341.3791

Based on observed means. The error term is Mean Square(Error) = 1339703216.688.

*. The mean difference is significant at the .05 level.

Mean Distance to Cities

	Plot Characteristics	N	Subset		
			1	2	3
Tukey B[a,,b,,c]	High Density	310	31782.7149		
	Other Pattern	320		43675.5106	
	Fishbone Pattern	320		47857.7480	
	Low Density	308			90905.3406

Means for groups in homogeneous subsets are displayed.
Based on observed means.
The error term is Mean Square(Error) = 1339703216.688.

a. Uses Harmonic Mean Sample Size = 314.402.

b. The group sizes are unequal. The harmonic mean of the group sizes is used. Type I error levels are not guaranteed. c. Alpha = .05.

Appendix 8. MANOVA distribution land cover types in respect to categories distance to roads and cities

1. **Distance to roads**

Multivariate Tests[c]

Effect		Value	F	Hypothesis df	Error df	Sig.
Intercept	Pillai's Trace	.303	20.337[a]	5.000	234.000	.000
	Wilks' Lambda	.697	20.337[a]	5.000	234.000	.000
	Hotelling's Trace	.435	20.337[a]	5.000	234.000	.000
	Roy's Largest Root	.435	20.337[a]	5.000	234.000	.000
Year	Pillai's Trace	.304	20.476[a]	5.000	234.000	.000
	Wilks' Lambda	.696	20.476[a]	5.000	234.000	.000
	Hotelling's Trace	.438	20.476[a]	5.000	234.000	.000
	Roy's Largest Root	.438	20.476[a]	5.000	234.000	.000
Distance_Road	Pillai's Trace	1.295	11.887	35.000	1190.000	.000
	Wilks' Lambda	.008	59.578	35.000	986.779	.000
	Hotelling's Trace	83.522	554.585	35.000	1162.000	.000
	Roy's Largest Root	83.132	2826.485[b]	7.000	238.000	.000

a. Exact statistic

b. The statistic is an upper bound on F that yields a lower bound on the significance level.

c. Design: Intercept + Year + Distance_Road

Tests of Between-Subjects Effects

Source	Dependent Variable	Type III Sum of Squares	df	Mean Square	F	Sig.
Corrected Model	Primary Forest	3.607E14	8	4.509E13	297.339	.000
	Clear Cut	3.532E12	8	4.415E11	50.683	.000
	Other	5.926E13	8	7.408E12	271.911	.000
	Secondary Forest	7.086E12	8	8.858E11	62.539	.000
	No Data (Clouds, Shadow, Water)	1.677E11	8	2.096E10	33.475	.000
Intercept	Primary Forest	1.241E13	1	1.241E13	81.831	.000
	Clear Cut	5.253E11	1	5.253E11	60.309	.000
	Other	2.377E12	1	2.377E12	87.256	.000
	Secondary Forest	1.028E12	1	1.028E12	72.579	.000
	No Data (Clouds, Shadow, Water)	2.913E9	1	2.913E9	4.653	.032
Year	Primary Forest	1.166E13	1	1.166E13	76.869	.000
	Clear Cut	5.322E11	1	5.322E11	61.101	.000
	Other	2.442E12	1	2.442E12	89.626	.000
	Secondary Forest	1.042E12	1	1.042E12	73.571	.000

Tests of Between-Subjects Effects

Source	Dependent Variable	Type III Sum of Squares	df	Mean Square	F	Sig.
	No Data (Clouds, Shadow, Water)	3.102E9	1	3.102E9	4.955	.027
Distance_Road	Primary Forest	3.482E14	7	4.975E13	328.074	.000
	Clear Cut	3.010E12	7	4.300E11	49.365	.000
	Other	5.692E13	7	8.131E12	298.458	.000
	Secondary Forest	6.065E12	7	8.665E11	61.176	.000
	No Data (Clouds, Shadow, Water)	1.648E11	7	2.355E10	37.604	.000
Error	Primary Forest	3.609E13	238	1.516E11		
	Clear Cut	2.073E12	238	8.711E9		
	Other	6.484E12	238	2.724E10		
	Secondary Forest	3.371E12	238	1.416E10		
	No Data (Clouds, Shadow, Water)	1.490E11	238	6.261E8		
Total	Primary Forest	9.727E14	247			
	Clear Cut	6.707E12	247			
	Other	8.692E13	247			
	Secondary Forest	1.279E13	247			
	No Data (Clouds, Shadow, Water)	4.624E11	247			
Corrected Total	Primary Forest	3.968E14	246			
	Clear Cut	5.605E12	246			
	Other	6.575E13	246			
	Secondary Forest	1.046E13	246			
	No Data (Clouds, Shadow, Water)	3.167E11	246			

a. R Squared = .909 (Adjusted R Squared = .906)

b. R Squared = .630 (Adjusted R Squared = .618)

c. R Squared = .901 (Adjusted R Squared = .898)

d. R Squared = .678 (Adjusted R Squared = .667)

e. R Squared = .529 (Adjusted R Squared = .514)

2. Distance to cities

Multivariate Tests[c]

Effect		Value	F	Hypothesis df	Error df	Sig.
Intercept	Pillai's Trace	.513	49.587[a]	5.000	235.000	.000
	Wilks' Lambda	.487	49.587[a]	5.000	235.000	.000
	Hotelling's Trace	1.055	49.587[a]	5.000	235.000	.000
	Roy's Largest Root	1.055	49.587[a]	5.000	235.000	.000
Year	Pillai's Trace	.509	48.777[a]	5.000	235.000	.000
	Wilks' Lambda	.491	48.777[a]	5.000	235.000	.000
	Hotelling's Trace	1.038	48.777[a]	5.000	235.000	.000
	Roy's Largest Root	1.038	48.777[a]	5.000	235.000	.000
Distance_Cities	Pillai's Trace	1.792	19.064	35.000	1195.000	.000
	Wilks' Lambda	.029	37.323	35.000	990.985	.000
	Hotelling's Trace	8.987	59.932	35.000	1167.000	.000
	Roy's Largest Root	5.019	171.351[b]	7.000	239.000	.000

a. Exact statistic

b. The statistic is an upper bound on F that yields a lower bound on the significance level.

c. Design: Intercept + Year + Distance_Cities

Tests of Between-Subjects Effects

Source	Dependent Variable	Type III Sum of Squares	df	Mean Square	F	Sig.
Corrected Model	Primary Forest	1.991E14	8	2.489E13	141.793	.000
	Clear Cut	1.882E12	8	2.353E11	30.398	.000
	Other	2.297E13	8	2.871E12	82.389	.000
	Secondary Forest	1.844E12	8	2.305E11	21.297	.000
	No Data (Clouds, Shadow, Water)	4.066E10	8	5.082E9	5.787	.000
Intercept	Primary Forest	1.214E13	1	1.214E13	69.137	.000
	Clear Cut	5.945E11	1	5.945E11	76.802	.000
	Other	2.220E12	1	2.220E12	63.713	.000
	Secondary Forest	1.016E12	1	1.016E12	93.877	.000
	No Data (Clouds, Shadow, Water)	5.110E9	1	5.110E9	5.819	.017
Year	Primary Forest	1.139E13	1	1.139E13	64.892	.000
	Clear Cut	6.022E11	1	6.022E11	77.801	.000
	Other	2.283E12	1	2.283E12	65.522	.000
	Secondary Forest	1.030E12	1	1.030E12	95.182	.000
	No Data (Clouds, Shadow, Water)	5.363E9	1	5.363E9	6.107	.014

Tests of Between-Subjects Effects

Source	Dependent Variable	Type III Sum of Squares	df	Mean Square	F	Sig.
Distance_Cities	Primary Forest	1.877E14	7	2.682E13	152.778	.000
	Clear Cut	1.280E12	7	1.829E11	23.626	.000
	Other	2.068E13	7	2.955E12	84.798	.000
	Secondary Forest	8.137E11	7	1.162E11	10.742	.000
	No Data (Clouds, Shadow, Water)	3.529E10	7	5.042E9	5.742	.000
Error	Primary Forest	4.196E13	239	1.755E11		
	Clear Cut	1.850E12	239	7.741E9		
	Other	8.327E12	239	3.484E10		
	Secondary Forest	2.586E12	239	1.082E10		
	No Data (Clouds, Shadow, Water)	2.099E11	239	8.782E8		
Total	Primary Forest	8.110E14	248			
	Clear Cut	4.935E12	248			
	Other	5.257E13	248			
	Secondary Forest	6.775E12	248			
	No Data (Clouds, Shadow, Water)	3.970E11	248			
Corrected Total	Primary Forest	2.411E14	247			
	Clear Cut	3.732E12	247			
	Other	3.129E13	247			
	Secondary Forest	4.430E12	247			
	No Data (Clouds, Shadow, Water)	2.505E11	247			

a. R Squared = .826 (Adjusted R Squared = .820)

b. R Squared = .504 (Adjusted R Squared = .488)

c. R Squared = .734 (Adjusted R Squared = .725)

d. R Squared = .416 (Adjusted R Squared = .397)

e. R Squared = .162 (Adjusted R Squared = .134)

Appendix 9. Distribution land cover types in respect to density

1. **MANOVA (no covariables)**

Density	1	Low	258
	2	High	245

Effect		Value	F	Hypothesis df	Error df	Sig.
Ýear	Pillai's Trace	.406	1.298	150.000	2205.000	.011
	Wilks' Lambda	.637	1.381	150.000	2166.046	.002
	Hotelling's Trace	.507	1.473	150.000	2177.000	.000
	Roy's Largest Root	.358	5.267[b]	30.000	441.000	.000
Density	Pillai's Trace	.613	138.676[a]	5.000	437.000	.000
	Wilks' Lambda	.387	138.676[a]	5.000	437.000	.000
	Hotelling's Trace	1.587	138.676[a]	5.000	437.000	.000
	Roy's Largest Root	1.587	138.676[a]	5.000	437.000	.000
Ýear * Density	Pillai's Trace	.399	1.274	150.000	2205.000	.016
	Wilks' Lambda	.645	1.340	150.000	2166.046	.005
	Hotelling's Trace	.486	1.412	150.000	2177.000	.001
	Roy's Largest Root	.323	4.747[b]	30.000	441.000	.000

a. Exact statistic

b. The statistic is an upper bound on F that yields a lower bound on the significance level.

c. Design: Intercept + Ýear + Density + Ýear * Density

Tests of Between-Subjects Effects

Source	Dependent Variable	Type III Sum of Squares	df	Mean Square	F	Sig.	Noncent. Parameter	Observed Power[b]
Corrected Model	Primary_Forest	3.380E6	61	55411.728	11.346	.000	692.129	1.000
	Clear_Cut	139414.516[c]	61	2285.484	3.417	.000	208.430	1.000
	Other	1.229E6	61	20148.174	7.017	.000	428.023	1.000
	Secondary_Forest	183053.708[e]	61	3000.880	5.977	.000	364.582	1.000
	No_Data	3003.013[f]	61	49.230	1.059	.365	64.577	.990
Intercept	Primary_Forest	5.170E7	1	5.170E7	10586.916	.000	10586.916	1.000
	Clear_Cut	64577.947	1	64577.947	96.546	.000	96.546	1.000
	Other	1106074.115	1	1106074.115	385.199	.000	385.199	1.000
	Secondary_Forest	105186.498	1	105186.498	209.496	.000	209.496	1.000
	No_Data	5092.537	1	5092.537	109.511	.000	109.511	1.000
Ýear	Primary_Forest	325289.134	30	10842.971	2.220	.000	66.608	1.000
	Clear_Cut	38520.927	30	1284.031	1.920	.003	57.590	.998
	Other	64233.082	30	2141.103	.746	.835	22.370	.720
	Secondary_Forest	48465.213	30	1615.507	3.218	.000	96.527	1.000
	No_Data	804.720	30	26.824	.577	.966	17.305	.568
Density	Primary_Forest	2689784.917	1	2689784.917	550.773	.000	550.773	1.000

Tests of Between-Subjects Effects

Source	Dependent Variable	Type III Sum of Squares	df	Mean Square	F	Sig.	Noncent. Parameter	Observed Power[b]
	Clear_Cut	64016.861	1	64016.861	95.707	.000	95.707	1.000
	Other	1084458.436	1	1084458.436	377.672	.000	377.672	1.000
	Secondary_Forest	89662.546	1	89662.546	178.578	.000	178.578	1.000
	No_Data	939.918	1	939.918	20.212	.000	20.212	.994
Ýear * Density	Primary_Forest	314937.080	30	10497.903	2.150	.001	64.488	.999
	Clear_Cut	38354.164	30	1278.472	1.911	.003	57.341	.998
	Other	63852.838	30	2128.428	.741	.840	22.237	.716
	Secondary_Forest	41424.275	30	1380.809	2.750	.000	82.503	1.000
	No_Data	1180.042	30	39.335	.846	.703	25.376	.792
Error	Primary_Forest	2153690.896	441	4883.653				
	Clear_Cut	294976.283	441	668.880				
	Other	1266301.634	441	2871.432				
	Secondary_Forest	221422.607	441	502.092				
	No_Data	20507.650	441	46.503				

a. R Squared = .611 (Adjusted R Squared = .557)

b. Computed using alpha = .05

c. R Squared = .321 (Adjusted R Squared = .227)

d. R Squared = .493 (Adjusted R Squared = .422)

e. R Squared = .453 (Adjusted R Squared = .377)

f. R Squared = .128 (Adjusted R Squared = .007)

Density of Roads

Dependent Variable	Density of Roads	Mean	Std. Error	95% Confidence Interval	
				Lower Bound	Upper Bound
Primary_Forest	Low	399.440	4.642	390.320	408.561
	High	251.555	4.764	242.195	260.914
Clear_Cut	Low	.050	1.692	-3.275	3.375
	High	22.650	1.737	19.238	26.063
Other	Low	.462	3.282	-5.986	6.910
	High	94.150	3.368	87.533	100.767
Secondary_Forest	Low	1.180	1.549	-1.864	4.224
	High	28.558	1.590	25.434	31.681
No_Data	Low	1.856	.417	1.036	2.676
	High	4.687	.428	3.846	5.529

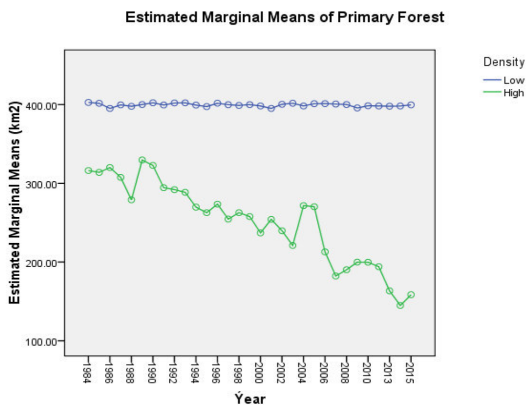

1. Mean Values of Primary Forest according to their difference of density

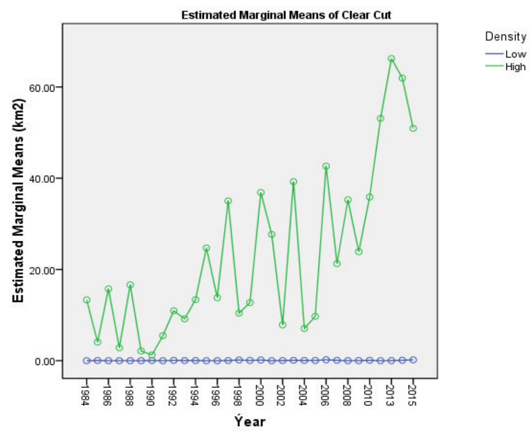

2. Mean Values of Clear Cut according to their difference of density

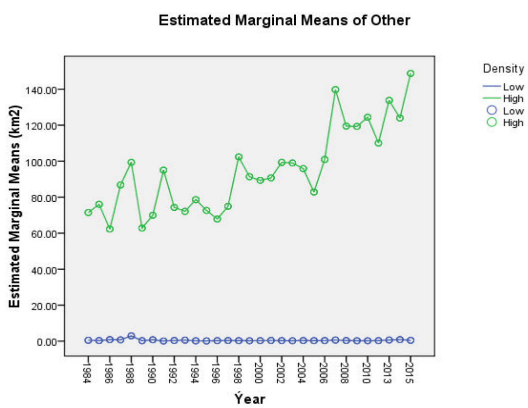

3. Mean Values of Other (Land Cover) according to their difference of density

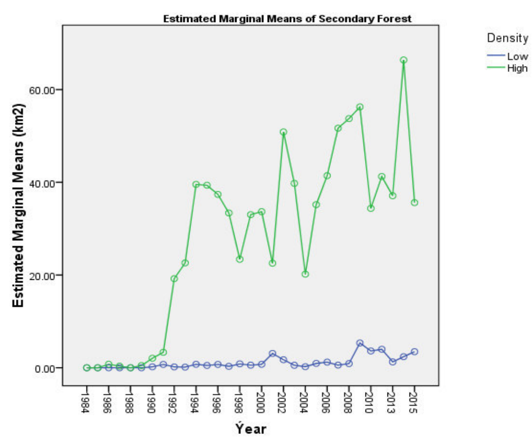

4. Mean Values of Secondary Forest according to their difference of density

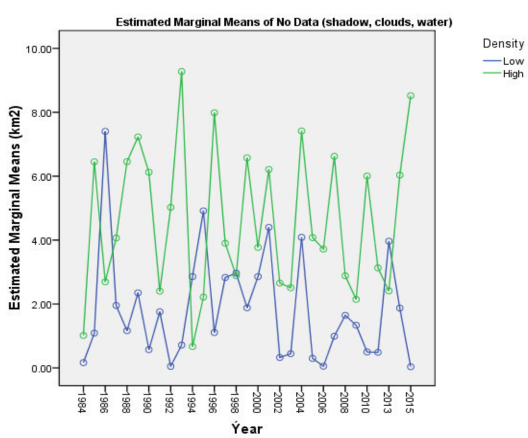

5. Mean Values of No Data according to their difference of density

2. MANCOVA (using distance to roads and cities as covariables)

Multivariate Tests[c]

Effect		Value	F	Hypothesis df	Error df	Sig.
Intercept	Pillai's Trace	.993	13194.780[a]	5.000	432.000	.000
	Wilks' Lambda	.007	13194.780[a]	5.000	432.000	.000
	Hotelling's Trace	152.717	13194.780[a]	5.000	432.000	.000
	Roy's Largest Root	152.717	13194.780[a]	5.000	432.000	.000
City_Mean	Pillai's Trace	.259	30.161[a]	5.000	432.000	.000
	Wilks' Lambda	.741	30.161[a]	5.000	432.000	.000
	Hotelling's Trace	.349	30.161[a]	5.000	432.000	.000
	Roy's Largest Root	.349	30.161[a]	5.000	432.000	.000
City_max	Pillai's Trace	.239	27.175[a]	5.000	432.000	.000
	Wilks' Lambda	.761	27.175[a]	5.000	432.000	.000
	Hotelling's Trace	.315	27.175[a]	5.000	432.000	.000
	Roy's Largest Root	.315	27.175[a]	5.000	432.000	.000
Road_mean	Pillai's Trace	.495	84.599[a]	5.000	432.000	.000
	Wilks' Lambda	.505	84.599[a]	5.000	432.000	.000
	Hotelling's Trace	.979	84.599[a]	5.000	432.000	.000
	Roy's Largest Root	.979	84.599[a]	5.000	432.000	.000
Road_min	Pillai's Trace	.414	61.080[a]	5.000	432.000	.000
	Wilks' Lambda	.586	61.080[a]	5.000	432.000	.000
	Hotelling's Trace	.707	61.080[a]	5.000	432.000	.000
	Roy's Largest Root	.707	61.080[a]	5.000	432.000	.000
Road_max	Pillai's Trace	.517	92.499[a]	5.000	432.000	.000
	Wilks' Lambda	.483	92.499[a]	5.000	432.000	.000
	Hotelling's Trace	1.071	92.499[a]	5.000	432.000	.000
	Roy's Largest Root	1.071	92.499[a]	5.000	432.000	.000
Density	Pillai's Trace	.520	93.431[a]	5.000	432.000	.000
	Wilks' Lambda	.480	93.431[a]	5.000	432.000	.000
	Hotelling's Trace	1.081	93.431[a]	5.000	432.000	.000
	Roy's Largest Root	1.081	93.431[a]	5.000	432.000	.000
Ýear	Pillai's Trace	.587	1.934	150.000	2180.000	.000
	Wilks' Lambda	.485	2.246	150.000	2141.321	.000
	Hotelling's Trace	.918	2.633	150.000	2152.000	.000
	Roy's Largest Root	.750	10.901[b]	30.000	436.000	.000
Density * Ýear	Pillai's Trace	.577	1.896	150.000	2180.000	.000
	Wilks' Lambda	.499	2.154	150.000	2141.321	.000
	Hotelling's Trace	.859	2.465	150.000	2152.000	.000
	Roy's Largest Root	.673	9.781[b]	30.000	436.000	.000

a. Exact statistic

b. The statistic is an upper bound on F that yields a lower bound on the significance level.

c. Design: Intercept + City_Mean + City_max + Road_mean + Road_min + Road_max + Density + Ýear + Density * Ýear

Tests of Between-Subjects Effects

Source	Dependent Variable	Type III Sum of Squares	df	Mean Square	F	Sig.
Corrected Model	Primary_Forest	4.551E6	66	68961.529	30.608	.000
	Clear_Cut	196894.483[b]	66	2983.250	5.477	.000
	Other	1.732E6	66	26248.843	15.001	.000
	Secondary_Forest	228407.816[d]	66	3460.724	8.570	.000
	No_Data	3348.952[e]	66	50.742	1.097	.292
Intercept	Primary_Forest	1253229.944	1	1253229.944	556.228	.000
	Clear_Cut	4.765	1	4.765	.009	.926
	Other	8335.617	1	8335.617	4.764	.030
	Secondary_Forest	12175.269	1	12175.269	30.150	.000
	No_Data	2.651	1	2.651	.057	.811
City_Mean	Primary_Forest	53580.219	1	53580.219	23.781	.000
	Clear_Cut	689.883	1	689.883	1.267	.261
	Other	9644.996	1	9644.996	5.512	.019
	Secondary_Forest	26615.493	1	26615.493	65.908	.000
	No_Data	103.149	1	103.149	2.231	.136
City_max	Primary_Forest	43035.894	1	43035.894	19.101	.000
	Clear_Cut	900.419	1	900.419	1.653	.199
	Other	6740.620	1	6740.620	3.852	.050
	Secondary_Forest	25300.205	1	25300.205	62.651	.000
	No_Data	90.333	1	90.333	1.953	.163
Road_mean	Primary_Forest	612768.538	1	612768.538	271.969	.000
	Clear_Cut	19036.113	1	19036.113	34.947	.000
	Other	236784.371	1	236784.371	135.320	.000
	Secondary_Forest	26072.165	1	26072.165	64.563	.000
	No_Data	.000	1	.000	.000	.998
Road_min	Primary_Forest	395824.273	1	395824.273	175.681	.000
	Clear_Cut	11453.357	1	11453.357	21.026	.000
	Other	153411.540	1	153411.540	87.673	.000
	Secondary_Forest	19320.779	1	19320.779	47.844	.000
	No_Data	.114	1	.114	.002	.960
Road_max	Primary_Forest	713605.322	1	713605.322	316.724	.000
	Clear_Cut	23534.705	1	23534.705	43.205	.000
	Other	277182.691	1	277182.691	158.407	.000

Tests of Between-Subjects Effects

Source	Dependent Variable	Type III Sum of Squares	df	Mean Square	F	Sig.
	Secondary_Forest	26705.414	1	26705.414	66.131	.000
	No_Data	.030	1	.030	.001	.980
Density	Primary_Forest	730106.245	1	730106.245	324.047	.000
	Clear_Cut	17728.406	1	17728.406	32.546	.000
	Other	285089.551	1	285089.551	162.926	.000
	Secondary_Forest	22939.219	1	22939.219	56.805	.000
	No_Data	407.738	1	407.738	8.817	.003
Ýear	Primary_Forest	343165.483	30	11438.849	5.077	.000
	Clear_Cut	39247.567	30	1308.252	2.402	.000
	Other	67720.225	30	2257.341	1.290	.143
	Secondary_Forest	49593.724	30	1653.124	4.094	.000
	No_Data	787.660	30	26.255	.568	.970
Density * Ýear	Primary_Forest	315622.834	30	10520.761	4.669	.000
	Clear_Cut	37070.940	30	1235.698	2.269	.000
	Other	67392.911	30	2246.430	1.284	.148
	Secondary_Forest	41807.523	30	1393.584	3.451	.000
	No_Data	1203.933	30	40.131	.868	.670
Error	Primary_Forest	982345.426	436	2253.086		
	Clear_Cut	237496.316	436	544.716		
	Other	762916.629	436	1749.809		
	Secondary_Forest	176068.498	436	403.827		
	No_Data	20161.711	436	46.242		
Total	Primary_Forest	5.945E7	503			
	Clear_Cut	495897.895	503			
	Other	3564096.867	503			
	Secondary_Forest	510454.321	503			
	No_Data	28775.092	503			
Corrected Total	Primary_Forest	5533806.308	502			
	Clear_Cut	434390.799	502			
	Other	2495340.271	502			
	Secondary_Forest	404476.315	502			
	No_Data	23510.663	502			

a. R Squared = .822 (Adjusted R Squared = .796), b. R Squared = .453 (Adjusted R Squared = .371), c. R Squared = .694 (Adjusted R Squared = .648), d. R Squared = .565 (Adjusted R Squared = .499), e. R Squared = .142 (Adjusted R Squared = .013)

Appendix 10. Distribution land cover types in respect to Pattern

1. **MANOVA (no covariables)**

Type of Pattern	1	Fishbone	267
	2	Other	278

Multivariate Tests[d]

Effect		Value	F	Hypothesis df	Error df	Sig.	Noncent. Parameter	Observed Power[b]
Ýear	Pillai's Trace	.838	3.239	150.000	2415.000	.000	485.919	1.000
	Wilks' Lambda	.328	3.999	150.000	2373.732	.000	592.522	1.000
	Hotelling's Trace	1.585	5.045	150.000	2387.000	.000	756.719	1.000
	Roy's Largest Root	1.281	20.617[c]	30.000	483.000	.000	618.522	1.000
Pattern	Pillai's Trace	.196	23.373[a]	5.000	479.000	.000	116.865	1.000
	Wilks' Lambda	.804	23.373[a]	5.000	479.000	.000	116.865	1.000
	Hotelling's Trace	.244	23.373[a]	5.000	479.000	.000	116.865	1.000
	Roy's Largest Root	.244	23.373[a]	5.000	479.000	.000	116.865	1.000
Ýear * Pattern	Pillai's Trace	.220	.742	150.000	2415.000	.991	111.286	.999
	Wilks' Lambda	.795	.750	150.000	2373.732	.989	111.186	.999
	Hotelling's Trace	.238	.758	150.000	2387.000	.986	113.671	.999
	Roy's Largest Root	.125	2.005[c]	30.000	483.000	.001	60.143	.999

a. Exact statistic

b. Computed using alpha = .05

c. The statistic is an upper bound on F that yields a lower bound on the significance level.

d. Design: Intercept + Ýear + Pattern + Ýear * Pattern

Tests of Between-Subjects Effects

Source	Dependent Variable	Type III Sum of Squares	df	Mean Square	F	Sig.	Noncent. Parameter	Observed Power[b]
Ýear	Primary_Forest	1980266.023	30	66008.867	14.765	.000	442.945	1.000
	Clear_Cut	68178.121	30	2272.604	6.362	.000	190.857	1.000
	Other	636526.369	30	21217.546	7.097	.000	212.913	1.000
	Secondary_Forest	199687.204	30	6656.240	10.380	.000	311.397	1.000
	No_Data	1927.394	30	64.246	1.377	.091	41.321	.972
Pattern	Primary_Forest	52391.503	1	52391.503	11.719	.001	11.719	.927
	Clear_Cut	10307.109	1	10307.109	28.854	.000	28.854	1.000
	Other	50696.043	1	50696.043	16.957	.000	16.957	.984
	Secondary_Forest	2636.135	1	2636.135	4.111	.043	4.111	.525
	No_Data	177.519	1	177.519	3.806	.052	3.806	.495
Ýear * Pattern	Primary_Forest	40077.344	30	1335.911	.299	1.000	8.964	.276
	Clear_Cut	10365.926	30	345.531	.967	.518	29.018	.862
	Other	60684.206	30	2022.807	.677	.904	20.298	.664
	Secondary_Forest	9957.847	30	331.928	.518	.985	15.528	.509
	No_Data	1364.832	30	45.494	.975	.506	29.260	.866
Error	Primary_Forest	2159339.454	483	4470.682				
	Clear_Cut	172537.580	483	357.221				
	Other	1443981.431	483	2989.610				
	Secondary_Forest	309729.951	483	641.263				
	No_Data	22529.497	483	46.645				

a. R Squared = .490 (Adjusted R Squared = .425)

b. Computed using alpha = .05
c. R Squared = .344 (Adjusted R Squared = .261)
d. R Squared = .340 (Adjusted R Squared = .257)
e. R Squared = .408 (Adjusted R Squared = .334)
f. R Squared = .136 (Adjusted R Squared = .027)

Type of Pattern

Dependent Variable	Type of Pattern	Mean	Std. Error	95% Confidence Interval	
				Lower Bound	Upper Bound
Primary_Forest	Fishbone	299.152	5.367	288.610	309.695
	Other	279.230	5.260	268.898	289.561
Clear_Cut	Fishbone	8.079	1.318	5.491	10.668
	Other	17.122	1.292	14.585	19.659
Other	Fishbone	58.469	3.838	50.931	66.008
	Other	78.340	3.761	70.952	85.727
Secondary_Forest	Fishbone	28.785	1.894	25.064	32.507
	Other	23.944	1.857	20.297	27.591
No_Data	Fishbone	3.689	.422	2.859	4.518
	Other	2.416	.414	1.603	3.229

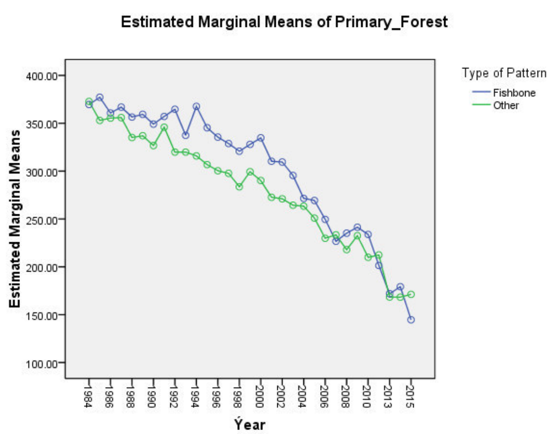

1. Mean Values of Primary Forest according to their difference in pattern

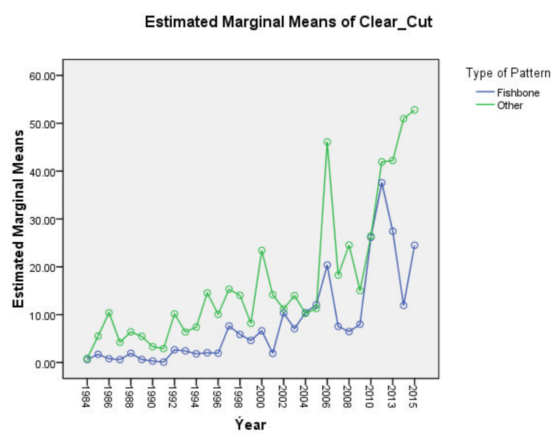

2. Mean Values of Clear Cut according to their difference in pattern

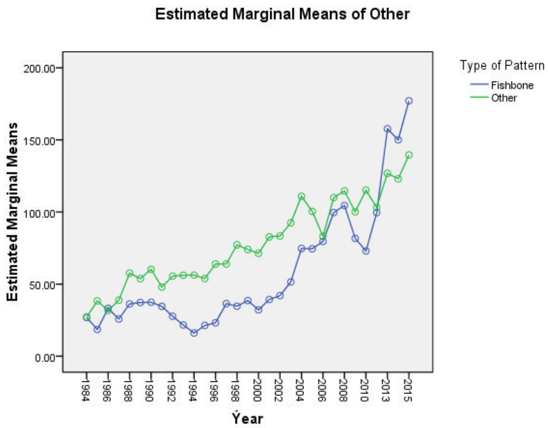

3. Mean Values of Other (Land Cover) according to their difference in pattern

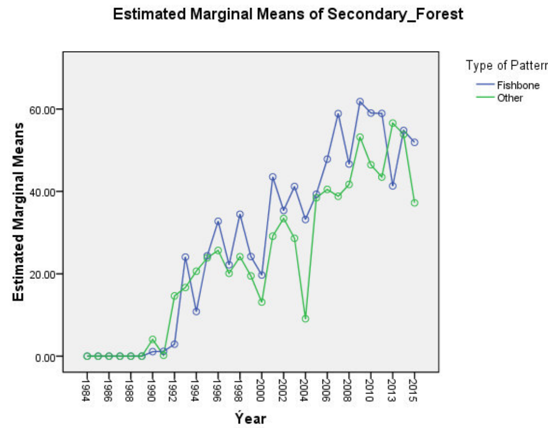

4. Mean Values of Secondary Forest according to their difference in pattern

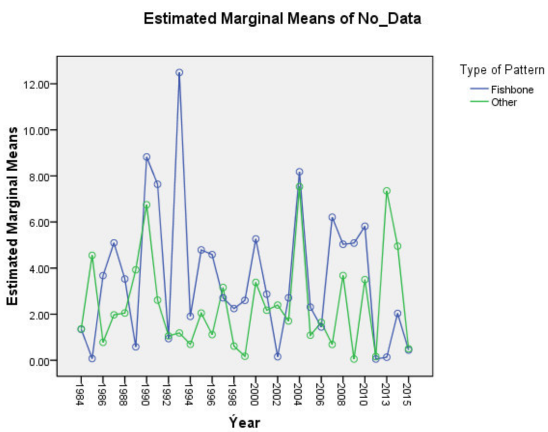

5. Mean Values of No Data according to their difference in pattern

2. MANCOVA (using distance to roads and cities as covariables)

Multivariate Tests[c]

Effect		Value	F	Hypothesis df	Error df	Sig.
Intercept	Pillai's Trace	.997	30603.768[a]	5.000	474.000	.000
	Wilks' Lambda	.003	30603.768[a]	5.000	474.000	.000
	Hotelling's Trace	322.825	30603.768[a]	5.000	474.000	.000
	Roy's Largest Root	322.825	30603.768[a]	5.000	474.000	.000
City_Mean	Pillai's Trace	.131	14.319[a]	5.000	474.000	.000
	Wilks' Lambda	.869	14.319[a]	5.000	474.000	.000
	Hotelling's Trace	.151	14.319[a]	5.000	474.000	.000
	Roy's Largest Root	.151	14.319[a]	5.000	474.000	.000
City_max	Pillai's Trace	.142	15.710[a]	5.000	474.000	.000
	Wilks' Lambda	.858	15.710[a]	5.000	474.000	.000
	Hotelling's Trace	.166	15.710[a]	5.000	474.000	.000
	Roy's Largest Root	.166	15.710[a]	5.000	474.000	.000
Road_mean	Pillai's Trace	.092	9.630[a]	5.000	474.000	.000
	Wilks' Lambda	.908	9.630[a]	5.000	474.000	.000
	Hotelling's Trace	.102	9.630[a]	5.000	474.000	.000
	Roy's Largest Root	.102	9.630[a]	5.000	474.000	.000
Road_min	Pillai's Trace	.046	4.535[a]	5.000	474.000	.000
	Wilks' Lambda	.954	4.535[a]	5.000	474.000	.000
	Hotelling's Trace	.048	4.535[a]	5.000	474.000	.000
	Roy's Largest Root	.048	4.535[a]	5.000	474.000	.000
Road_max	Pillai's Trace	.169	19.229[a]	5.000	474.000	.000
	Wilks' Lambda	.831	19.229[a]	5.000	474.000	.000
	Hotelling's Trace	.203	19.229[a]	5.000	474.000	.000
	Roy's Largest Root	.203	19.229[a]	5.000	474.000	.000
Pattern	Pillai's Trace	.298	40.218[a]	5.000	474.000	.000
	Wilks' Lambda	.702	40.218[a]	5.000	474.000	.000
	Hotelling's Trace	.424	40.218[a]	5.000	474.000	.000
	Roy's Largest Root	.424	40.218[a]	5.000	474.000	.000
Ýear	Pillai's Trace	.952	3.750	150.000	2390.000	.000

Multivariate Tests[c]

Effect		Value	F	Hypothesis df	Error df	Sig.
	Wilks' Lambda	.249	5.078	150.000	2349.008	.000
	Hotelling's Trace	2.274	7.161	150.000	2362.000	.000
	Roy's Largest Root	1.950	31.076[b]	30.000	478.000	.000
Pattern * Ýear	Pillai's Trace	.256	.859	150.000	2390.000	.888
	Wilks' Lambda	.766	.867	150.000	2349.008	.872
	Hotelling's Trace	.278	.876	150.000	2362.000	.854
	Roy's Largest Root	.139	2.223[b]	30.000	478.000	.000

a. Exact statistic

b. The statistic is an upper bound on F that yields a lower bound on the significance level.

c. Design: Intercept + City_Mean + City_max + Road_mean + Road_min + Road_max + Pattern + Ýear + Pattern * Ýear

Tests of Between-Subjects Effects

Source	Dependent Variable	Type III Sum of Squares	df	Mean Square	F	Sig.
Corrected Model	Primary_Forest	3.007E6	66	45561.643	17.807	.000
	Clear_Cut	103464.076[b]	66	1567.638	4.698	.000
	Other	1.204E6	66	18248.503	8.861	.000
	Secondary_Forest	261897.603[d]	66	3968.145	7.250	.000
	No_Data	4002.791[e]	66	60.648	1.313	.059
Intercept	Primary_Forest	479950.757	1	479950.757	187.584	.000
	Clear_Cut	7178.040	1	7178.040	21.513	.000
	Other	340116.943	1	340116.943	165.146	.000
	Secondary_Forest	262.967	1	262.967	.480	.489
	No_Data	7.943	1	7.943	.172	.679
City_Mean	Primary_Forest	124699.507	1	124699.507	48.738	.000
	Clear_Cut	3028.373	1	3028.373	9.076	.003
	Other	135443.281	1	135443.281	65.766	.000
	Secondary_Forest	3365.844	1	3365.844	6.149	.013
	No_Data	223.736	1	223.736	4.846	.028
City_max	Primary_Forest	142504.796	1	142504.796	55.697	.000
	Clear_Cut	3062.873	1	3062.873	9.180	.003
	Other	148628.636	1	148628.636	72.168	.000
	Secondary_Forest	2891.346	1	2891.346	5.282	.022
	No_Data	218.256	1	218.256	4.727	.030

Tests of Between-Subjects Effects

Source	Dependent Variable	Type III Sum of Squares	df	Mean Square	F	Sig.
Road_mean	Primary_Forest	109517.476	1	109517.476	42.804	.000
	Clear_Cut	4650.103	1	4650.103	13.937	.000
	Other	47571.411	1	47571.411	23.099	.000
	Secondary_Forest	3101.401	1	3101.401	5.666	.018
	No_Data	86.634	1	86.634	1.876	.171
Road_min	Primary_Forest	21771.716	1	21771.716	8.509	.004
	Clear_Cut	4.289	1	4.289	.013	.910
	Other	7010.412	1	7010.412	3.404	.066
	Secondary_Forest	1916.918	1	1916.918	3.502	.062
	No_Data	163.190	1	163.190	3.534	.061
Road_max	Primary_Forest	213822.778	1	213822.778	83.571	.000
	Clear_Cut	5446.981	1	5446.981	16.325	.000
	Other	83293.216	1	83293.216	40.444	.000
	Secondary_Forest	9425.915	1	9425.915	17.221	.000
	No_Data	48.007	1	48.007	1.040	.308
Pattern	Primary_Forest	53854.650	1	53854.650	21.049	.000
	Clear_Cut	12582.696	1	12582.696	37.711	.000
	Other	57225.482	1	57225.482	27.786	.000
	Secondary_Forest	4119.209	1	4119.209	7.526	.006
	No_Data	225.303	1	225.303	4.880	.028
Ýear	Primary_Forest	1949500.910	30	64983.364	25.398	.000
	Clear_Cut	66745.658	30	2224.855	6.668	.000
	Other	625463.809	30	20848.794	10.123	.000
	Secondary_Forest	199899.576	30	6663.319	12.174	.000
	No_Data	1888.799	30	62.960	1.364	.098
Pattern * Ýear	Primary_Forest	53114.036	30	1770.468	.692	.891
	Clear_Cut	9909.258	30	330.309	.990	.484
	Other	77048.625	30	2568.287	1.247	.175
	Secondary_Forest	9412.516	30	313.751	.573	.968
	No_Data	1365.630	30	45.521	.986	.490
Error	Primary_Forest	1223006.141	478	2558.590		
	Clear_Cut	159490.593	478	333.662		
	Other	984435.394	478	2059.488		
	Secondary_Forest	261638.788	478	547.361		
	No_Data	22070.824	478	46.173		
Total	Primary_Forest	4.975E7	545			

Tests of Between-Subjects Effects

Source	Dependent Variable	Type III Sum of Squares	df	Mean Square	F	Sig.
	Clear_Cut	350746.248	545			
	Other	4753962.121	545			
	Secondary_Forest	900952.568	545			
	No_Data	31108.281	545			
Corrected Total	Primary_Forest	4230074.568	544			
	Clear_Cut	262954.669	544			
	Other	2188836.607	544			
	Secondary_Forest	523536.390	544			
	No_Data	26073.615	544			

a. R Squared = .711 (Adjusted R Squared = .671)

b. R Squared = .393 (Adjusted R Squared = .310)

c. R Squared = .550 (Adjusted R Squared = .488)

d. R Squared = .500 (Adjusted R Squared = .431)

e. R Squared = .154 (Adjusted R Squared = .037)